

# ResearchOnline@JCU

This file is part of the following reference:

**Bochow, Shaun (2016) *Characterisation of Cherax quadricarinatus densovirus: the first virus characterised from Australian freshwater crayfish*. PhD thesis, James Cook University.**

Access to this file is available from:

<http://researchonline.jcu.edu.au/48889/>

*The author has certified to JCU that they have made a reasonable effort to gain permission and acknowledge the owner of any third party copyright material included in this document. If you believe that this is not the case, please contact*

*[ResearchOnline@jcu.edu.au](mailto:ResearchOnline@jcu.edu.au) and quote  
<http://researchonline.jcu.edu.au/48889/>*

Characterisation of *Cherax quadricarinatus*  
densovirus; the first virus characterised from  
Australian freshwater crayfish

Thesis submitted by

Shaun Bochow

Bsc Science (Aquaculture)

Hons Class 1 (Microbiology & Immunology)

August 2016

**For the degree of Doctor of Philosophy**

**in**

**Microbiology & Immunology**

**College of Public Health, Medical and Veterinary Science**

**James Cook University**

## STATEMENT OF ACCESS DECLARATION

I, the undersigned, author of this work, understand that James Cook University will make this thesis available for use within the University Library and, via the Australian Digital Theses Network, for use elsewhere.

I understand that, as an unpublished work, a thesis has significant protection under Copyright Act and, I do not wish to place any further restriction on access to this work.

Signature

Date:

## **STATEMENT OF SOURCES DECLARATION**

I declare that this thesis is my own work and has not been submitted in any form for another degree or diploma at any university or other institution of tertiary education. Information derived from the published or unpublished work of others has been acknowledged in the text and a list of references is given

Signature

Date:

# **STATEMENT OF SOURCES ELECTRONIC COPY DECLARATION**

I, the undersigned, the author of this work, declare that the electronic copy of this thesis provided to the James Cook University Library is an accurate copy of the print thesis submitted, within limits of the technology available.

Signature

Date:

## DECLARATION OF ETHICS

The research presented and reported in this thesis was conducted within the guidelines for research ethics outlined in the *National Statement on Ethics Conduct in Research Involving Human* (1999), *The Joint NHMCR/AVCC Statement and Guidelines on Research Practice* (1997), the *James Cook University Policy on Experimentation Ethics, Standard Practices and Guidelines* (2001), and the *James Cook University Statement and Guidelines on Research Practice* (2001). The proposed research methodology received clearance from the James Cook University Experimentation Ethics Review (Approval numbers A1922 and A2053).

Signature

Date:

## STATEMENT OF Co-AUTHORS

Bochow, S., Condon, K., Elliman, J. and Owens, L. (2015) First complete genome of an Ambidensovirus; *Cherax quadricarinatus* densovirus, from freshwater crayfish *Cherax quadricarinatus*. *Marine Genomics* **24, Part 3**: 305-312

Author	Contribution
Shaun Bochow	Infected, isolated and purified the virus from <i>Cherax quadricarinatus</i> at James Cook University Extracted viral DNA Sequenced genome using PCR with random and specific primers Performed the bioinformatics analysis of the genome Prepared manuscript drafts
Kelly Condon	Provided the original virus inoculum Assisted with DNA extraction and PCR Assisted with manuscript preparation
Jennifer Elliman	Consulted on PCR trouble shooting and optimising PCR Manuscript revision
Leigh Owens	Provided funding to complete work Manuscript direction and revision Coordinated the Aquatic Fish Pathology Laboratory where the work was undertaken

## STATEMENT OF THE CONTRIBUTION OF OTHERS

The staff at the Queensland Government's Tropical and Aquatic Animal Health Laboratory provided the original tissue infected with the virus that was the focus of this project.

I was the recipient of an Australian Postgraduate Award.

This study was partially funded by Indo-Australia Biotechnology Grant BF50090.

Funding was provided in the form of competitive grants from Graduate Research Scheme Grants-in aid Conference Funding

Dr Ian Hewson of Cornell University provided unpublished echinoderm sequences.

Rusaini contributed to the histology of CqDV used in Chapter 4.

Associate Professor Leigh Owens, Dr Jennifer Elliman and Kelly Condon provided editorial support.

The northern Queensland farms provided the *C. quadricarinatus* for this project at no cost.

Dr Kathryn Green and Mr Richard Webb from the Centre for Microscopy and Microanalysis at the University of Queensland processed samples from caesium chloride bands and gills and took transmission electron microscopy pictures used in this project.

## ACKNOWLEDGEMENTS

The staff of the Queensland Government's former Tropical and Aquatic Animal Health Laboratory are gratefully acknowledged for providing CqDV infected tissue for this project.

I would like to thank Associate Professor Leigh Owens and Dr Jennifer Elliman who have been my supervisors during Honours and now PhD. They have been a valuable source of information and have helped keep me on track to complete this project. I am grateful for the opportunity that they have given me.

To Kelly Condon, my friend and mentor, you have been a rock throughout this project. To have someone of your calibre in my corner, in this, a very difficult environment to operate in, has been immeasurable. I have enjoyed all the talks, laughs and rough times that we have shared over the last few years. Because of your training and tutelage at the bench, I now have skills applicable to the real world. I wish you all the very best of luck in your PhD. Stay calm, breath, and don't let the voices in your head lead you down the path that leads to a lab on fire.

A special thankyou to Alyssa Budd from the MEEL lab. Working with you has been very insightful and I learned a lot in a very short time. I am glad my 'slaughtered' RNA made you laugh.

To the wonderful technicians at the vet school that I have worked with over the years: you guys are awesome! You deserve a medal for keeping the labs and the equipment in a 'working state' despite having no time or money to do so. I hope things improve for you in the future.

Thankyou to James Cook University for the Australian Postgraduate Award and the conditions attached.

Finally I would like to thank my family, my parents Kathy and Kevin, my brothers Matthew and Simon. My family have provided financial support throughout my PhD,

particularly when I was funding the research myself. I have appreciated being able to just turn up on your front door step with a bag of washing, looking for a hot meal. Having somewhere to retreat to, to clear my head and refocus on my goals has been invaluable in helping me through the hard times.

## ABSTRACT

Early disease investigations in *Cherax* spp. were observational in nature. Investigators found a variety of pathogens including fungi, ciliates, platyhelminthes, nematodes and viruses. To date, the viral flora identified have been studied using histopathology and transmission electron microscopy. There have been two transmission trials carried out using *Cherax* spp. infecting viruses, a Reo-like virus and a parvovirus-like virus. Despite multiple detections of viruses in *Cherax* spp., there has been no molecular characterisation of any of these pathogens. Of the various viral flora identified in *Cherax* spp., four were classified as parvovirus-like. These include Cherax destructor systemic parvo-like virus, Cherax quadricarinatus gill parvo-like virus, spawner-isolated mortality like virus and Cherax quadricarinatus parvo-like virus (now Cherax quadricarinatus densovirus, CqDV). The focus of this project was to characterise, for the first time, a *Cherax* spp. infecting virus, CqDV. The isolate was obtained from the staff at the Queensland Government's former Tropical and Aquatic Animal Health Laboratory. Infected tissue was used to recreate the disease at James Cook University. As well as confirming the results of Bowater *et al.* (2002), we extended these results, characterising the tissue tropism of CqDV using quantitative real-time PCR (qPCR). We revealed that CqDV preferentially targets ectodermal tissues, consistent with histopathology observations, and that infection is systemic. CqDV was detected in the heart and muscle, most likely from infected haemocytes in the haemocoel. The genome of CqDV was sequenced using primer walking. The CqDV genome is 6,334 nucleotides in length (GenBank: KP410261) and has four open reading frames (ORFs), three (non structural proteins, NS3, NS1 and NS2) on the sense strand and one (viral protein, VP) on the anti-sense strand, indicating an ambisense organisation. Bioinformatics analysis of the ORFs identified highly conserved motifs characteristic of the family *Parvoviridae*, including endonuclease and helicase motifs in the NS1 protein and a phospholipase A<sub>2</sub> motif in the VP. Phylogenetic analysis firmly placed CqDV in the subfamily *Densovirinae*, genus *Ambidensovirus*, species *Decapod ambidensovirus*, virus variant Cherax quadricarinatus densovirus. The CqDV isolate grouped with the blattodean-infecting densoviruses but its genome was architecturally similar to the *Lipidopteran ambidensovirus 1* group. The CqDV genome shared 75 % amino acid homology across the entire genome with sea star associated densovirus (SSaDV). Although CqDV and SSaDV are phylogenetically similar, they are geographically and

environmentally distinct from each other, infecting two different orders, a unique feature not observed in the *Densovirinae* to date. Sequencing of the transcriptome revealed four introns in the NS ORFs. These introns could produce four new hypothetical proteins. These included two truncated isoforms of NS3, and one truncated isoform each of NS1 and NS2. The new hypothetical proteins were all in frame. Finally CqDV's ability to cause disease in another commercially cultured crayfish, *C. destructor* was assessed. Although qPCR was able to detect CqDV in *C. destructor* + CqDV treatment group, no clinical signs of disease were observed. Future work should investigate if CqDV is replicating in *C. destructor* and whether or not it can be re-isolated and is still infectious to *C. quadricarinatus*. Future work should also focus on characterising the protein expression of CqDV. CqDV's ability to cause disease in echinoderms and SSaDV's ability to cause disease in freshwater crayfish should also be assessed.

# TABLE OF CONTENTS

STATEMENT OF ACCESS DECLARATION .....	i
STATEMENT OF SOURCES DECLARATION .....	ii
STATEMENT OF SOURCES ELECTRONIC COPY DECLARATION .....	iii
DECLARATION OF ETHICS .....	iv
STATEMENT OF Co-AUTHORS .....	v
STATEMENT OF THE CONTRIBUTION OF OTHERS .....	vi
ACKNOWLEDGEMENTS .....	vii
ABSTRACT .....	ix
LIST OF FIGURES.....	xvii
LIST OF TABLES .....	xxi
ABBREVIATIONS .....	xxii
<b>CHAPTER 1: General introduction .....</b>	<b>1</b>
<b>1.1 Introduction .....</b>	<b>2</b>
<b>CHAPTER 2: Literature review .....</b>	<b>6</b>
<b>2.1 Introduction .....</b>	<b>7</b>
<b>2.2 <i>Parvoviridae</i> .....</b>	<b>8</b>
2.2.1 Introduction .....	8
2.2.2 Replication.....	10
2.2.3 Expression strategies of subfamily <i>Densovirinae</i> .....	10
2.2.3.1 Genus <i>Ambidensovirus</i> .....	11
2.2.3.2 Genus <i>Iteradensovirus</i> .....	14
2.2.3.3 Genus <i>Brevidensovirus</i> .....	15
2.2.3.4 Genus <i>Penstyldensovirus</i> .....	15
2.2.4 RNA interference .....	16
2.2.5 Encoded proteins in the <i>Parvoviridae</i> .....	16
2.2.5.1 Non-structural protein 3 .....	16
2.2.5.2 Non-structural protein 1 .....	17
2.2.5.3 Non-structural protein 2 .....	20
2.2.5.4 Viral protein.....	22
2.2.6 Phylogeny of the <i>Densovirinae</i> .....	24
<b>2.3 Viral flora of <i>Cherax</i> species.....</b>	<b>28</b>
2.3.1 Bacilliform virus of <i>Cherax</i> species.....	28

2.3.2 White spot syndrome virus.....	29
2.3.3 Totiviridae .....	30
2.3.4 <i>Circoviridae/Picornaviridae</i> .....	30
2.3.5 Presumptive reovirus.....	31
<b>2.4 <i>Densovirinae</i> of freshwater crustacean species .....</b>	<b>32</b>
2.4.1 <i>Densovirinae</i> of <i>Cherax</i> species .....	32
2.4.2 <i>Cherax destructor</i> systemic parvo-like virus .....	32
2.4.3 Putative gill parvovirus of <i>Cherax quadricarinatus</i> .....	33
2.4.4 Spawner isolated mortality virus .....	33
2.4.5 <i>Cherax quadricarinatus</i> parvovirus like .....	34
2.4.6 <i>Penaeus merguensis</i> densovirus.....	35
<b>2.5 <i>Densovirinae</i> of <i>Macrobrachium</i> species.....</b>	<b>35</b>
2.5.1 <i>Macrobrachium</i> hepatopancreatic parvovirus .....	35
2.5.2 <i>Penaeus stylirostris</i> penstyldensovirus of <i>Macrobrachium rosenbergii</i> .....	36
<b>2.6 Unclassified parvovirus-like pathology .....</b>	<b>37</b>
<b>2.7 Future work on characterisation of crustacean viruses .....</b>	<b>37</b>
<b>2.8 Conclusion.....</b>	<b>40</b>
<b>CHAPTER 3: General materials and methods .....</b>	<b>41</b>
<b>3.1 General husbandry of <i>Cherax</i> species .....</b>	<b>42</b>
<b>3.2 Purification of virus from <i>Cherax quadricarinatus</i> .....</b>	<b>42</b>
3.2.1 Clarified viral homogenate .....	42
3.2.2 Transmission electron microscopy .....	43
<b>3.3 Molecular biology .....</b>	<b>44</b>
3.3.1 Nucleic acid extraction.....	44
3.3.2 Polymerase chain reaction.....	44
3.3.3 Electrophoresis .....	44
3.3.4 Cloning .....	45
<b>3.4 Quantitative real-time polymerase chain reaction .....</b>	<b>45</b>
3.4.1 Preparation of synthetic control for quantitative real-time polymerase chain reaction.....	45
3.4.2 Standard curve preparation.....	46
3.4.3 SYBR green quantitative real-time polymerase chain reaction.....	47
<b>3.5 Histopathology .....</b>	<b>48</b>
<b>3.6 Bioinformatics analysis.....</b>	<b>48</b>

<b>CHAPTER 4: Tissue tropism of <i>Cherax quadricarinatus</i> densovirus using histopathology, TEM and quantitative real-time PCR</b>	<b>49</b>
<b>4.1 Introduction</b>	<b>50</b>
<b>4.2 Materials and Methods</b>	<b>51</b>
4.2.1 Experimental <i>Cherax quadricarinatus</i>	51
4.2.2 Experimental trial	51
4.2.3 Histopathology	51
4.2.4 Viral purification and transmission electron microscopy	52
4.2.5 Molecular biology	52
4.2.5.1 Nucleic acid extraction	52
4.2.5.2 Preparation of synthetic control for quantitative real-time polymerase chain reaction	52
4.2.5.3 Standard curve preparation for quantitative real-time PCR	52
4.2.5.4 Defining measurement uncertainty	52
4.2.5.5 Quantitative real-time polymerase chain reaction	53
4.2.6 Statistical analysis	53
<b>4.3 Results</b>	<b>53</b>
4.3.1 Infection trial	53
4.3.2 Histopathology	56
4.3.3 Viral purification and transmission electron microscopy	58
4.3.4 Quantitative real-time polymerase chain reaction	61
<b>4.4 Discussion</b>	<b>63</b>
4.4.1 Gross signs of disease	63
4.4.2 Histopathology	65
4.4.3 Transmission electron microscopy	65
4.4.4 Quantitative real-time polymerase chain reaction	66
<b>4.5 Conclusion</b>	<b>66</b>
<b>CHAPTER 5: First complete genome of an <i>Ambidensovirus</i>, <i>Cherax quadricarinatus</i> densovirus, from freshwater redclaw <i>Cherax quadricarinatus</i></b>	<b>67</b>
<b>5.1 Introduction</b>	<b>68</b>
<b>5.2 Materials and methods</b>	<b>69</b>
5.2.1 Purification of virus from <i>Cherax quadricarinatus</i>	69
5.2.2 Molecular biology	69
5.2.2.1 Nucleic acid extraction	69

5.2.2.2 Polymerase chain reaction .....	69
5.2.2.3 Electrophoresis.....	71
5.2.2.4 Cloning .....	71
5.2.3 Bioinformatical analysis.....	71
<b>5.3 Results .....</b>	<b>72</b>
5.3.1 Polymerase chain reaction.....	72
5.3.2 Phylogeny .....	73
5.3.3 Genome annotation .....	76
5.3.3.1 ORF 1 – NS3 equivalent.....	77
5.3.3.2 ORF 2 – NS1 equivalent.....	77
5.3.3.3 ORF 3 – NS2 equivalent.....	78
5.3.3.4 ORF 4 – VP equivalent.....	79
5.3.3.5 Inverted terminal repeats and untranslated regions.....	79
<b>5.4 Discussion.....</b>	<b>80</b>
5.4.1 Amino acid homology.....	81
5.4.2 Phylogeny .....	82
<b>5.5 Conclusion.....</b>	<b>84</b>
<b>CHAPTER 6: Partial transcriptome of <i>Cherax quadricarinatus</i></b>	
<b>densovirus.....</b>	<b>85</b>
<b>6.1 Introduction .....</b>	<b>86</b>
<b>6.2 Materials and methods .....</b>	<b>87</b>
6.2.1 <i>Cherax quadricarinatus</i> .....	87
6.2.2 Clarified homogenate.....	87
6.2.3 Infection trial .....	87
6.2.4 Molecular biology.....	88
6.2.4.1 Nucleic acid extraction.....	88
6.2.4.2 Total RNA extraction .....	89
6.2.4.3 RNA quality check .....	89
6.2.4.4 RNA ligase-mediated rapid amplification of cDNA ends polymerase chain reaction .....	89
6.2.4.5 Tetro cDNA synthesis .....	90
6.2.4.6 Polymerase chain reaction .....	90
6.2.4.7 Cloning .....	90

6.2.4.8 Preparation of synthetic control for quantitative real-time polymerase chain reaction .....	91
6.2.4.9 Standard curve preparation .....	91
6.2.4.10 Quantitative real-time polymerase chain reaction.....	91
6.2.5 Statistical analysis .....	92
<b>6.3 Results .....</b>	<b>95</b>
6.3.1 Infection trial .....	95
6.3.2 Quantitative real-time polymerase chain reaction .....	95
6.3.3 RNA quality check.....	95
6.3.4 Partial transcriptome analysis .....	97
<b>6.4 Discussion.....</b>	<b>100</b>
<b>6.5 Conclusion.....</b>	<b>102</b>
<b>CHAPTER 7: Translocation of <i>Cherax</i> species crayfish across zoogeographical zones within Australia; potential to spread highly pathogenic <i>Cherax quadricarinatus</i> densovirus .....</b>	<b>104</b>
<b>7.1 Introduction .....</b>	<b>105</b>
<b>7.2 Materials and methods .....</b>	<b>107</b>
7.2.1 Experimental <i>Cherax</i> species .....	107
7.2.2 Experimental trial .....	107
7.2.3 Histopathology.....	108
7.2.4 Molecular biology.....	108
7.2.4.1 Nucleic acid extraction.....	108
7.2.4.2 Preparation of synthetic control for quantitative real-time polymerase chain reaction .....	108
7.2.4.3 Standard curve preparation .....	108
7.2.4.4 SYBR Green quantitative real-time polymerase chain reaction.....	108
7.2.5 Statistical analysis.....	109
<b>7.3 Results .....</b>	<b>109</b>
7.3.1 Infection trial .....	109
7.3.2 Histology .....	110
7.3.3 Quantitative real-time polymerase chain reaction .....	112
<b>7.4 Discussion.....</b>	<b>113</b>
<b>7.5 Conclusion.....</b>	<b>116</b>
<b>CHAPTER 8: General discussion.....</b>	<b>117</b>

<b>8.1 Background.....</b>	<b>118</b>
<b>8.2 Results .....</b>	<b>118</b>
<b>8.3 Future work .....</b>	<b>122</b>
<b>8.4 Implications.....</b>	<b>122</b>
<b>APPENDIX 1 .....</b>	<b>124</b>
<b>Media and buffers.....</b>	<b>124</b>
<b>APPENDIX 2 .....</b>	<b>126</b>
<b>Publications.....</b>	<b>126</b>
<b>REFERENCE LIST .....</b>	<b>127</b>

## LIST OF FIGURES

- Figure 2.1: Phylogenetic analysis of full-length NS1 amino acids of the subfamily *Densovirinae* by the Maximum Likelihood method. The percentage of trees in which the associated taxa clustered together is shown on branches. Viral genera are bracketed on the right. The tree is drawn to scale, with branch lengths measured in the number of substitutions per site. Abbreviations with the Aust postscript represent Australian isolates. ....25
- Figure 4.1: Lesions of a moribund *C. quadricarinatus* infected with CqDV. A. blister filling the branchial cavity (black circles). B. arrow indicates blisters filling the branchial chamber between gill and carapace. C. the viscous, gelatinous substance that makes up the blister. D. arrows indicate the blister covers the inside of the cephalothorax, (arrow indicates blisters). E. arrows indicate white spots characteristic of moribund *C. quadricarinatus*. F. arrows point to white spots that are etched on the inside of the brachial carapace. ....55
- Figure 4.2: A. secondary gill filament (sec) (scale bar: 200µM). B. heavily infected cuticular epidermis (cep) (carapace, crp) with a lack of apoptosis (scale bar: 50µM). C. heavily infected gastric sieve (gss) (setae, ste) epidermis (epi) (scale bar: 200µM). D. midgut epithelium (emc) with infected cells (scale bar: 50µM). E. antennal gland tubules (agn) with healthy cells (scale bar: 50µM). F abdominal muscle (Mus) with infected cep (scale bar: 200µM). G. hepatopancreas (Hep) with lumen (lum) and the sinus (sin) with infected cells (scale bar: 50µM). H. sec (scale bar: 50µM). Stains: A-F H&E, G: Feulgen stain counterstained with alcoholic picric acid; H: Feulgen strain. Arrows point out basophilic inclusion bodies that are characteristic of CqDV infection.....57
- Figure 4.3: A. the first (see 3.2.2) band representing CqDV in caesium chloride. B. viral particles stained with 1% uranyle acetate with

size of capsid indicated (scale bar: 100 nm). C. insert (red box) of cluster of capsids, note the empty particle bottom right (scale bar: 25nm). .....	58
Figure 4.4: A. chromatin is being marginated (mnc) and virogenic stroma (vgs) forming (10 $\mu$ m) B. virogenic stroma is established and chromatin is fully marginated (10 $\mu$ m) C. signet ring formed with marginated nucleolus (nls) (10 $\mu$ m) D. elongated mitochondria (mca) (1 $\mu$ m) E. virogenic stroma filling the nucleus (5 $\mu$ m) F. intact infected cells with fully formed inclusion bodies (10 $\mu$ m). TEM produced from dissected gill tissue originating from a <i>C. quadricarinatus</i> experimentally infected with CqDV. ....	60
Figure 4.5: Paracrystalline arrays of CqDV (arrow) (scale bar: 1 $\mu$ m).....	61
Figure 4.6: A. average copy number mg <sup>-1</sup> of tissue from six organs ( <i>n</i> =10) with error bars showing the standard error of the mean. B. is the trellis diagram showing significant difference values of the one-way ANOVA between the various organs. ....	63
Figure 5.1: Phylogenetic analysis of full-length NS1 amino acids of the subfamily <i>Densovirinae</i> by the Maximum Likelihood method. The percentage of trees in which the associated taxa clustered together is shown on branches. Viral genera are bracketed on the right. The tree is drawn to scale, with branch lengths measured in the number of substitutions per site. Abbreviations with the Aust postscript represent Australian isolates. ....	74
Figure 5.2: Phylogenetic analysis of NS1 amino acids of the genus <i>Ambidensovirus</i> by Maximum Likelihood method. The percentage of trees in which the associated taxa clustered together is shown on branches. The tree is drawn to scale, with branch lengths measured in the number of substitutions per site.....	76
Figure 5.3: Organisation of the CqDV genome, above the line indicates top strand and below the line indicates bottom strand. Filled in boxes indicate hairpins, empty boxes indicate ORFs, bracketed numbers indicate reading frame. ORFs, UTRs and potential promoters are marked with nucleotide positions.....	77

Figure 5.4: Amino acid alignments of CqDV with AdDV and BgDV1. Metal binding domain (motif 1), endonuclease (motif 2), and helicase superfamily 3 motifs (A, B, C).....	78
Figure 5.5: Hairpin structures of CqDV. (A) Hairpin of left hand side, note the two TA nucleotides that are not complementary, blue circled A is the terminus. (B) Hairpin on the right and side, note the two AT nucleotides that are not complementary, red circled T is the terminus. The miss-matched nucleotides occur at the same position on both termini. ....	80
Figure 6.1: Left side of CqDV (between nt 1 and 3,153) showing NS genes (orange). The hairpin is marked in yellow, P3 promoter in purple, PCR primers in green and polyadenylation signal in blue. ....	93
Figure 6.2: Right side of CqDV (between nt 6,334 and 3,029) showing VP genes (orange). The hairpin is marked in yellow, P97 promoter in purple, PCR primers in green and polyadenylation signals in blue. ....	94
Figure 6.3: Viral copies $\text{mg}^{-1}$ of CqDV in gill tissue of <i>C. quadricarinatus</i> between 3 and 120 hours post-injection of clarified homogenate. There was no significant difference between time points ( $P >$ 0.05).....	95
Figure 6.4: Electropherograms of heat denatured total RNA (A, B) and non- denatured RNA (C, D). There was no difference between treatments of the RNA. A and C; B and D are paired samples of A15-052.5 and A15-052.11 respectively. Peaks 5S, 18S and 28S are at approximately nt 25, 2,000 and 4,000 respectively. X-axis represents nucleotides and the Y-axis represents sample intensity. ....	96
Figure 6.5: A. Left hand side of the CqDV genome showing hairpin (HP), promoter (P3) and NS genes. Below the solid black line are the four splices sites A, B, C and D represented by inverted triangles orientated against the NS genes above the black line. B. The sequence of the four clones showing where the splice sites were found. C. New hypothetical ORFs generated from	

splicing of the mRNA from CqDV. Superscript numbers indicate nucleotide position on the CqDV un-spliced genome. / represent the splice sites. N with subscript represents number of nucleotides between sequences presented. Underlined ATG is the start codon of NS1. Bold ATG indicates new start codons from spliced cDNA. Bold TAA indicates stop codons. ....99

Figure 7.1: Mortality of *Cherax* species over 61 days of the trial. Although the negative control *C. destructor* apparently suffered higher mortalities than the *C. destructor* + CqDV treatment, it was not statistically significant ( $P > 0.05$ ). .... 110

Figure 7.2: Epithelial cells of the three control and treatment groups. A. *C. destructor* control group did not show any lesions (long arrows). B. *C. destructor* + CqDV did not show basophilic inclusion bodies characteristic of CqDV (long arrows). C. *C. quadricarinatus* + CqDV, short arrows indicate large basophilic inclusion bodies. cep: cuticular epidermis, crp: carapace. All figures are stained with H&E. .... 111

Figure 7.3: Mean copy number of CqDV  $\text{mg}^{-1}$  of hemolymph of each treatment group. .... 112

## LIST OF TABLES

Table 2.1: Comparison of <i>Densovirinae</i> donor and acceptor sites .....	11
Table 2.2: Members of the <i>Ambidensovirus</i> that contain NLS in NS3 .....	17
Table 2.3: Heat map showing percentage of amino acids that are identical to each other between the <i>Ambidensovirus</i> NS1. Black indicates highest homology, to light grey with the least homology <sup>ab</sup> .....	27
Table 2.4: Comparison of the characterisation between penaeid-infecting <i>Densovirinae</i> and <i>Cherax</i> spp. infecting parvovirus .....	39
Table 3.1: Primers used to create the real time clone and run SYBR Green qPCR .....	47
Table 4.1: Measurement uncertainty of qPCR for detecting CqDV, Taura syndrome virus (TSV); yellow head virus (YHV); <i>Penaeus</i> <i>stylirostris</i> penstyldensoviurs (PstDV); white spot syndrome virus (WSSV). .....	62
Table 5.1: Primers used to sequence the CqDV genome .....	70
Table 5.2: Sequences used to construct phylogenetic tree .....	72
Table 5.3: Percentage of amino acids that are identical between the <i>Ambidensovirus</i> NS1 including CqDV and echinoderm sequences <sup>ab</sup> .....	75
Table 5.4: Motifs present in uncharacterized echinoderm densovirus.....	84
Table 6.1: Experimental design of <i>C. quadricarinatus</i> randomly distributed in three systems. ....	88
Table 6.2: Primers used in the investigation of the CqDV transcriptome .....	92
Table 6.3: Comparison of <i>Densovirinae</i> donor and acceptor sites of the NS genes.....	97
Table 7.1: Distribution of crayfish in CqDV infection trial.....	107
Table 8.1: Comparison of the characterisation between penaeid infecting <i>Densovirinae</i> and <i>Cherax</i> spp. infecting parvovirus showing the knowledge gaps in CqDV filled by this study.....	121

## ABBREVIATIONS

BLAST	Basic local alignment search tool
bp	Base pair
cDNA	Complementary DNA
DNA	Deoxyribonucleic acid
ITR	Inverted terminal repeat
kb	Kilobase (kbp = 1,000 base pairs)
mRNA	Messenger RNA
NCBI	National Center for Biotechnology Information
NLS	Nuclear location signal
NS	Non-structural protein of parvovirus
nt	Nucleotide
ORFs	Open reading frames
PCR	Polymerase chain reaction
PLA <sub>2</sub>	Phospholipase A2 motif
qPCR	Quantitative real-time polymerase chain reaction
RCR	Rolling circle replication
RIN	RNA integrity number
RLM-RACE	RNA ligase mediated rapid amplification of cDNA ends
RNA	ribonucleic acid
RNAi	RNA interference
RT-PCR	Reverse transcriptase polymerase chain reaction
ssDNA	Single stranded DNA
TAAHL	Tropical and aquatic animal health laboratory
UTR	Untranslated region
VP	Viral capsid protein of parvovirus
VP1	The largest VP, encodes a unique region at its C terminus
5'	5 prime (directionality of DNA and RNA)
3'	3 prime (directionality of DNA and RNA)

## **CHAPTER 1: General introduction**

## 1.1 Introduction

*Cherax quadricarinatus*, commonly known as redclaw crayfish, are a member of the *Parastacidae*, which have a restricted distribution to the southern hemisphere.

*C. quadricarinatus* are native to the tropical freshwater streams and rivers of Queensland, Cape York Peninsula, Northern Territory and Papua New Guinea (Jones, 1990). Within *Cherax*, three species are commercially cultured in Australia. They are *C. quadricarinatus* in northern Australia, *C. tenuimanus* in south-western Australia (given that *C. tenuimanus* and *C. cainii* are closely related (Munasinghe *et al.*, 2004), and previous literature may have used incorrect nomenclature, I have used the *C. tenuimanus*, which has been used in the literature) and *C. destructor* in south-eastern and western Australia. Production systems are purpose-built earthen ponds or agricultural farm dams and culture is considered semi-intensive (Merrick and Lambert, 1991). *C. quadricarinatus* have also been exported overseas for culture (Jones *et al.*, 1994).

Viral diseases of crustaceans have only been known for the past fifty years. The first crustacean virus was visualised using transmission electron microscopy (TEM) in *Macropipus depurator* (Vago, 1966). In subsequent years, Bonami and Vago (1971) visualised via TEM, a new virus in *M. depurator* that was found to be different to the virus identified by Vago (1966). Then in 1974 the first virus of penaeid prawns, *Penaeus duorarum*, was identified (Couch, 1974b) and partially characterised (Couch, 1974a). Since these initial reports, a large number of viruses have been identified and characterised in penaeid prawns (Lightner *et al.*, 1983; Lightner and Redman, 1985; Bonami *et al.*, 1990; Boonyaratpalin *et al.*, 1993; Bonami *et al.*, 1995; Overstreet *et al.*, 1997; Chang *et al.*, 1998; La Fauce *et al.*, 2007; Mello *et al.*, 2011). In contrast, pathogens of cultured freshwater crayfish in Australia remain poorly studied.

Early reports on disease in Australian crayfish were observational in nature. Typically, fresh mounts, squash preparations and histopathology were used to opportunistically search for pathogens. These investigations found fungi, ciliates, platyhelminthes and nematodes (Carstairs, 1978; Herbert, 1987). The first virus of *Cherax* spp. identified in Australia was a subclinical baculovirus (Anderson and Prior, 1992). Since then, many

pathogens have been observed including *Cherax* Giardavirus-like virus (Edgerton *et al.*, 1994), vibriosis (Eaves and Ketterer, 1994), *Cherax quadricarinatus* bacilliform virus (Edgerton, 1996), *Coxiella rickettsia* (Tan and Owens, 2000), presumptive hepatopancreatic reovirus (Edgerton *et al.*, 2000; Hayakijkosol and Owens, 2011) and presumptive *Circoviridae* or *Picornaviridae* (Jones and Lawrence, 2001). Surveys have also identified pathological lesions of interest in cultured freshwater crayfish in Australia (Edgerton and Owens, 1999; Jones and Lawrence, 2001). To date, four parvovirus-like pathogens have been observed in Australian freshwater crayfish.

The family *Parvoviridae* are small, isometric, non-enveloped viruses that contain a linear single stranded DNA and have a wide host range. The viral genome is 4 to 6 kilobases (kb) and is characterised as having 3 to 5 genes bracketed by self-priming hairpins (Tattersall, 2008). The family *Parvoviridae* is divided into two sub-families, the subfamily *Parvovirinae* that infect the vertebrates and the subfamily *Densovirinae* that infect the arthropods (Bergoin and Tijssen, 2008; Tattersall, 2008; Cotmore *et al.*, 2013).

*Densovirinae* are a major concern to the commercial rearing of insects and penaeid crustaceans (Bonami *et al.*, 1990; La Fauce *et al.*, 2007; Liu *et al.*, 2011). Clinical signs of infection include lethargy, anorexia, paralysis, melanisation, inhibition of moulting and metamorphosis and uniquely to *Cherax quadricarinatus* parvo-like virus (CqPV), inner branchial membrane blistering (Bowater *et al.*, 2002; Bergoin and Tijssen, 2008). Histopathology is generally characterised by hypertrophied and densely stained nuclei (Shike *et al.*, 2000).

The subfamilies in the family *Parvoviridae* share a similar genome organisation. The left side of the genome, or the 5' half, codes for the non-structural (NS) genes while the right side or the 3' half, codes for the viral protein (VP) genes. The genus *Ambidensovirus* within the subfamily *Densovirinae* are unique as they have coding regions on both strands of ssDNA. By convention, the top strand codes for the NS genes so that they are on the left side, while the bottom strand, codes for the VP genes on the right side of the genome. There is little sequence homology between members of the *Parvoviridae*, with the exception of a few enzyme motifs (Bergoin and Tijssen, 2008).

The NS genes of the *Parvoviridae* are multifunctional proteins that carry out a wide range of tasks during the viral lifecycle. Non-structural protein 1 (NS1), encodes highly conserved endonuclease and helicase amino acid motifs that play a role in viral replication and host cell damage (Ilyina and Koonin, 1992; Koonin, 1993; Op De Beeck and Caillet-Fauquet, 1997; Hickman and Dyda, 2005). The function of non-structural protein 2 (NS2) remains poorly understood. Members of the genus *Ambidensovirus* also encode a unique protein, non-structural protein 3 (NS3). It is believed that NS3 has a role in viral DNA replication (Abd-Alla *et al.*, 2004). The viral proteins have many functions, including effecting cell entry (Zádori *et al.*, 2001) and nuclear location (Vihinen-Ranta *et al.*, 2002).

There have been four parvoviruses reported in *Cherax* spp. using histopathology and TEM. The first parvovirus-like pathology was seen in a single moribund *C. destructor* opportunistically collected from a pond side and the virus was designated *Cherax destructor systemic parvo-like virus* (CdSPV) (Edgerton *et al.*, 1997). The second parvo-like virus was found in *C. quadricarinatus* supplied from a commercial farm in northern Australia after a (GAV) (penaeid infecting virus) challenge experiment (Edgerton *et al.*, 2000). The third *Cherax* spp. parvo-like virus was identified using spawner-isolated mortality virus (suspected parvo-like virus of penaeids) specific *in situ* probe, which returned a positive result (Owens and McElnea, 2000). To date, none of these viruses have been isolated and used to recreate disease.

The most rigorously studied *C. quadricarinatus* virus is CqPV. Over four months, an epizootic occurred in juvenile and adult *C. quadricarinatus*. Histopathology of moribund *C. quadricarinatus* found early stage eosinophilic and late stage basophilic inclusions with hypertrophic nuclei. The inclusions stained Feulgen positive indicating DNA. Infection was systemic, infecting cuticular epithelium, foregut, midgut and hindgut epithelium, connective tissue, antennal gland, haematopoietic tissue, epithelial cells of the seminiferous tubules and interstitial tissue of the ovary. TEM of infected tissue revealed a non-enveloped hexagonal particle with a mean diameter of 19.5 nm. Clarified homogenate was used to successfully recreate the disease in healthy *C. quadricarinatus*. The injected *C. quadricarinatus* displayed the same symptoms and histopathology as the infected, farmed *C. quadricarinatus*. The only notable difference was the blistering of the inner-branchial membrane observed in *C. quadricarinatus*

injected with CqPV (Bowater *et al.*, 2002).

There is a dearth of information on the pathogens that infect *Cherax* species. Almost all of the studies involving *Cherax* spp. pathogens are opportunistic and observational. Histopathology and TEM have been used to place the pathogens in high-level taxonomic groups because molecular characterisation has not been attempted. The prevalence, distribution and impact on culture of these pathogens in Australia is currently unknown; though, with the exception of CqPV, there are no reports suggesting that these pathogens can cause epizootics in cultured freshwater crayfish.

The aim of this research thesis is to characterise the pathogen reported by Bowater *et al.* (2002). The pathogen was provided by the staff of the Queensland Government's former Tropical and Aquatic Animal Health Laboratory. We set out to 1. recreate the disease in healthy *C. quadricarinatus*, confirm the results of Bowater *et al.* (2002) and characterise the tissue tropism using quantitative real-time PCR; 2. sequence the genome of CqPV and propose a formal taxonomic position using the method of Cotmore *et al.* (2013); 3. characterise the transcriptome of CqPV and 4. assess CqPV's ability to cause disease in other commercially cultured *Cherax* species. This will be the first parvo-like virus to be characterised from *Cherax* spp. and will lead to a faster response time should this pathogen become an issue once more in cultured *C. quadricarinatus*.

## **CHAPTER 2: Literature review**

## 2.1 Introduction

Crustacean aquaculture production was 6.4 million tonnes or 10 % of global aquaculture in 2012 (FAO). Viral disease such as *Penaeus stylirostris penstyldensovirus 1* (PstDV1) (formally *Penaeus stylirostris densovirus*, infectious hypodermal and hematopoietic necrosis virus, see Cotmore *et al.* (2013) for most recent taxonomy) (Lightner *et al.*, 1983), yellow head virus (YHV) (Boonyaratpalin *et al.*, 1993), *Penaeus merguensis* hependensovirus (PmeDV) (formally *Penaeus merguensis densovirus*, hepatopancreatic parvovirus) (Bonami *et al.*, 1995; La Fauce and Owens, 2007), white spot syndrome virus (WSSV) (Chang *et al.*, 1998), Taura syndrome virus (TSV) (Overstreet *et al.*, 1997) and more recently infectious myonecrosis virus (IMNV) (Mello *et al.*, 2011) have all caused significant losses and continue to be a major inhibitory factor in penaeid production (Flegel, 2012).

Australia has a burgeoning freshwater crustacean aquaculture industry. There are several geographically distinct species cultured in varying culture systems. Species include *Cherax quadricarinatus* (redclaw) in northern Australia (Ghanawi and Saoud, 2012), *C. destructor* (yabbies) in southern Australia (Mills and McCloud, 1983), and *C. tenuimanus* (marron) in south-western Australia (Morrissy, 1979). These species are the main freshwater crayfish species cultured in Australia (Jones *et al.*, 1994).

Production began in 1984 with 8 tonnes, reaching a combined peak production in 2003 of 564 tonnes. Since then, production has steadily declined to 140 tonnes in 2013 (FAO). Although not commercially cultured in Australia, *Macrobrachium rosenbergii* is also an important freshwater species cultured overseas (Lin and Boonyaratpalin, 1988). These species are cultured in earthen ponds with varying input from farmers. *C. quadricarinatus* is the only species that is produced in Australia using intensive commercial hatchery techniques. These fresh water species are marketed at restaurants and by the aquarium trade. Like the penaeid prawn industry, the freshwater crustacean industry has viral disease issues.

Diseases of freshwater crustaceans have been sporadic. Many of the viral diseases reported in Australia are case studies of individuals and rarely of epizootics. The viral diseases associated with freshwater crayfish have been poorly studied, with

histopathology being the main detection tool. Viral diseases include *Cherax* bacilliform virus (Anderson and Prior, 1992; Edgerton, 1996), *Cherax* Giadivirus-like virus (Edgerton *et al.*, 1994), *Cherax* destructor systemic parvo-like virus (Edgerton *et al.*, 1997), presumptive hepatopancreatic reovirus and putative gill parvovirus (Edgerton *et al.*, 2000), presumptive spawner-isolated mortality virus (Owens and McElnea, 2000), presumptive *Circoviridae* or *Picornaviridae* (Jones and Lawrence, 2001), and *Cherax* quadricarinatus parvo-like virus (CqPV) (Bowater *et al.*, 2002). With the exception of the hepatopancreatic reovirus and CqPV, most viruses have not been purified and characterised but remain a concern to the industry as the instances of disease is likely to increase with the intensification of the industry (Edgerton *et al.*, 2002). This is best illustrated by the development of the penaeid prawn industry, which has suffered considerable setbacks due to viral disease and the lack of diagnostics in its infancy (Lightner and Redman, 1998).

In order for the Australian freshwater crayfish industry to progress, development of detection and surveillance tools for the purposes of biosecurity need to be addressed. Viral isolation and purification for the purposes of sequencing viral genomes will greatly aid in the characterisation of viral pathogens. Such information can be used to develop diagnostic tools that can help produce specific pathogen free stock for the industry. Knowledge of viral aetiology will also aid in biosecurity protocols that can reduce the spread of viral disease. This review will focus on parvoviruses, particularly CqPV (Bowater *et al.*, 2002) as this virus caused an epizootic, is partially characterised and viral material is available for further work. To date, the only sequence data on any viral genomes that infect Australian freshwater crustaceans comes from *Macrobrachium rosenbergii* nodavirus (Hayakijkosol *et al.*, 2012).

## ***2.2 Parvoviridae***

### **2.2.1 Introduction**

The family *Parvoviridae* are small isometric non-enveloped, linear ssDNA viruses that have a wide host range. The viral genome is between 4 and 6 kb and is characterised by self-priming hairpins. Hairpins are essential for the unique rolling-hairpin replication

that define the replication strategy of this group of viruses (Tattersall, 2008). The family are classified into two subfamilies, the subfamily *Parvovirinae* infecting vertebrates and the subfamily *Densovirinae* infecting arthropods (Tattersall, 2008; Cotmore *et al.*, 2013). The new taxonomy proposed by Cotmore *et al.* (2013) suggest that the subfamily *Densovirinae* be broken into the following genera; *Ambidensovirus*, *Brevidensovirus*, *Hepandensovirus*, *Iteradensovirus* and *Penstyldensovirus*. Of these, the *Hepandensovirus* and *Penstyldensovirus* are pathogenic to crustaceans. This review will focus on the *Densovirinae*, using examples from the *Parvoviridae* when necessary.

Of importance to this review are the subfamily *Densovirinae* and the strictly aquatic animal infecting densovirus. Important viruses to crustacean aquaculture include the genera *Hepandensovirus* and *Penstyldensovirus* which are pathogenic to commercially important crustaceans such as the penaeids (Lightner *et al.*, 1983; Bonami *et al.*, 1995) causing substantial losses (Lightner *et al.*, 1983; Lightner and Redman, 1985; Shike *et al.*, 2000). The only other known densovirus to infect a marine invertebrate is the sea star-associated densovirus (SSaDV) which is the suggested agent of sea-star wasting disease (Hewson *et al.*, 2014). Clinical signs of parvovirus infection include, but are not limited to lethargy, anorexia, paralysis, slow melanization and inhibition of moulting and metamorphosis (Bergoin and Tijssen, 2008) and uniquely to CqPV, inner brachial membrane blistering (Bowater *et al.*, 2002). Histological examination shows hypertrophied and densely stained nuclei (Shike *et al.*, 2000).

Members of the family *Parvoviridae* share a similar genome organisation. By convention, the non-structural (NS) genes are coded on the left half of the genome and the viral protein (VP) genes are coded on the right half of the sense orientation of the single strand of DNA. The genus *Ambidensovirus* are unique as they have coding regions on both strands of ssDNA, hence the ‘Ambi’ prefix. In this instance, the sense strand, codes for the NS genes on the left half and the anti-sense codes for VP genes on the right half. Viruses of the genus *Ambidensovirus* package both strands in separate capsids in equimolecular ratios (Tijssen *et al.*, 2006) and also encode the unique NS3 gene. There is little nucleotide homology between the subfamilies (Bergoin and Tijssen, 2008).

### 2.2.2 Replication

Parvovirus replication resembles rolling circle replication of bacteriophage and is called rolling hairpin replication in parvovirus biology. The model of replication has been established using members of the *Parvovirinae*, but as they share similar homotelomeric and heterotelomeric hairpins, replication is most likely functionally similar in the *Densovirinae*. The model was first proposed by Tattersall and Ward (1976) using Minute Virus of Mice (MVM). The 3' hairpin directs synthesis, filling in the gap between the 3' and 5' hairpin (the majority of the coding capacity of the genome). The 5' hairpin is melted and copied on the new 3'-5' DNA strand. The newly copied hairpin folds back onto its self, allowing synthesis to continue and at the same time displacing the original strand. This produces a concatemer of genomes that can continue synthesising new genomes. The concatemer can grow to a tetramer intermediate at which point a single strand nick is introduced by NS1 at the 5' end of a genome within the tetramer. The ssDNA is displaced by the continued copying of the genome from the now free 3' -OH. Non-structural protein 1 (NS1) remains attached to the end of the 5' nicked ssDNA and a separate NS1 packages the genome into the pre-formed capsid in a 3'-5' orientation, using the helicase function of NS1 (King *et al.*, 2001). Nicking at both ends of homotelomeric hairpins allows equimolar ratios of genome packaging, while only the 3' end can be nicked in heterotelomeric hairpins (Cotmore and Tattersall, 2014). In a new cell, the genome is released in the 3'-5' orientation (Cotmore *et al.*, 2010), exposing the 3' end to host machinery, synthesising the initial duplex that leads to the transcription of NS transcripts (Cotmore and Tattersall, 2013). Once NS1 is translated, it then regulates transcription from the promoters found on the parvovirus genome (Doerig *et al.*, 1990; Yang *et al.*, 2008).

### 2.2.3 Expression strategies of subfamily *Densovirinae*

Although varied, the splicing and leaky scanning mechanism of translation allow the compact genome of the *Densovirinae* to increase its' coding capacity. The splicing eliminates the need for multiple mRNA leader sequences before each gene and can generate new open reading frames (ORFs) from the same DNA sequence. The conserved sequences of the donor and acceptor sites have been calculated for eukaryotic

proteins. The consensus donor and acceptor sites are AG/GTAAGT and a pyrimidine (C/T) rich tract followed by CAG/G respectively (Shapiro and Senapathy, 1987). The donor and acceptor sites of the *Densovirinae* described are presented in Table 2.1. The leaking scanning of start codons also allows the *Densovirinae* to translate multiple proteins from a single mRNA. Together these multicistronic RNAs save space on the genome, and have most likely contributed to the compact genomes.

Table 2.1: Comparison of *Densovirinae* donor and acceptor sites

Species (accession number)	Gene	Donor site	nt position	Acceptor site	nt position
Consensus <sup>a</sup>		AG/GTAAGT <sup>b</sup>	NA	CAG/N	NA
PfdV (AB028936)	NS3	AC/AAAGCT	312	TAT/A	1120
	VP	GT/GTAAGT	4991	TTT/A	4785
	VP	TA/ATCTAC	4553	TGA/C	4397
BgDV (AY189948)	NS3/NS1 + NS2	AG/GTACGT	275	GAG/A	1699
	VP	CA/ATACGG	4425	TAG/G	4192
	VP	AA/ATATGC	4417	TAG/G	4192
CpDV (FJ810126)	NS1	CG/GTAAGT	1721	CAG/A	1774
GmDV (L32896)	NS3	AG/GTATGT	655	CAG/A	1362
JcDV (S47266)	NS3	GG/TATGTC	564	AGA/T	1254
MIDV (AY461507)	NS3	AG/GTATGT	653	CAG/A	1356
AdDV (HQ827781)	NS3	AG/TAGAAG	241	CCG/T	840
	VP	AG/GTGCAG	4758	TTT/C	4405
	VP	TC/CGGTAC	4535	TTT/C	4406
	VP	AC/GTGAGT	4434	CAG/A	4259
PstDV1 (AF273215)	NS1	AT/GTAAGT	288	CAG/A	423

<sup>a</sup> Shapiro and Senapathy, 1987

<sup>b</sup> / indicates splice site

### 2.2.3.1 Genus *Ambidensovirus*

Within in the genus *Ambidensovirus* there are various strategies to express proteins during the viral lifecycle. Three transcriptomes have been sequenced in the species *Lepidopteran ambidensovirus 1*; *Galleria mellonella* densovirus (GmDV) (L32896) (Tijssen *et al.*, 2003), *Mythimna loreyi* densovirus (MIDV) (AY461507) (Fédière *et al.*, 2004) and *Junonia coenia* densovirus (JcDV) (S47266) (Wang *et al.*, 2013). Northern blotting demonstrated that these genomes produce two NS transcripts of approximately 2.5 and 1.8 kb and a single viral protein (VP) transcript of 2.6 kb. Splicing of the larger NS transcript produces the 1.8 kb transcript by removing an intron containing the NS3 ORF. Uniquely, the JcDV intron removes the A from the NS1 ATG start codon. The splicing leaves the NS1 start codons in an unfavorable context for translation (incomplete Kozak consensus sequence (Kozak, 1995)), leading to leaky scanning translation of NS1 while NS2 is in a more favorable context. The larger unspliced

transcript has more favorable context around the first start codon (Kozak, 1986) leading to NS3 translation only.

A single large ORF encodes the VP of these genomes and produces a single unspliced VP transcript. The 3' end of GmDV, MIDV and JcDV NS and VP transcripts overlapped by 60, 57 and 61 nucleotides (nt) respectively, though the significance of this is unknown. Expression of the GmDV, MIDV and JcDV VP ORFs in baculovirus expression systems yielded four proteins that were able to auto-assemble into capsids indistinguishable from wild type capsids. This data suggest that the VPs are translated from a single transcript via leaky scanning mechanism. In the case of JcDV, this was confirmed by removing the first in frame start codon, resulting in VP 2-4 expression only (Croizier et al., 2000). The genome of *Pseudoplusia includens* densovirus PiDV (JX645046) shares approximately 80% sequence similarity to GmDV and MIDV. The transcriptome of PiDV has been hypothesized to be the same as GmDV and MIDV (Huynh et al., 2012) as its splicing sites are conserved on the PiDV genome and are therefore most likely functional.

The species *Dipteran ambidensovirus 1* have a similar expression strategy as above as the NS transcript is spliced and the VP transcript is not. *Culex pipens* densovirus (CpDV) (FJ810126) produces two NS transcripts of 2.4 and 1.8 kb and a single VP of 2.3 kb. However, unlike species *Lepidopteran ambidensovirus 1*, the start sites for the NS transcripts are not the same. The 2.4 kb transcript starts at nt 416 while the 1.8 kb transcript starts at nt 1,045. The splicing occurs at the same place on both NS mRNAs between nt 1,721 and 1,773. The splicing brings in frame NS1 and 2 N- and C-terminal sequences. The VP transcript starts at nt 4,961, 3 nt downstream of the second ATG start codon and is unspliced but overlaps with the NS transcript by 12 nt. The first start codon is at nt 4,985, but this is only 1 nt downstream of the promoter at 4,986-4,991 (Baquerizo-Audiot et al., 2009). As this start codon is so close to the promoter, Baquerizo-Audiot et al. (2009) suggested that the ribosome bypassed this start codon in favor of the second. However, *Acheta domesticus* densovirus (AdDV) only has a single nt between the promoter and the start of the VP yet produces a VP mRNA transcript (see below). SDS-PAGE analysis of the CpDV proteins showed 4 structural proteins, however, VP4 is too small to form part of the capsid and was suggested to be a product of proteolytic cleavage from a larger VP.

Unlike the species *Lepidopteran ambidensovirus 1* and the species *Dipteran ambidensovirus 1*, species *Blattodean ambidensovirus 1*; *Periplaneta fuliginosa* densovirus (PfdV) (AB028936), *Blattella germanica* densovirus (BgDV) (AY189948) and species *Orthopteran ambidensovirus 1* (AdDV) (HQ827781) have multiple spliced mRNA variants of both the NS and VP transcripts. The BgDV genome produced 5 NS transcripts detected by northern blotting. Sequencing of the respective cDNA revealed a large 2.3 kb NS transcript that produced NS3. A smaller 1.6 kb spliced variant of the large NS transcript produced NS1 and 2. Translation of NS1 and 2 occurred through leaky scanning, with the NS1 start codon in an unfavorable context compared to NS2. Unlike GmDV and MIDV, BgDV also had an 872 nt spliced variant which produced the C terminal end of NS1 only. The significance of this is unknown. These 3 transcripts overlapped the VP transcript by 48 nt. Two additional large transcripts of 3.9 and 3.2 kb were also detected. These transcripts overlapped the VP transcript by 1,650 nt. The BgDV VP transcript was also spliced to produce two transcripts. The unspliced ORF1 transcript produced the largest VP, VP2, while the smaller spliced transcript produced VP1 from the first in frame start codon and VP3 via leaky scanning at the second in frame start codon (Kapelinskaya *et al.*, 2011).

Although architecturally similar, the PfdV (AB028936) genome produces more VP mRNA variants. Sequencing of the VP cDNA produced 2 abundant transcripts and at least 6 other low abundant mRNAs. The splicing connected the two major VP ORFs together resulting in a new larger ORF. Together the splicing produced 5 structural proteins (Yamagishi *et al.*, 1999). Like other densovirus, two NS mRNA transcripts of 2.6 and 1.9 kb were found upon northern blotting of RNA and overlap the VP transcript by 7 nt. The larger of the two transcripts directs synthesis of NS3 while the smaller NS1 and 2. Like GmDV and MIDV, the first in-frame start codon of NS1 is in an unfavorable context compared to the NS2 start codon. Thus NS1 and NS2 are translated by a leaky scanning mechanism (Yang *et al.*, 2008).

Like GmDV, and MIDV, northern blotting of AdDV RNA revealed two NS transcripts of 2.5 and 1.8 kb and a single VP band of 2.5 kb. The large transcript coded for NS3 while the smaller spliced variant removed much of NS3 and coded for NS1 and 2 via leaky scanning mechanism. The VP transcript started at nt 5,236 within the promoter

element and 1 nt downstream of this promoter is the first start codon. Liu *et al.* (2011) proposed that the short 5' untranslated region (UTR) lead to leaky scanning of this start codon. Upon cloning of the VP transcript, 3 spliced variants were found which overlapped the NS transcript by 34 nt. The large unspliced transcript coded by the larger ORF A translated VP2. A 175 nt splice between nt 4,260-4,434 removed the N terminus of ORF A and the C terminus of ORF B, bringing the two ORFs in frame and producing VP1. The smaller transcripts removed the C terminus of ORF B lead to leaky scanning of VP 2, 3 and 4. The expression strategy of these VPs is different to that of the species *Lepidopteran ambidensovirus 1*, and more closely resemble that of the vertebrate parvoviruses (Cassinotti *et al.*, 1988; Berns, 1990).

#### 2.2.3.2 Genus *Iteradensovirus*

Transcriptome analysis has been completed on five *Iteradensovirus* genomes. Unlike other member of the *Densovirinae*, *Papilio polyxenes* densovirus (PpDV) (JX110122), *Sibine fusca* densovirus (SfDV) (JX020762), *Casphalia extranea* densovirus (CeDV) (AF375296), *Bombyx mori* densovirus (BmDV) (AY033435), and *Dendrolimus punctatus* densovirus (DpIDV) (KF963252) do not have spliced genomes. Northern blotting of the PpDV RNA extracts showed 2.3 kb and 2.0 kb bands representing the NS and VP mRNAs. Cloning of the cDNA revealed two separate bands for NS1 and NS2 driven by a single promoter. The 5' UTR of the NS1 transcript was 3-4 nt long, making it less likely to be transcribed efficiently except for SfDV, which had an extra transcription start site 26 nt upstream of the NS1 start codon. This was confirmed by the difficulty the authors had in obtaining NS1 related 5' RACE products. The NS2 transcripts started with CAGT 118 nt (CeDV, SfDV and DpIDV) or 124 nt (BmDV and PpDV) up-stream of the NS2 start codon and had favorable Kozak sequence. Both NS1 and 2 shared the same polyadenylation signal downstream of the VP promoter. Because of this, there was a 9-12 nt overlap between the NS and VP transcripts. The VP 5' UTR was also short, (between 11-14 nt) with an unfavorable Kozak sequence much like the *Lepidopteran ambidensovirus 1* and is likely to generate leaky scanning of the VP genes (Yu and Tijssen, 2014). Although not sequenced yet, alignments of HaDV2 (HQ613271) and DpDV (AY665654) found the conserved CAGT sequence in the latter while HaDV2 had AAGT at the same position. VP promoters and NS and VP

polyadenylation signals are in a similar pattern to the other five genomes, it likely that DpDV shares a similar transcription map.

#### 2.2.3.3 Genus *Brevidensovirus*

The transcriptome map of *Dipteran brevidensovirus 2*, *Aedes albopictus* densovirus (AalDV2) (X74945) is similar to that of the *Iteradenosovirus* transcriptome maps as the genome is not spliced. There were two NS transcripts but these were driven by individual promoters. Northern blotting showed a NS specific 3.4 kb band and VP specific 3.4 and 1.3 kb bands. Analysis of mutants showed NS1 was expressed from promoter P7 with transcription starting at CAGT, 6 nt upstream of the NS1 start codon. NS2 was expressed from the P7.4 promoter 11 nt downstream of P7, with NS2 transcription starting at CAGT, 68 nt upstream of the NS2 start codon which also had a favorable Kozak sequence. The VP transcript starts at CAGT, 158 nt upstream of the VP start codon. Both the NS and VP transcripts use the same polyadenylation signal at 3,662 and terminate at 3,680. Pham *et al.* (2013) noted that no clear TAT like motif could be found for the VP; however, at 2,410 there is a TATAAAT promoter sequence which is 23 nt up stream from the start of the VP transcript. This promoter is most likely the functional promoter that drives VP transcription.

#### 2.2.3.4 Genus *Penstyldensovirus*

The only transcriptome to be sequenced from the *Penstyldensovirus* is species *Decapod penstyldensovirus 1* (PstDV1) (AF273215). This virus has caused significant economic damage to the aquaculture of prawns (Lightner *et al.*, 1983). Northern blotting of total RNA revealed 5 bands of 4.1, 0.9, 2.6, 1.9, and 1.3 kb, the latter three representing predicted sizes of the left, middle and right ORFs of PstDV1. The 4.1 and 0.9 kb transcript were positive for PstDV1 but their origin is unknown. The 135 nt splice between nt 288-422 creates a frame shift that results in translation of NS1. NS2 is produced from its own transcript that originates at either nt 466 or 467, which has a moderately strong Kozak sequence. Although not experimentally demonstrated, it is likely that leaky scanning of the single VP transcript produces capsid proteins of PstDV1 (Dhar *et al.*, 2010).

## 2.2.4 RNA interference

The RNA transcripts of all the *Ambidensovirus* sequenced have overlapping RNA transcripts that may play a part in the life cycle of these viruses through the RNA interference (RNAi) pathway. The RNAi pathway is an intracellular mechanism, which is proposed as an antiviral pathway in plants (Baulcombe, 2004) and arthropods (Robalino *et al.*, 2004; Robalino *et al.*, 2005). The pathways involve a stepwise process of recognition and cleavage of dsRNA and the loading of the cleaved dsRNA into a RNA-induced silencing complex (RISC) (see Zamore *et al.* (2000), Pillai *et al.* (2007), Obbard *et al.* (2009), and La Fauce and Owens (2012) for reviews). The various pathways are activated by a distinct RNA species, use different enzymes and proteins and are located in different parts of the cell. Kapelinskaya *et al.* (2011) suggest the overlap in the transcripts of BgDV creates a dsRNA that may be loaded into one of these pathways. Furthermore, microRNAs have been identified on the *Aedes aegypti* densovirus (AaeDV) genome (Wang *et al.*, 2015). The fate of these virus-derived dsRNAs needs further investigation to identify if they play a role the infectious lifecycle of these viruses.

## 2.2.5 Encoded proteins in the *Parvoviridae*

### 2.2.5.1 Non-structural protein 3

The genus *Ambidensovirus* are unique among the family *Parvoviridae* as they encode an ambisense genome and a unique NS3 gene at the start of their genome. Bioinformatical analysis of PfDV NS3 has found metal binding and zinc finger motifs of DNA binding proteins (Yamagishi *et al.*, 1999), although protein BLASTs show very little homology to any known protein. Studies of site-specific mutants of JcDV NS3 resulted in negative ELISAs for viral particles compared to positive controls on Ld 652 cells and in *Spodoptera littoralis* larvae. Replicative form DNA was also assayed by Southern blot; the NS3 mutant infected cells did not produce any detectible replicative form DNA while viral DNA synthesis was clearly observed in infected control cells. Infection was recovered with the addition of JcDV and MIDV NS3 expressing plasmids. The data clearly demonstrate that NS3 is required for viral DNA replication in

Ld 652 cells and *S. littoralis* larvae and that the NS3 proteins of different densoviruses have similar functions (Abd-Alla *et al.*, 2004).

Western blots of BgDV found that NS3 was predominantly located in the nucleus (Martynova *et al.*, 2014), supporting the previous results that NS3 is involved in replication which takes place in the nucleus. Bioinformatical analysis of BgDV did not find a nuclear location signal and it is not known how NS3 moves into the nucleus. However, Martynova *et al.* (2014) noted that the size of BgDV NS3 was slightly larger than expected and that might be a result of posttranslational modification. However, further investigation of NS3 amino acids of the genus *Ambidensovirus* identified several putative NLSs that would allow NS3 to translocate into the nucleus (Table 2.2). Similar bioinformatics results have been found by Owens (2013) who identified a number of putative NLS in the genomes of PstDV and PmeDV. Mutational studies are needed to identify if these NLSs are functional.

Table 2.2: Members of the *Ambidensovirus* that contain NLS in NS3

Accession number	Species	Virus abbreviation	Sequence
KM052275	Unclassified <sup>a</sup>	SSaDV	<sup>130</sup> PPKKKV
JX645046	<i>Lepidopteran ambidensovirus 1</i>	PiDV	<sup>204</sup> PNNKRRK
L32896	<i>Lepidopteran ambidensovirus 1</i>	GmDV	<sup>203</sup> PNNKQRRY
S47266	<i>Lepidopteran ambidensovirus 1</i>	JcDV	<sup>157</sup> PNKKRRY
AY461507	<i>Lepidopteran ambidensovirus 1</i>	MIDV	<sup>203</sup> PNKKRRY
JQ894784	<i>Lepidopteran ambidensovirus 1</i>	HaDV	<sup>203</sup> PNKKRRY

<sup>a</sup> most likely an *Ambidensovirus* member

#### 2.2.5.2 Non-structural protein 1

The non-structural proteins of the family *Parvoviridae* are multifunctional proteins that carry out a wide variety of tasks during the viral lifecycle. Although the nomenclature is similar between the subfamily *Parvovirinae* and subfamily *Densovirinae*, they share very little nucleotide homology. However, the *Parvoviridae* have two conserved endonuclease and helicase amino acid motifs that perform various roles during the viral lifecycle.

The endonuclease motif of NS1 plays a role in viral replication and host cell damage. Alignments of known rolling circle replication (RCR) initiator proteins have revealed

three conserved motifs (motif 1, 2 and 3) that are involved in rolling circle replication (Ilyina and Koonin, 1992). Two of these motifs have been identified (motif 2 and 3) in the *Parvoviridae*. The two H motif (HuHuuu, where 'u' is any bulky hydrophobic residue) is thought to be a metalloenzyme that binds a copper ion, and requires  $Mg^{2+}$  or  $Mn^{2+}$  to catalyse its reaction. The second motif is the active site Y, which together with the two H motif, nick the viral DNA. Experimental mutation of these amino acid motifs in the MVM NS1 protein demonstrated that these motifs are absolutely required for site-specific nicking of viral origin DNA (Nüesch et al., 1995). Once nicked, the NS1 protein covalently links to the 5' end, leaving the 3' hydroxyl end to be extended by host DNA polymerase. Replication is initiated from the 3' hairpin creating a complementary strand that forms the basis of the replicative form of the viral DNA. Genomes are then excised from the concatemer with the introduction of a site and strand specific nick by NS1 as previously described (section 2.2.2) (see Berns (1990), Cotmore and Tattersall (1996), Cotmore and Tattersall (2014)). Purified baculovirus-expressed N terminal fusion recombinant proteins of PfDV were assayed with a 5'-hexachloro fluorescein probe 1 containing NS1 binding sequences and a 3'-hexachloro fluorescein probe 2 that did not contain the NS1 binding site, to determine endonuclease activity. The results indicated that the PfDV NS1 was able to cleave probe 1 containing the NS1 binding sequence (Han et al., 2013).

The endonuclease function of NS1 also affects the host cell. Transformed rat fibroblasts expressing MVM NS1 were used to demonstrate that NS1 was able to interfere with host cell DNA replication and caused nicks in the host chromatin that was hypothesised to be a result of the NS1 endonuclease. Together these functions of NS1 led to an arrest of transformed cells in S phase (Op De Beeck and Caillet-Fauquet, 1997) allowing for viral DNA propagation. These results were substantiated in HepG2 expressing mutated B19 NS1 (metal binding motif) using a baculovirus expression system. Using a single-cell neutral and alkaline gel electrophoresis (comet) assay, DNA damage was assessed and shown to occur less in mutant NS1 compared to wild type B19 NS1. The damage was attributed to single stand breaks, an attribute of NS1 during viral DNA replication. Furthermore, the accumulated DNA damage led to apoptotic cell death (Kivovich et al., 2012). These results demonstrate that the endonuclease function of NS1 during viral DNA replication has the ability to damage host DNA, affect cell cycle progression and is functionally conserved among the family *Parvoviridae*.

The helicase function of NS1 is also highly conserved in NS1 of the *Parvoviridae* and belongs to the superfamily 3 (SF3) helicases (Gorbalenya *et al.*, 1990; Koonin, 1993). The SF3 helicases are encoded by small DNA and RNA viruses and contain three Walker-type motifs A, B and C (Koonin, 1993). Helicases are ATP-dependent enzymes that unwind duplex DNA for DNA replication (Hickman and Dyda, 2005). ATPase activity has been assessed using purified MVM NS1 and was shown to hydrolyse labelled ( $\gamma$ -<sup>32</sup>P)ATP. Helicase function was also assessed using a radiolabelled oligodeoxynucleotide annealed to ssDNA. Incubation of MVM purified NS1 and the substrate showed that the labelled oligonucleotide was displaced (Wilson *et al.*, 1991). Similar results were obtained with baculovirus expressed and purified mutant and wild type PfDV NS1. Using a colorimetric assay to detect inorganic phosphate released from ATP in combination with ssDNA, Yang *et al.* (2006) demonstrated that wild type NS1 ATPase was stimulated while mutant NS1 could not be stimulated. Next, a displacement assay (a 28-mer substrate with annealed primer) was used to assess helicase activity in the presence of mutant and wild type NS1. Gel electrophoresis showed that NS1 wild type successfully unwound the primer from the substrate while the mutants failed to displace the primer. The wild type NS1 also specifically interacted with (CAC)<sub>x4</sub> sequence of the inverted terminal repeat (ITR) and most likely facilitated strand displacement for replication. Although the endonuclease and helicase domains represent the major functions of NS1, the protein has many other functions that aid in the viral lifecycle.

As well as its role in DNA replication, NS1 also interacts with cellular factors and can affect the host cell environment (Labow *et al.*, 1987; Momoeda *et al.*, 1994). Parvovirus B19 can initiate apoptosis in erythroleukemia K562 and mega-karyocytic UT/-7/Epo cell lines. NS1 was stably maintained in these cells and expression induced by isopropyl  $\beta$ -D-1-thiogalactopyranoside (IPTG). Induction of NS1 resulted in chromatin condensation, cell rounding, cytoplasmic blebbing and DNA fragmentation. Terminal deoxynucleotidyl transferase dUTP nick-end labelling (TUNEL) staining identified cells with fragmented nuclear DNA, hallmarks of cellular apoptosis. Mutation of the NS1 helicase domain resulted in significantly reduced apoptosis (Moffatt *et al.*, 1998). However this study also demonstrated that wild-type NS1 was able to activate caspase 3 which led to apoptosis, though the mechanism of activation is unknown (Moffatt *et al.*,

1998). These results were similar to Ohshima *et al.* (1998) who used parvovirus H1 to infect C6 rat glioblastoma cells. Using caspase 1 and caspase 3 inhibitors Ac-YVAD-CHO and Ac-DEVD-CHO respectively, apoptosis was demonstrated to be caspase 3 – dependent.

Luciferase reporter plasmids under control of either RNA polymerase II or T7 RNA polymerase promoters were used to assay the effect of PfdV NS1 on luciferase expressions on Sf9 cells. The results showed that NS1 only inhibited the RNA polymerase II promoter (Yang *et al.*, 2009). To further identify the specific area of NS1 protein that caused the inhibition, two plasmids were constructed, either with NS1 N-terminal half (DNA binding domain) or the C- terminal half (ATPase motif). These plasmids were co-transfected with the reporter plasmid in Sf9 cells. A decrease in luciferase was only recorded in the plasmid with the C- terminal half. The ATPase motif of this plasmid was then mutated and the experiment repeated. The mutated ATPase motif containing plasmid was incapable of inhibiting luciferase. The results indicate that NS1 can inhibit protein synthesis and is dependent on ATP binding activity of NS1. When NS1 was co-expressed with PfdV NS2 and NS3, cell necrosis was observed as a result of a loss of mitochondrial trans-membrane potential and progressive ATP depletion. These results are similar to that of Nykky *et al.* (2014) who used confocal microscopy to demonstrate canine parvovirus was associated with mitochondria throughout infection and sometimes inside the mitochondria. During early infection, loss of membrane potential was counteracted by extracellular regulated kinases 1 and 2 which inhibited intrinsic mitochondria-dependent apoptosis. However, once NS1 was expressed, depolarisation of the mitochondria could not be stopped and resulted in cell death. These results demonstrate that NS1 is a pleiotropic protein which has a complex relationship with the host cell. It induces cytotoxic effects in a variety of ways, by disrupting the mitochondrion, *trans* activation of host cell factors that facilitate apoptosis, and degradation of the host cell chromatin, ultimately leading to cellular death.

#### 2.2.5.3 Non-structural protein 2

The function of NS2 of the subfamily *Densovirinae* is poorly understood and little is known about the role NS2 plays in viral propagation. The study of NS2 mutant

parvovirus has provided an insight into the role NS2 plays in the lifecycle of parvoviruses. Murine A9 (normal MVM<sub>p</sub> host cell), Simian Virus 40-transformed newborn human kidney cell line 324K and 4 other cell lines were used to assay the effect of mutant NS2 on the lifecycle of MVM. Plaquing ability of NS2 mutants were reduced 3 to 4 orders of magnitude on A9 cells compared to 324K cells (though plaque morphologies varied between mutants) while wild-type MVM plaqued similarly on both. NS2 mutant monomer replicative form and ssDNA were reduced compared to wild-type infection after release into S phase on A9 cells. On 324K cells mutant NS2 replicated its monomer replicative form DNA to wild-type levels, although there was a reduction in accumulation of progeny single strand DNA. This data suggests that NS2 is involved in replication of the viral genome (Naeger *et al.*, 1990). Like mutant MVM, NS2 mutant H1 was not able to replicate efficiently in host rat fibroblasts with comparatively less ssDNA to wild-type. However, viral RNA was at wild-type levels, yet the level of capsid protein VP2 compared to wild-type was reduced (Li and Rhode 3rd, 1991). Like mutant H1, there is no effect to viral RNA transcription in NS2 mutants of MVM vs wild-type MVM on A9. Despite this, translation of viral proteins, particularly the capsid protein, is significantly less in NS2 mutants compared to wild-type MVM. However, on 324K, the ratio of RNA to protein was similar to that of wild-type MVM (Naeger *et al.*, 1993). To investigate the role NS2 plays post-transcription a luciferase gene was added to the H1 capsid protein under control of P38 and the 3' UTR was sequentially deleted. The results indicate that the 3' UTR is essential for NS2 dependent protein synthesis (Li and Rhode 3rd, 1993). However, in pulse-chase experiments on 324K, MVM NS2 mutant infected cells showed comparable VP synthesis to wild-type, but that assembly of the VP proteins was defective. These experiments demonstrate that NS2 has a role in viral assembly (Cotmore *et al.*, 1997).

Compared to the *Parvovirinae*, very little work has been done to characterise NS2 in the *Densovirinae*. Experiments with NS2 mutants of the *Densovirinae* have demonstrated similar results to those of *Parvovirinae*. Experiments by Azarkh *et al.* (2008) using AeDNV have shown that NS2 has a nuclear location signal (NLS) and is located in the nucleus early in infection and in the cytoplasm late in infection. The authors created a NS2-null mutant and infected C6/36 cells. Viral capsid synthesis was detected using immunofluorescence antibody assay in both NS2 mutants and wild-type infections. However, analysis of viral DNA using qPCR revealed a 52-fold decrease in total viral

DNA copies in lysates and a 41-fold decrease in viral encapsidated DNA. The results demonstrate, that like MVM, NS2 plays a role in viral replication, though it is unclear if it is translation of viral mRNA and/or assembly of the capsid that is affected by a mutant NS2 phenotype.

#### 2.2.5.4 Viral protein

The tough viral capsid encapsulates the viral genome protecting it from the elements. The capsid is made of 60 overlapping proteins generally designated VP1-4. Transcriptional regulation and post-transcriptional modification from one or two capsid proteins produce the varying VP1-4 proteins (Simpson *et al.*, 1998; Hueffer and Parrish, 2003). VP1 (the largest VP) encodes a unique region (VP1u) at its N terminal end that encodes motifs essential for the viral lifecycle and host tropism. This region is externalized during entry, which facilitates successful infection.

The phospholipase A<sub>2</sub> (PLA<sub>2</sub>) motif has a calcium-binding loop and a catalytic site that are conserved among both the subfamily *Parvovirinae* and members of the genus *Ambidensovirus* and *Iteradensovirus* (Zádori *et al.*, 2001). The PLA<sub>2</sub> is positioned on the inside of the capsid of MVM and PPV. Alkali denaturation and renaturation and heat shock were used on purified capsid to assess the activity PLA<sub>2</sub> using mixed micelles assay. The PLA<sub>2</sub> activity was 50-100 fold higher for alkali treatment and 20-50 times higher after heat shock. Mutational studies demonstrate that the PLA<sub>2</sub> is required for endosomal escape into the cytosol. These results are supported by Farr *et al.* (2005) who used adenovirus and polyethyleneimine (PEI) (transfection reagent) to rescue PLA<sub>2</sub> mutant MVM infections in cell culture. Their results indicate that MVM, PEI and adenovirus need to be trapped in the same endosome, resulting in the release of the PLA<sub>2</sub> mutant MVM from the endosome.

There are conflicting reports on the location of B19 VP1u (and thus PLA<sub>2</sub>) during infection. VP1u of B19 was expressed in bacteria with the resulting fusion proteins used to immunise rabbits. The rabbit antisera was used in western blots against serum-derived viral capsids and baculovirus-derived capsids. The antisera immunoprecipitated both types of capsids. The results indicated that B19 VP1u is on the outside of the capsid prior to internalisation (Rosenfeld *et al.*, 1992). Contrary to this, Ros *et al.*

(2006) used monoclonal antibodies (MAb 1417-1) directed against the B19 VP1u residues 30 to 42 and a monoclonal antibody against intact capsids (MAb 850-55D) to show that the VP1u was internal. Furthermore, like MVM, heat treatment of intact capsids increased the reactivity of MAb 1417-1. Although initially internal, the B19 VP1u becomes external during primary attachment before internalisation unlike MVM. Leisi *et al.* (2013) used a recombinant protein spanning the first N terminal 160 amino acids to demonstrate that VP1u first binds to the outside of the cell (UT7/Epo cells) and then is internalised. A truncated VP1u, delta 128 (removal of amino acids 128-160, the PLA<sub>2</sub>) was used to investigate if the PLA<sub>2</sub> domain played a role in internalisation. Immunoflorescent staining demonstrated that the truncated VP1u of B19 was not internalised in the absence of the PLA<sub>2</sub> confirming previous results that the PLA<sub>2</sub> is required downstream in the infection pathway. It is not known how parvovirus that do not code a PLA<sub>2</sub> escape the endosome.

The VP1u contains basic amino acids that are homologous to NLSs. The NLSs are thought to move the capsid into the nucleus of the cell to begin replication and are found in both the *Parvovirinae* and *Densovirinae*. CPV VP1 N terminus is positioned on the inside of the capsid. Antibodies directed against VP1u at 1, 4 and 8 hours post infection show that at 4 and 8 hours, VP1u can be detected around and inside the nucleus (Vihinen-Ranta *et al.*, 2002). These results suggest that during infection, a conformational change occurs, exposing the VP1u to the cellular environment. Co-injection of capsids and antibodies reduced transport of the capsid to the nucleus. Furthermore, mutation of the NLS diminished infectivity of CPV, indicating that the N terminus of VP1 has a role to play in viral entry to the nucleus (Vihinen-Ranta *et al.*, 2002). These results are supported by Lombardo *et al.* (2002) who used several mutant strains of MVM to study NLSs and a nuclear localization motif (NLM) found in VP1 and VP2. They found that the BC1 and to a lesser extent BC2 (the first and second set of basic amino acids on the N terminal end of VP1) and NLM (at the C terminal end) act independently to move VP1 into the nucleus, while NLM is used to move single VP2 proteins into the nucleus. Mutational studies also demonstrated that the VP1/2 oligomer requires BC1, BC2 and NLM to move into the nucleus.

*Densovirinae* also code NLS on their VPs. HeLa cells were transfected using a BgDV VP1-GFP fusion protein under the control of the cytomegalovirus promoter.

Immunohistochemistry demonstrated that the BgDV VP1 protein was strictly nuclear (Kozlova and Mukha, 2015). However, not all parvovirus have a NLS in their VPs. A bioinformatical analysis by Owens (2013) suggested that PstDV does not have a functional NLS as evidenced by the lack of capsids in the nucleus and eosinophilic staining. The nuclear pore is approximately 25-27 nm (Feldherr *et al.*, 1984; Dworetzky *et al.*, 1988), large enough for a parvovirus capsid to move through the pore unassisted.

### **2.2.6 Phylogeny of the *Densovirinae***

The phylogeny of the *Parvoviridae* is constantly being updated as more genomes are sequenced and characterised. The nomenclature governing the writing of *Parvoviridae* names is that the name of the host the virus infects is not italicised as per Cotmore *et al.* (2013) and will be followed in this thesis. For inclusion into the family, the genomes must meet certain criteria set out by the International Committee on Taxonomy of Viruses (ICTV). These include: 1. the viral particle has been isolated from an unambiguous host; 2. the genome has been sequenced; 3. the genome is non-segmented and contains non-structural and viral particle coding regions that meets the required size constraints and organisation; 4. conserved motif patterns are consistent with that of a parvovirus; and 5. observed epizootic and experimentally induced mortalities are compatible with dissemination by infection (Cotmore *et al.*, 2013). The phylogeny of the *Parvoviridae* is displayed in Figure 2.1. This data has been collated from the accession numbers provided by Cotmore *et al.* (2013) and the evolutionary history was inferred by using the Maximum Likelihood method based on the JTT matrix-based model (Jones *et al.*, 1992). The tree with the highest log likelihood (-10506.8125) is shown for the amino acid homology of NS1 subfamily *Densovirinae*. Initial tree(s) for the heuristic search were obtained automatically by applying Neighbor-Join and BioNJ algorithms to a matrix of pairwise distances estimated using a JTT model, and then selecting the topology with superior log likelihood value. The analysis involved 37 amino acid sequences (SSaDV, KM052275 was included because it affects marine invertebrates). All positions containing gaps and missing data were eliminated. There were a total of 254 positions in the final dataset. Evolutionary analyses were conducted in MEGA6 (Tamura *et al.*, 2013).

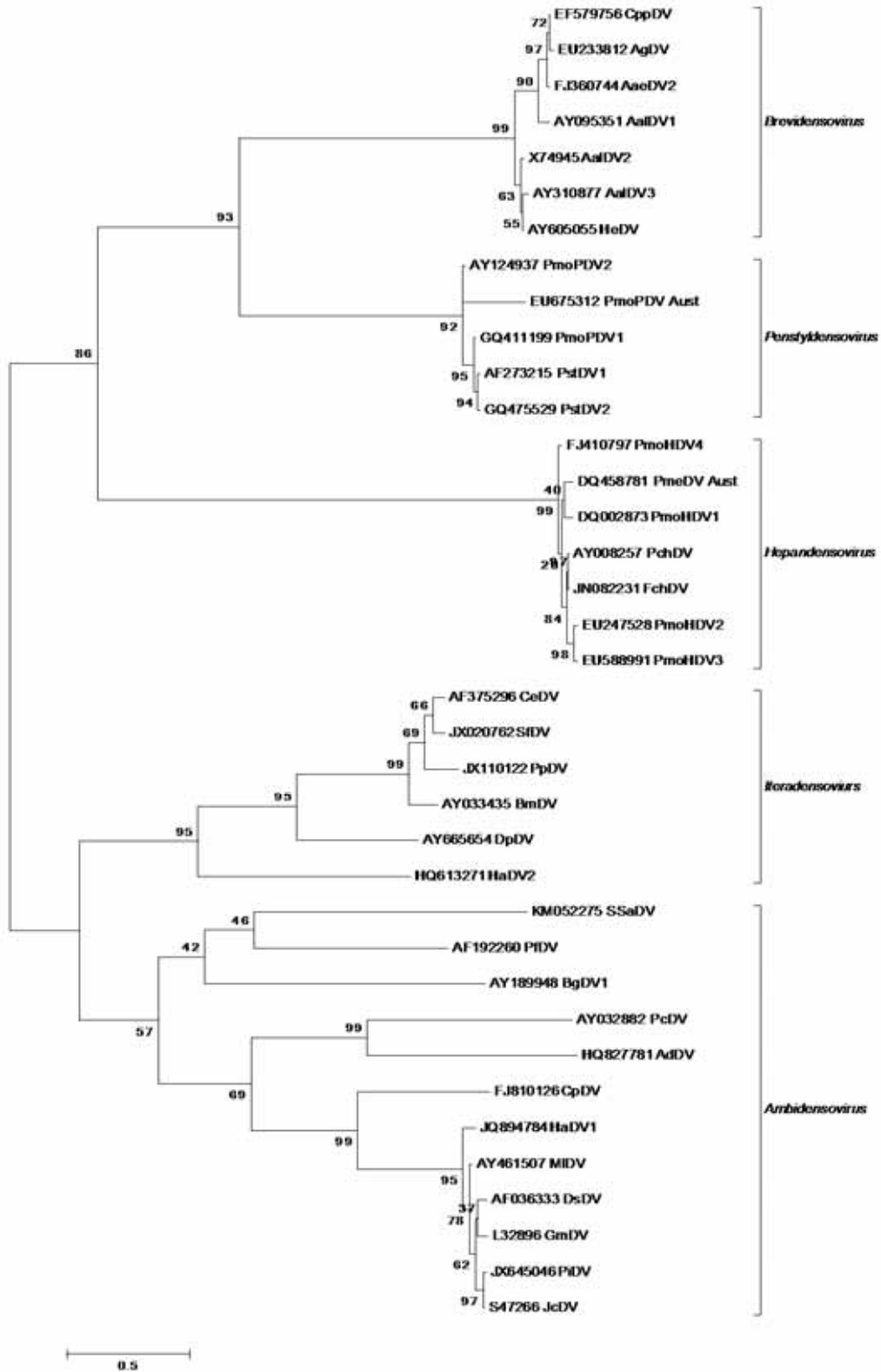


Figure 2.1: Phylogenetic analysis of full-length NS1 amino acids of the subfamily *Densovirinae* by the Maximum Likelihood method. The percentage of trees in which the associated taxa clustered together is shown on branches. Viral genera are bracketed on the right. The tree is drawn to scale, with branch lengths measured in the number of substitutions per site. Abbreviations with the Aust postscript represent Australian isolates.

The genomes in each genus are architecturally similar in their organisation with the exception of the *Ambidensovirus*. Within the *Ambidensovirus*, PfDV, BgDV1, PcDV, and AdDV share the same organisation, having a split ORF that codes for the VP. The CpDV and closely related HaDV1, MIDV, DsDV, GmDV, PiDV and JcDV share a single ORF for their VPs. SSaDV is unique in this respect, as it groups closer with the first group (split VP ORF) yet has a single ORF coding for the VP. Table 2.3 displays the percentage of bases that are identical within the genera *Ambidensovirus*. The architecturally similar viruses share greater than 87 % amino acid homology while SSaDV shares 19 to 28 % homology with the split ORF group. The SSaDV is also associated with sea star wasting disease (Hewson *et al.*, 2014), making this virus the first marine infecting *Ambidensovirus*.

Most *Densovirinae* have a highly specific host range with few exceptions. The MIDV can infect *Spodoptera littoralis*, *Pectinophora gossypiella*, *Sesamia cretica*, *Chilo agamemnon*, and *Ostrinia nubilalis* (Fédière *et al.*, 2004). PfDV can infect various members of the genus *Periplaneta*, while JcDV can infect various members of the order *Lepidoptera* (Bergoin and Tijssen, 2008). The crustacean virus PstDV infects various species of penaeid prawn including *Penaeus stylirostris* which is highly susceptible while *P. vannamei* and *P. monodon* are less susceptible (Bell and Lightner, 1984). With the exception of SSaDV, host tropism does not extend outside of the host order, even between somewhat related *Densovirinae* genomes. However, SSaDV has a wide host range, infecting at least two families, *Asteriidae* and *Asterinidae*, and at least twenty different species of asteroid (Hewson *et al.*, 2014), a unique feature among the *Densovirinae*.

Table 2.3: Heat map showing percentage of amino acids that are identical to each other between the *Ambidensovirus* NS1. Black indicates highest homology, to light grey with the least homology<sup>ab</sup>

	PcDV	AdDV	CpDV	HaDV1	DsDV	PiDV	JcDV	GmDV	MIDV	SSaDV	BgDV1	PfDV
PcDV		35	24.5	25.9	25.5	25.9	26.1	26.1	26.9	21.5	23.1	25.3
AdDV	35		25.8	26.2	26	25.8	26.2	24.8	26	19.9	21.7	22.8
CpDV	24.5	25.8		48.6	49.6	49.3	49.6	49.3	50.2	24.9	24.9	25.6
HaDV1	25.9	26.2	48.6		87.9	87.7	88.4	87.2	90.3	27.3	27.1	28.4
DsDV	25.5	26	49.6	87.9		92.3	92.8	92.1	92.5	27.7	27.1	27.9
PiDV	25.9	25.8	49.3	87.7	92.3		97.6	92.8	93.4	27.8	27.1	28.4
JcDV	26.1	26.2	49.6	88.4	92.8	97.6		92.7	93.9	28	27.1	28.1
GmDV	26.1	24.8	49.3	87.2	92.1	92.8	92.7		94.1	27.7	27.1	28.8
MIDV	26.9	26	50.2	90.3	92.5	93.4	93.9	94.1		27	27.5	28.3
SSaDV	21.5	19.9	24.9	27.3	27.7	27.8	28	27.7	27		26.5	28
BgDV1	23.1	21.7	24.9	27.1	27.1	27.1	27.1	27.1	27.5	26.5		29.4
PfDV	25.3	22.8	25.6	28.4	27.9	28.4	28.1	28.8	28.3	28	29.4	

<sup>a</sup> Accession numbers for genomes are presented in Figure 2.1

<sup>b</sup> Heat map reproduced from Geneious 6.1.8

## 2.3 Viral flora of *Cherax* species

Combined culture of *P. monodon*, *P. vannamei*, *P. japonicus* and *P. stylirostris* was \$ (USD) 21.1 billion in 2013 (FAO). However, aquaculture of marine prawns has been affected by many viral pathogens. Viruses include PstDV1 (Lightner *et al.*, 1983), YHV (Boonyaratpalin *et al.*, 1993), PmeDV (Bonami *et al.*, 1995; La Fauce *et al.*, 2007), WSSV (Chang *et al.*, 1998), TSV (Overstreet *et al.*, 1997) and more recently IMNV (Mello *et al.*, 2011). These virus have caused significant losses and continue to be a major inhibitory factor in penaeid production (Flegel, 2012). Although comparatively small, the growth of the fresh water crayfish aquaculture industry will likely be associated with an increase in disease outbreaks (Edgerton *et al.*, 2002).

Combined culture of *C. destructor*, *C. tenuimanus*, and *C. quadricarinatus* was comparatively low at \$ (USD) 3.9 million in 2013. Like the marine prawns, many pathogens have been reported in cultured freshwater crayfish. However, most diseases of crayfish are not isolated and in some cases, reported for individual crayfish only. Pathogens include bacteria, fungi, and epibionts (see Herbert (1987) and Longshaw (2011) for review). The information on viral disease in freshwater crayfish is severely lacking, with histology being the main tool used for detection and diagnosis. This review will detail the viral pathogens of the *Cherax* spp. The *Densovirinae* will be reviewed under section 2.4 *Densovirinae* of freshwater crustacean species.

### 2.3.1 Bacilliform virus of *Cherax* species

The first case of disease in commercially cultured *Cherax* spp. in Australia came from routine histology. Farmed *C. quadricarinatus* were found with hypertrophied amorphous eosinophilic inclusion in hepatopancreatic epithelial cells. Examination by TEM revealed a rod shaped  $34 \times 154$  nm nucleocapsid which was assigned *Cherax quadricarinatus* baculovirus (now bacilliform virus) (CqBV) (Anderson and Prior, 1992).

Second and third generation *C. quadricarinatus* originating from Australia and grown in California USA, were examined during routine histology. Like the Australian

*C. quadricarinatus*, these specimens presented similar pathology to CqBV of Australia. The enveloped CqBV-like virion, 47 nm × 216 nm, was considerably larger than that found in Australia but infected the same tissue with the same histological changes (Groff *et al.*, 1993). Hauck *et al.* (2001) also reported that juvenile *C. quadricarinatus* from Utah submitted for routine histology had the same histological changes though the nucleocapsid was 38 nm × 180 nm. CqBV was identified in Australia again in 1996 from farmed *C. quadricarinatus* and presented the same histopathological changes. However, TEM of this virus showed the nucleocapsid was closer in size as that reported by Groff at 53.3 nm × 212.2 nm (Edgerton, 1996; Edgerton and Owens, 1999). Based on the TEM of these viruses, it is likely that there are at least two strains of CqBV; however, molecular techniques are needed to confirm this. There are conflicting reports on the virulence of CqBV, with Anderson and Prior (1992), Hauck *et al.* (2001) and Romero and Jiménez (2002) reporting that CqBV was not associated with morbidity or mortality, contrary to Groff *et al.* (1993), Edgerton *et al.* (1995) and Edgerton *et al.* (2002) who reported poor health and mortality attributed to CqBV.

A single case of bacilliform virus has been reported in *C. destructor*. Like CqBV, *Cherax destructor* bacilliform virus (CdBV) infected the hepatopancreatic epithelium. Histopathological changes were described as above and TEM found a 49 x 263 nm nucleocapsid. The health status of the *C. destructor* were not reported (Edgerton, 1996). There have been no further reports of CdBV published.

### **2.3.2 White spot syndrome virus**

White spot syndrome virus is highly virulent to prawns and is found in many crustacean species (Stentiford *et al.*, 2009). Infection trials have been carried out with WSSV and *Cherax* species. *C. destructor* was challenged with the Thai isolate from *P. monodon* by intramuscular injection and oral feeding of infected *P. monodon*. Mortality of the WSSV injected group was 100 % 3 days post-injection. Histopathological changes were found in *C. destructor* that were consistent with WSSV infection (Edgerton, 2004). The two replicates that were fed WSSV-infected tissue were less susceptible. During the trial, water temperature dropped to 16 °C for 24 hours inducing stress in one replicate. This was the only replicate to show histopathological changes consistent with WSSV

infection. The remaining *C. destructor* orally challenged showed no WSSV infection but suffered high mortality that could not be attributed to a cause (Edgerton, 2004).

Infection trials with *C. quadricarinatus* have produced similar results. Intramuscular injection of WSSV into *C. quadricarinatus* produced between 82 – 100 % mortality over 12 days. TEM of haemolymph showed WSSV capsids while *in situ* hybridization was positive in WSSV injected groups but negative in control groups (Shi *et al.*, 2000). However, false positive PCR results have been demonstrated using OIE listed WSSV primers (Claydon *et al.*, 2004). Taken together, the results suggest that *Cherax* spp. are susceptible to WSSV and could potentially become carriers of WSSV.

### **2.3.3 Totiviridae**

The *Totiviridae* are dsRNA viruses that are associated with protozoan hosts and have been found to infect penaeid prawns (Poulos *et al.*, 2006). The first report of *Cherax* Giardiavirus (CGV) came from farmed *C. quadricarinatus* during a survey of northern Queensland farms. Histological changes in the hepatopancreas included mildly hypertrophic nuclei with amorphous nuclear inclusion that stained eosinophilic (presumed early stage) or purple-red (presumed late stage) using hematoxylin and eosin. When stained with acridine orange, nuclei were yellow-green indicating dsRNA. TEM of inclusions identified a 25 nm icosahedral capsid arranged in paracrystalline arrays within the nucleus. The prevalence of CGV was up to 52 % in the seven farms surveyed, though the lesion was not associated with clinical signs of infection. An association between mortality and CGV could not be firmly established (Edgerton *et al.*, 1994). However, intensity of infection was much higher in juvenile *C. quadricarinatus* compared to adults (Edgerton and Owens, 1997). Between 1992 and 1996 CGV was reported to increase in intensity in farms surveyed (Edgerton and Owens, 1999).

### **2.3.4 Circoviridae/Picornaviridae**

A CGV-like virus has also been found in *C. albidus*. Histological changes were similar to those described above and TEM found a 13-19 nm virion in paracrystalline arrays (Jones and Lawrence, 2001). The *C. albidus* CGV-like virus was also associated with an

isolated mortality event. The distribution of *C. albidus* CGV-like virus was wide spread in dams in Western Australia, but with low prevalence. The authors suggest the pathogen as either a *Circoviridae* or *Picornaviridae*. Without proper characterisation, it is difficult to assign the virus a taxonomic rank.

### 2.3.5 Presumptive reovirus

A transmission trial was undertaken to investigate the pathogenesis of gill-associated virus (GAV) to *C. quadricarinatus*. *C. quadricarinatus* used in the trial suffered chronic mortalities leading up to and during the trial. This batch of *C. quadricarinatus* was also associated with mortalities in the holding tanks at the farm. Histopathological investigation of a single *C. quadricarinatus* from this group revealed cytoplasmic inclusions in hepatopancreatocytes at or near the distal tips of tubules throughout the hepatopancreas. TEM of the lesion revealed a virogenic stroma containing hexagonal and pentagonal viral particles of 35-40 nm. The particle was suggested to be a reovirus. The chronic mortalities could not be singularly attributed to the reovirus as bacteraemia and a parvovirus were also found in this batch of *C. quadricarinatus* (Edgerton *et al.*, 2000).

Transmission trials with a presumptive reovirus were carried out. Histologically positive *C. quadricarinatus* had their hepatopancreai removed and viral isolation performed. TEM of the extract revealed a capsid size of 50 nm. The clarified homogenate was injected into grossly normal *C. quadricarinatus* or *C. quadricarinatus* were orally challenged with infected hepatopancreas. *C. quadricarinatus* injected with the extract suffered 20 % mortality though histopathological examination revealed only 3 % of hepatopancreatic tubules showed presumptive reovirus-like lesions. Orally challenged *C. quadricarinatus* suffered 5% mortality but 27 % of tubules were histologically positive for presumptive reovirus-like lesions. Reverse transcription-PCR (RT-PCR) using reovirus-specific primers did not amplify any reovirus (Hayakijkosol and Owens, 2011). Further characterisation of the presumptive reovirus is needed to confirm the viruses' taxonomic standing and its impact on the culture of *C. quadricarinatus*.

## **2.4 *Densovirinae* of freshwater crustacean species**

### **2.4.1 *Densovirinae* of *Cherax* species**

*Densovirinae* infection is characterised by a hypertrophied nuclei with a haloed inclusion body consisting of virogenic stroma containing virions upon histological and TEM examination. Gross signs of infection vary depending on species infected, but can include lethargy, anorexia, paralysis, inhibition of moulting and metamorphosis, poor growth, reduced preening activity and increased surface fouling (Bell and Lightner, 1984; Lightner and Redman, 1985; Bergoin and Tijssen, 2008). *Densovirinae* members characterised from penaeid prawns include PstDV1 (Lightner *et al.*, 1983) PmeDV (Bonami *et al.*, 1995; La Fauce *et al.*, 2007). These viruses have caused significant losses and continue to be a major inhibitory factor in penaeid production (Flegel, 2012). Instances of parvovirus-like pathology have been recorded in farmed *Cherax* spp. though these have not been as well characterised and their prevalence, distribution and effect on the commercial culture of *Cherax* spp. remains unknown.

### **2.4.2 *Cherax destructor* systemic parvo-like virus**

*Cherax destructor* systemic parvo-like virus (CdSPV) was the first parvovirus reported in a *Cherax* spp. The description came from a single moribund *C. destructor* collected opportunistically at the side of a pond. The *C. destructor* was moribund and exhibited patches of opaque musculature. Histopathological examination revealed hypertrophied nuclei with eosinophilic Cowdry Type A inclusions. The inclusions were reported as Feulgen negative. Extensive necrosis of gill tissue was observed, characterised by masses of pyknotic and karyorrhectic nuclei, melanisation and hypertrophied inclusions were also observed in gill tissue. Hypertrophied inclusions was also observed in the hepatopancreas, intestinal tissue, endothelial cells and hindgut myoepithelial cells, epicardium, abdominal muscle and spongy connective tissue. TEM showed Cowdry Type A inclusion in hypertrophied nuclei. The chromatin was marginated and rarefied and the viroplasm was associated with the nucleolus but centrally located with a halo. Icosahedral capsids were observed in the viroplasm and were between 17 and 20 nm (Edgerton *et al.*, 1997). The virus was not isolated nor was there any reports of a further

investigation at the farm. It is also unclear if CdSPV caused the morbidity as Edgerton *et al.* (1997) noted large numbers of bacteria during histology observations. Since the original report from south Australia, parvo-like pathology has not been observed in *C. destructor*, despite extensive routine disease surveillance of farmed *Cherax* spp. in Western Australia (Jones and Lawrence, 2001).

#### **2.4.3 Putative gill parvovirus of *Cherax quadricarinatus***

A putative gill parvovirus was discovered during a failed transmission trial using GAV. Leading up to and during the trial, *C. quadricarinatus* were lethargic and suffered chronic mortality. Histopathological investigations found a common lesion in both injected and control *C. quadricarinatus* that was not consistent with GAV.

Histopathology of gill epithelial nuclei showed hypertrophic nuclei that were either empty or slightly basophilic. TEM showed marginated chromatin and nucleoli. Capsids of 20 nm were scattered throughout a centrally located viroplasm (Edgerton *et al.*, 2000). From these observations the virus was tentatively assigned as parvovirus-like. No attempt was made to purify the virus, recreate disease, or characterize the genome of the pathogen. The TEM of this virus and CdSPV are not similar, with the viroplasm of this virus was not associated with the nucleolus as it is in CdSPV. It was not reported if the putative gill parvovirus was systemic.

#### **2.4.4 Spawner isolated mortality virus**

Spawner-isolated mortality virus (SMV) was first reported in wild caught female *P. monodon* brood stock in 1993. The spawners suffered high mortality with gross signs of disease including lethargy, failure to feed, redness of carapace and pleopods. Infection trials with clarified homogenate were able to replicate the disease in *P. monodon*. TEM of infected *P. monodon* revealed a 20 nm icosahedral virion (Fraser and Owens, 1996). In 1996 SMV was found to be associated with midcrop mortality syndrome as infected *P. monodon* tested positive to an SMV gene probe (Owens *et al.*, 1998).

*C. quadricarinatus* suffering high mortality, low yield and stress-related mortalities in a single pond were investigated. Histological analysis did not find any signs of viral

disease that could be attributed to the mortalities. Nevertheless, *C. quadricarinatus* were tested with the SMV gene probe developed by Owens *et al.* (1998). The results indicate that the *C. quadricarinatus* were infected with SMV. Organs included the hepatopancreas, midgut epithelium, glands associated with the midgut, epithelium of seminal ducts and follicle cells surrounding oocytes (Owens and McElnea, 2000). TEM and PCR were not used to confirm the *in situ* hybridisation results and SMV has not been reported in *C. quadricarinatus* since this report.

#### **2.4.5 Cherax quadricarinatus parvovirus like**

*Cherax quadricarinatus* parvo-like (CqPV) is the second virus of *Cherax* spp. to have been isolated and used to recreate disease. CqPV caused the only reported viral epizootic on a *C. quadricarinatus* farm. Mortalities of up to 96 % occurred in two earthen ponds stocked with juvenile *C. quadricarinatus* over four-months. Mortalities continued in other ponds on the same farm stocked with adults resulting in complete destocking and pond disinfection. Clinical signs of infection included anorexia, orange discolouration and weak tail flicking when handled. Bowater *et al.* (2002) described early stage infection as having small eosinophilic inclusion bodies in slightly enlarged nuclei. Late stage infection was described as having large basophilic inclusion bodies in hypertrophied nuclei that were Feulgen positive. Endodermal, ectodermal and mesodermal tissues were infected including gills, cuticular epithelium, foregut, midgut and hindgut epithelium, connective tissue, antennal gland, haematopoietic tissue, epithelial cells of the seminiferous tubules and interstitial tissue of the ovary. TEM of infected tissue revealed margined chromatin and displacement of the nucleolus. Icosahedral capsids of 19.5 nm were regularly seen in the stroma.

Transmission trials with cell free extract from the original diseased *C. quadricarinatus* were used in a transmission trial. The injected *C. quadricarinatus* presented with the same gross signs as those on the farm. However, inner branchial membrane blistering was observed in injected *C. quadricarinatus*, which has not been reported for any other crustacean virus. The first mortality occurred 17 days post-injection and continued for 73 days when the last *C. quadricarinatus* died. Histology was the same as that reported above (Bowater *et al.*, 2002).

#### **2.4.6 *Penaeus merguensis* densovirus**

*Penaeus merguensis* densovirus is a major pathogen of many penaeid species worldwide (La Fauce *et al.*, 2007). *C. quadricarinatus* were tested for their susceptibility to the Australian isolate of PmeDV. *C. quadricarinatus* were intramuscularly injected with PmeDV or orally challenged and subjected to overcrowding. Cumulative mortality of orally challenged, overcrowded *C. quadricarinatus* was the highest at 46.6 %. This treatment also had the highest number of positive PmeDV infected individuals at 90 % based on quantitative real-time PCR. However, histopathology of treatment groups showed no signs of infection with PmeDV. Other infections observed included *Coxiella cheraxi* and fungal hyphae. Quantitative real-time PCR revealed a 3-log lower viral copy numbers at the end of the trial compared to the inoculum used. La Fauce and Owens (2007) concluded PmeDV did not replicate and *C. quadricarinatus* was a potential short-term carrier.

### **2.5 *Densovirinae* of *Macrobrachium* species**

#### **2.5.1 *Macrobrachium* hepatopancreatic parvovirus**

The first report of parvovirus infection from *Macrobrachium rosenbergii* came from cultured postlarvae in Malaysia. Specimens were originally used in an iron toxicity study. Histological examination at the end of the trial revealed inclusions ranging from amorphous pale basophilic to large basophilic hypertrophied nuclei surrounded by a partial halo that were Feulgen positive. Infection occurred in the hepatopancreatic tubule epithelial cells, much like PmeDV (Lightner and Redman, 1985). TEM of the infected cells showed that the nucleolus was displaced to the nuclear membrane by a large virogenic stroma. Within the virogenic stroma were spherical particles of 29 nm presumed to be parvovirus-like. Closer examination of the capsids found that some were encased in an electron dense structure (Figure 4 of that publication), which has not been reported for any other *Densovirinae* member. *Macrobrachium* HPV (MHPV) was not associated with any mortality; laboratory stress did not increase the infection intensity or prevalence (Anderson *et al.*, 1990). *In situ* hybridisation of MHPV using a *P. chinensis* PchDV genomic probe were undertaken on the infected *M. rosenbergii*.

Control *P. chinensis* PchDV reacted strongly while MHPV infected *M. rosenbergii* were negative. The large size difference in capsid (PmeDV, 22-24 nm) and the negative gene probe results indicate that MHPV is not related to PmeDV (Lightner *et al.*, 1994).

A similar parvovirus to MHPV has been reported from larvae and brood stock *M. rosenbergii* from Thailand. During a survey of cultured *M. rosenbergii* a similar pathology to MHPV was seen but with some distinct differences. Small eosinophilic inclusions as well as larger hypertrophied basophilic inclusions with partial halos were noted in the tubule epithelial cells of the hepatopancreas (Gangnonngiw *et al.*, 2009a). The eosinophilic inclusion was not reported by Anderson *et al.* (1990). TEM revealed 25-30 nm capsids in the inclusion, similar to those of MHPV; however, capsid in the inclusions did not have an 'electron dense structure' around them. Digestion of the inclusion with mung bean nuclease demonstrated the Thailand parvo-like virus consisted of ssDNA. Like the MHPV, Thailand parvo-like virus was negative for *in situ* hybridisation using PmeDV and PstDV probes; additionally, this virus was negative for PmeDV and PstDV PCR (Gangnonngiw *et al.*, 2009a). The lack of molecular characterisation makes it impossible to say if these two pathogens are the same. They are at the very least, highly similar.

### **2.5.2 *Penaeus stylirostris* penstyldensovirus of *Macrobrachium rosenbergii***

Larval *M. rosenbergii* suffering high mortalities and sub-adults suffering runtting were examined for a causative agent. Histological examination revealed eosinophilic Cowdry Type A and B inclusions in the epithelial cells of the hepatopancreas. The *M. rosenbergii* were then screened by PCR for PstDV, PmeDV, WSSV, TSV, YHV, *Macrobrachium rosenbergii* nodavirus and extra small virus. A positive PstDV amplicon was found. The sequence was used in a phylogenetic tree to show that it was highly related to Thailand PstDV. Furthermore, *in situ* hybridisation specific to PstDV was positive and Hsieh *et al.* (2006) concluded that the agent causing the mortalities and runtting was PstDV. However, PstDV does not infect tissues of endodermal origin and does not produce a Cowdry Type B inclusion (Lightner *et al.*, 1983), indeed, *Densovirinae* have not been reported to produce both Cowdry Type A and B at the same time. PstDV does cause runt deformity syndrome in some hosts (Bell and

Lightner, 1984). Further characterisation of this virus, such as full-length genome sequence, TEM and transmission trials would be of great value in further characterisation of this virus.

## **2.6 Unclassified parvovirus-like pathology**

Uncharacterised lesions that are typical of parvovirus have been reported in *C. quadricarinatus* from Australia and Ecuador. The principle lesion described by Rusaini *et al.* (2013) in the gills of *C. quadricarinatus* was a hypertrophied nucleus with rarefied chromatin without a Cowdry Type A inclusion that stained a faint basophilic colour (Rusaini, 2013). These lesions were associated with pyknotic and karyorrhetic nuclei. TEM of the lesion did not identify any capsid-like structures, but slight rarefied chromatin and karyolysis were observed (Rusaini, 2013). Suppression subtractive hybridisation libraries failed to find any parvovirus like sequences or any other pathogen.

Cowdry Type A inclusions have been reported from farmed *C. quadricarinatus* on two separate farms in 1997 in Ecuador. Inclusions were present in the stomach hypodermis and antennal gland. These organs were infiltrated by haemocytes and affected areas contained pyknotic and karyorrhetic cells. *In situ* hybridisation using PstDV and WSSV specific probes failed to react with the infected tissue. On Farm J, these lesions were associated with 90 % mortality in nursery ponds and on Farm Z 70 % mortality in grow out ponds (Romero and Jiménez, 2002). TEM investigation of the lesions was not reported and it is unclear if this is a parvovirus; however, the histology is typical of parvovirus infection.

## **2.7 Future work on characterisation of crustacean viruses**

When considering the future of characterisation of crustacean viruses, it is useful to consider the methods previously used with characterisation of penaeid viruses. The initial report of a highly pathogenic parvovirus in commercially cultured penaeid prawns was made in 1980 (Lightner *et al.*, 1983). Since then, a large body of work has been carried out characterising the *Densovirinae* that infect penaeids (Table 2.4).

PstDV1 and PmeDV have been studied extensively using histology, TEM and molecular biology to characterise the pathogens while little is known about SMV. A systematic approach has been applied where histology is used to characterise the type of lesion and the tissue infected. TEM provides a general taxonomic rank to the pathogen and also aids in purification of the virus as viral morphology aids setting up density dependent purification. Clarified homogenate is then used to recreate the disease and test host tropism; partially fulfilling Koch's postulates (Rivers, 1937). This has led to genome sequencing, diagnostic PCRs, assignment of phylogeny and effective laboratory based treatments of these pathogens. Table 2.4 details the characterisation of these two parvoviruses compared to that of the presumptive fresh water crayfish parvoviruses.

Table 2.4: Comparison of the characterisation between penaeid-infecting *Densovirinae* and *Cherax* spp. infecting parvovirus

Pathogen	Histology	TEM	Transmission trial	Genome sequence	Transcriptome sequence	qPCR	Treatment
<b>PstDV1<sup>a</sup></b>	Lightner <i>et al.</i> (1983)	Lightner <i>et al.</i> (1983)	Bell and Lightner (1984)	Shike <i>et al.</i> (2000)	Dhar <i>et al.</i> (2010)	Tang and Lightner (2001), Dhar <i>et al.</i> (2002)	ND
<b>PmeDV<sup>a</sup></b>	Lightner and Redman (1985)	Bonami <i>et al.</i> (1995)	Catap <i>et al.</i> (2003)	Sukhumsirichart <i>et al.</i> (2006)	ND	Owens <i>et al.</i> (2014)	Owens <i>et al.</i> (2014)
<b>SMV<sup>ab</sup></b>	(Owens <i>et al.</i> , 1998) <sup>b</sup> Owens and McElnea (2000)	Owens <i>et al.</i> (1998) <sup>b</sup>	Owens <i>et al.</i> (1998) <sup>b</sup>	ND	ND	ND	ND
<b>CqPV<sup>b</sup></b>	Bowater <i>et al.</i> (2002)	Bowater <i>et al.</i> (2002)	Bowater <i>et al.</i> (2002)	ND	ND	ND	ND
<b>CdSPV</b>	Edgerton <i>et al.</i> (1997)	Edgerton <i>et al.</i> (1997)	ND	ND	ND	ND	ND
<b>Putative gill parvovirus<sup>b</sup></b>	Edgerton <i>et al.</i> (2000)	Edgerton <i>et al.</i> (2000)	ND	ND	ND	ND	ND

<sup>a</sup> *P. monodon*, <sup>b</sup> *C. quadricarinatus*, ND no data

## 2.8 Conclusion

Viruses that infect *Cherax* spp. are poorly characterised and have not moved past virion morphology and pathology (Table 2.4). CqPV (Bowater *et al.*, 2002) is the only known parvovirus to cause farm wide epizootics and the only *Cherax* spp. parvovirus to be purified and used to recreate the original disease. The lack of knowledge on *Cherax* spp. virus and their impacts on production is best demonstrated by the export of *Cherax* spp. around the world. After the initial report of a bacilliform virus in *C. quadricarinatus* from Australia, *C. quadricarinatus* were examined overseas and found to be infected with a highly similar virus. With proper characterisation of *Cherax* spp. virus, the potential to export exotic disease to other countries can be mitigated.

This thesis will aim to characterise CqPV and fill some of the knowledge gaps that exist with this pathogen. Clarified homogenate kindly provided by staff from the Queensland Government former Tropical and Aquatic Animal Health Laboratory will be used to recreate the disease at James Cook University. From infected *C. quadricarinatus*, caesium chloride purified virus and moribund *C. quadricarinatus* will be used to sequence the genome of CqPV. Once sequenced, the genome will be submitted to phylogenetic analysis to identify CqPV taxonomic standing and identify if CqPV is related to penaeid prawn-infecting densoviruses. Genomic sequencing will allow the development of a quantitative real-time PCR to further study aspects of the CqPV biology such as tissue tropism. To further characterise the genome, the transcription map will be sequenced and compared to other members of the *Densovirinae*. Finally, using histopathology and quantitative real-time PCR, host tropism of CqPV to other commercially cultured crayfish in Australia will be assessed as CqPV is the only known viral epizootic to occur in freshwater crayfish from Australia.

## **CHAPTER 3: General materials and methods**

### **3.1 General husbandry of *Cherax* species**

*Cherax quadricarinatus* and *C. destructor* were sourced from commercial farms in northern Queensland and New South Wales, Australia respectively. Crayfish were housed at James Cook University's Aquatic Pathology Laboratory in 1,000 L individually recirculating plastic aquaria. Hides were made from PVC piping cut into lengths and heavy-duty shade cloth anchored to the bottom by a rock, allowing the edges to float. Hides were provided for the crayfish as protection against cannibalism during moulting. Crayfish were maintained on a 12 h day/night photoperiod at 26 °C and monitored twice daily. Feed consisted of commercial chicken pellets fed once every second day and tinned sardines once a week to satiation. Water was exchanged every 7 days at a rate of 50 %; any biological debris was siphoned off. Experimental crayfish were allowed to acclimate for a minimum of two weeks before the start of the experiments.

James Cook University does not require an Animal Ethics Permit for experimentation on invertebrates (State of Queensland law). Nevertheless, all care was taken to provide the appropriate husbandry pre, during and after experimentation. Crayfish were monitored at least twice daily during experiments and moribund crayfish were removed and processed as appropriate for downstream analysis.

### **3.2 Purification of virus from *Cherax quadricarinatus***

#### **3.2.1 Clarified viral homogenate**

Frozen homogenate of *C. quadricarinatus* infected with CqDV was provided courtesy of the staff from the Tropical and Aquatic Animal Health Laboratory (TAAHL), Townsville, Queensland (Bowater *et al.*, 2002). The homogenate was used to experimentally infect *C. quadricarinatus* at James Cook University. Moribund *C. quadricarinatus* were dissected removing gills, cuticular epithelium of the brachial carapace, antennal gland, uropods, pleopods and chelipeds. The dissected tissue was freeze (-20 °C) thawed three times before being homogenized using an Ultra-Turrax T 25 (IKA Works (Asia) Sdn Bhd) as described previously (Bowater *et al.*, 2002). The

tissue was homogenized at a tissue to TNH buffer (Appendix 1) ratio of 1:4 (Bowater *et al.*, 2002). Tissue homogenate was clarified in a Sorvall RC 6+ centrifuge (Thermo Scientific, Victoria) using a F12S-6x500 LEX rotor for 10 min at 610 g at 4 °C. The supernatant was removed, centrifuged for 10 min at 3,830 g at 4 °C before a final centrifugation for 30 min at 24,520 g at 4 °C. Clarified supernatant was passed through a 0.45 µm syringe filter. The extract was confirmed free of bacteria by inoculation of 100 µL onto a sheep blood agar plate (Appendix 1) and incubated overnight at 28 °C. Clarified homogenate was stored at -80 °C until required.

### **3.2.2 Transmission electron microscopy**

Bacterial free, clarified supernatant was ultracentrifuged in an Optima L-90K Ultracentrifuge (Beckman Coulter, NSW) using a 55.2 Ti rotor at 145,421 g for 2.75 h at 4 °C. The pellet was re-suspended overnight at 4 °C in 500-1,000 µL of TN buffer (Appendix 1). The resuspended pellet was purified in a caesium chloride gradient isopycally formed using a density of 1.39 g cm<sup>-3</sup> (38.0 %) (Shike *et al.*, 2000) at 167,241 g for 18 h at 4 °C in a SW 55 Ti rotor. Presumptive viral fractions were removed using a gel loading pipette tip and individually stored in microfuge tubes. Fractions were purified again using caesium chloride as described above. The fractions were collected and diluted in approximately 30 µL of TN buffer.

The 30 µL aliquot of the presumptive viral fraction in caesium chloride was submitted for transmission electron microscopy (TEM) analysis. The sample was stained with 1 % uranyl acetate and viewed using transmission electron microscopy at the Centre for Microscopy and Microanalysis at University of Queensland.

The equivalent fractions not sent for TEM were ultracentrifuged using a 55.2 Ti rotor at 160,326 g for 2.75 h at 4 °C. The pellet was re-suspended in approximately 500 µL of TN buffer overnight at 4 °C before being stored at -20 °C for molecular biology.

### **3.3 Molecular biology**

#### **3.3.1 Nucleic acid extraction**

Viral nucleic acid was extracted from caesium chloride purified viral fractions and tissues from experimentally infected and control *C. quadricarinatus* and *C. destructor*. Extractions were completed using a High Pure Viral Nucleic Acid Kit (Cat. 11858874001, Roche, NSW) as per manufacturer's instructions and DNA stored at -20 °C.

#### **3.3.2 Polymerase chain reaction**

PCR reaction mixture was either MyFi (BIO-21117, Bioline, NSW) or Mango Taq (BIO-21083, Bioline, NSW) with 0.2 mM each dNTP (BIO-39025, Bioline, NSW) 1 mM MgCl<sub>2</sub> (BIO-37026, Bioline, NSW), 0.2 μM each primer and nuclease free water to a total volume of 25 μL. Cycling consisted of an initial melt of 94 °C for 2 minutes followed by 35 cycles of 94 °C for 30 seconds, annealing at the appropriate T<sub>m</sub> for the primer combination used for 20 seconds (see Appendix 3), extension at 72 °C for appropriate time based on expected product length; where an expected amplicon size was not known, an extension time of 60 seconds was used. A finale extension at 72 °C for 7 minutes was used before the reaction was stopped and held at 4 °C. Thermal cycling was conducted using either a GeneTouch thermal cycler (Bioer Technology, China) or a C1000 Touch thermal cycler (Bio-Rad, Gladesville). Amplicons from PCRs carried out at the TAAHL, Townsville, Queensland were also supplied for cloning and sequencing.

#### **3.3.3 Electrophoresis**

PCR amplicons were visualized by agarose gel electrophoresis. Agarose (Cat. 9010B, Scientifix, Victoria) gel was prepared and run in 1x TAE (40 mM Tris, 20 mM acetic acid, and 1 mM EDTA) buffer was stained with 0.05 μL ml<sup>-1</sup> Gel Red (Cat. 41003, Biotium, Fisher Biotec, Australia). The gels were loaded with 20 μL of PCR product and subjected to 35 min at 200 volts with a 100 bp DNA ladder (G3131, Promega,

NSW) (2 % gel) or 50 volts for 3.5 hours with a HyperLadder 1 kb DNA ladder (BIO-33025, Bioline, NSW) (1 % gel). The gels were visualised on a UV transilluminator (GeneSnap Syngene Synoptics, Cambridge, England).

### **3.3.4 Cloning**

PCR amplicons were excised from gels using individual scalpel blades (SBLDCL, Livingstone, NSW) and purified using an Agarose Gel DNA Extraction Kit (Cat. 11696505001, Roche, NSW). Purified amplicons were cloned into competent *Escherichia coli* JM109 cells (A1360, Promega, NSW) using the pGEM-T Easy Vector System (A1380, Promega, NSW), or One shot TOP10 chemically competent *E. coli* using the pCR4-TOPO TA vector (K4575-01, Life Technologies, VIC) as per manufacturer's instructions. Transformed *E. coli* were grown for 16 - 18 hours at 37 °C on lysogeny broth (LB) (Bertani, 1951) agar (Appendix 1) supplemented with 100 µg mL<sup>-1</sup> or 50 µg mL<sup>-1</sup> ampicillin (Cat. A9393-5G Sigma-Aldrich, NSW) for pGEM and TOPO clones respectively. Three white colonies were selected from each agar plate and cultured at 150 rpm (Bioline incubator shaker 8500 Edwards Instruments, NSW) for 16 - 18 hours in lysogeny broth (Bertani, 1951) (Appendix 1) supplemented with 100 µg mL<sup>-1</sup> or 50 µg mL<sup>-1</sup> ampicillin (A9393-5G, Sigma-Aldrich, NSW) for pGEM and TOPO cells respectively. Plasmid DNA was extracted using a High Pure Plasmid Isolation kit (Cat. 11754777001 Roche, NSW) as per manufacturer's instruction. Plasmid extracts were submitted to Macrogen Inc. (Seoul, Korea) or the Australian Genome Research Facility (Brisbane node) for sequencing analysis.

## **3.4 Quantitative real-time polymerase chain reaction**

### **3.4.1 Preparation of synthetic control for quantitative real-time polymerase chain reaction**

Total nucleic acid was extracted from caesium chloride purified CqDV (3.2.2) and used as template for PCR to generate a synthetic control for qPCR. The reaction consisted of 2x MyFi Mix (Cat. BIO-25049 Bioline, NSW) 20 pmol/µL of primer CqDV 379 F and BgF3 R (Table 3.1), 1 µL of template and DEPC-treated water (BIO-38030 Bioline,

NSW) to 25  $\mu\text{L}$ . Cycling conditions consisted of an initial hold of 95  $^{\circ}\text{C}$  for 2 minutes followed by 34 cycles of annealing at 56  $^{\circ}\text{C}$  for 20 seconds, extension of 72  $^{\circ}\text{C}$  for 20 seconds followed by 72  $^{\circ}\text{C}$  for 7 minutes before holding at 4  $^{\circ}\text{C}$ . PCR was carried out on a GeneTouch thermal cycler (Bioer Technology, China). PCR product was cleaned using a High Pure PCR Product Purification Kit (Cat. 11732668001 Roche, NSW) as per manufacturer's instructions. Purified PCR product was cloned into One Shot TOP10 chemically competent *E. coli* using the pCR4-TOPO TA vector (Cat. K4575-01 Life Technologies, VIC) as per manufacturer's instructions. Transformed *E. coli* were grown overnight at 37  $^{\circ}\text{C}$  on lysogeny broth (LB) (Bertani, 1951) agar supplemented with 50  $\mu\text{g mL}^{-1}$  ampicillin (Cat. A9393-5G Sigma-Aldrich, NSW). Three colonies were picked from the agar and grown overnight at 37  $^{\circ}\text{C}$  in LB supplemented with 50  $\mu\text{g mL}^{-1}$  ampicillin (Cat. A9393-5G Sigma-Aldrich, NSW) and shaken (Bioline incubator shaker 8500 Edwards Instruments, NSW) at 150 rpm. Plasmid DNA was extracted using a High Pure Plasmid Isolation kit (Cat. 11754777001 Roche, NSW) as per manufacturer's instruction. Plasmid extracts were submitted to Macrogen Inc. (Seoul, Korea) for sequencing. The sequence was confirmed as the 1,105 bp product. The clone became the positive control for the quantitative real-time PCR (qPCR).

### **3.4.2 Standard curve preparation**

A standard curve was prepared for the qPCR, following the method of Owens *et al.* (2014) using the clone generated from section 3.4.1; this was also used as a synthetic control. The clone was cultured for 18 hours in 30 mL of LB supplemented with 50  $\mu\text{g mL}^{-1}$  ampicillin (Sigma-Aldrich) at 150 rpm (Bioline incubator shaker 8500). A 100  $\mu\text{L}$  aliquot of culture was used in a 12 x 10 fold serial dilution while the 30 mL culture was frozen at -80  $^{\circ}\text{C}$  to prevent further bacterial growth. Copy number was calculated by plating triplicate 20  $\mu\text{L}$  aliquots of each dilution on LB agar plates supplemented with 50  $\mu\text{g mL}^{-1}$  ampicillin (Sigma-Aldrich) and incubated for 18 hours. Colony forming units were counted for each dilution and used to calculate the plasmid copy number in the 30 mL culture. The 30 mL culture was thawed and plasmids extracted and eluted in 100  $\mu\text{L}$  as previously described (3.3.4). A 10  $\mu\text{L}$  aliquot was used in a 12 x 10 fold serial dilution in DEPC-treated water (BIO-38030, Bioline) and stored at -20  $^{\circ}\text{C}$  for qPCR. A 2.5  $\mu\text{L}$  aliquot of each dilution was used as template in

each qPCR to construct the standard curve. The copy number of the standard curve is presented in Appendix 4.

### 3.4.3 SYBR green quantitative real-time polymerase chain reaction

Nucleic acid was subjected to a SYBR Green qPCR to determine the copy number of CqDV. The reaction mix consisted of 2x SensiFast SYBR No ROX Buffer (BIO-98002 Bioline, NSW), 20 pmol  $\mu\text{L}^{-1}$  of primers CqDV 5 Fq and 2A Rq (Table 3.1), 5 mM  $\text{MgCl}_2$  (BIO-37026 Bioline, NSW), 2.5  $\mu\text{L}$  of  $10^{-4}$  diluted template and DEPC-treated water (BIO-38030, Bioline) to a final volume of 20  $\mu\text{L}$ . Cycling was carried on a Corbett Rotor-Gene 6000 (Qiagen, VIC) and consisted of an initial hold of 95 °C for 3 minutes followed by 45 cycles of 95 °C for 30 seconds and 60 °C for 15 seconds while acquiring on channel Green, and a final hold of 60 °C for 5 minutes. A melt analysis consisting of a ramp from 79 – 89 °C acquiring every 0.5 °C with gain optimisation on all samples was conducted at the end of PCR amplification.

The SYBR assay was tested on *C. quadricarinatus* and *C. destructor*. Both crayfish species were confirmed negative for CqDV infection using standard PCR using primers that amplified all of the open reading frames of CqDV (Table 5.1). Confirmed negative tissue was then run in the SYBR assay along with positive controls. The SYBR assay was able to differentiate between positive and negative crayfish samples (data not shown).

Table 3.1: Primers used to create the real time clone and run SYBR Green qPCR

Assay	Primer name	Sequence	CqDV position	Product length
PCR	CqDV 379 F	GTA AGC ATG GCT TGC GTA TAC G	379-400	1,105
	BgF3 R	GGA TGT ACT TGG CTC AAC G	1464-1483	
qPCR	CqDV 5 Fq	CGC TGT GGA GAG TGC ACT AGA GGC	433-456	281
	2A Rq	TCT GAA TCA ATC TCC TCA CGA TCG C	689-713	

### **3.5 Histopathology**

Histopathology was carried following the methods described by (Bell and Lightner, 1988). Briefly, moribund *C. quadricarinatus* and *C. destructor* were dissected longitudinally, one side was placed in Davidson's fixative (Appendix 1) for 48 h, before being stored in 70 % ethanol. The other section was frozen at -20 °C for molecular biology. Fixed *C. quadricarinatus* were removed and trimmed into histocassettes before being dehydrated in ethanol and xylene washes. Tissue was then embedded in paraffin wax and 5 µm sections were trimmed. Sections were stained with haematoxylin and eosin (H&E), or Feulgen or Feulgen counterstained with alcoholic picric acid. Stained sections were viewed using an Olympus BX53 connected to an Olympus DP21 digital camera.

### **3.6 Bioinformatics analysis**

Sequencing data was analysed using Geneious 6.1.6 (Geneious version 6.1 created by Biomatters, available from <http://www.geneious.com>), and the tools available at National Center for Biotechnology Information (NCBI). These included Basic Local Alignment Search Tool (BLASTn and BLASTx) and Open Reading Frame (ORF) finder tool (<http://www.ncbi.nlm.nih.gov>).

**CHAPTER 4: Tissue tropism of *Cherax quadricarinatus*  
densovirus using histopathology, TEM and quantitative real-  
time PCR**

## 4.1 Introduction

*Densovirinae* within the family *Parvoviridae* infect invertebrates and are a major concern to the commercial rearing of insects and penaeid crustaceans (Bonami *et al.*, 1990; La Fauce *et al.*, 2007; Liu *et al.*, 2011). The classical histopathological lesion observed is hypertrophied nuclei with a haloed inclusion body consisting of virogenic stroma containing virions (Bergoin and Tijssen, 2008). In freshwater crustaceans, histological lesions and virions have been found in the giant freshwater prawn *Macrobrachium rosenbergii* that resemble those of genus *Hepadensovirus* (Anderson *et al.*, 1990; Gangnonngiw *et al.*, 2009b). Within the freshwater crayfish *Cherax* spp., a number of parvo-like virus have been observed including *Cherax destructor* systemic parvo-like virus (CdSPV) (Edgerton *et al.*, 1997), putative gill parvovirus in *C. quadricarinatus* (Edgerton *et al.*, 2000) and spawner isolated mortality virus (Owens and McElnea, 2000). Additional viruses reported in histopathological surveys of cultured *C. quadricarinatus* include *Cherax quadricarinatus* bacilliform virus, *Cherax quadricarinatus* Giardiavirus-like virus (Edgerton and Owens, 1999) and *Cherax reovirus* (Hayakijkosol and Owens, 2011). To date, these pathogens have not been characterised and their effect on farmed *Cherax* spp. remains unknown.

In Australia, Bowater *et al.* (2002) reported a parvo-like virus, *Cherax quadricarinatus* parvo-like virus (CqPV), which caused on-farm epizootics and experimentally induced mortalities in *C. quadricarinatus*. Histopathological investigation revealed two types of inclusions, early (eosinophilic) and late stage (basophilic) intranuclear inclusion bodies found in tissue of endodermal, ectodermal and mesodermal origin. Transmission trials were able to re-create the disease and pathology associated with CqPV infection.

The genome of CqPV was sequenced (GenBank KP410261), revealing a genus *Ambidensovirus* genome organisation with functional motifs characteristic of the family *Parvoviridae* (Bochow *et al.*, 2015). Phylogenetic analysis firmly placed CqPV in the genus *Ambidensovirus*, species *Decapod ambidensovirus*, variant *Cherax quadricarinatus* densovirus (CqDV). This study produces new results on tissue tropism determined by the first quantitative real-time PCR (qPCR) analysis of CqDV and

confirms and extends on the report of Bowater *et al.* (2002). Unlike the original paper, we found that CqDV preferentially infected cells of ectodermal origin.

## **4.2 Materials and Methods**

### **4.2.1 Experimental *Cherax quadricarinatus***

*C. quadricarinatus* were housed as previously described in 3.1.

### **4.2.2 Experimental trial**

Clarified homogenate was prepared as previously described in 3.2.1.

*C. quadricarinatus* were divided into two treatments, control *C. quadricarinatus* ( $n = 10$ ) and *C. quadricarinatus* + CqDV ( $n = 10$ ). *C. quadricarinatus* with a mean body weight of 25.7 g were injected using sterile Terumo 1 mL luer slip syringes (Cat. 1018242, SSS Australia Healthcare Supplies, North Murarrie, Queensland) and BD Microlance 3, 30 gauge needles (Cat. 1263187, SSS Australia Healthcare Supplies) with 90  $\mu$ L (or  $\sim 10^7$  copies) of CqDV clarified supernatant on the lateral left side of the ventral nerve ganglia of the first abdominal segment. Control *C. quadricarinatus* were not injected. The trial finished when all *C. quadricarinatus* + CqDV were moribund (57 days). When moribund, all *C. quadricarinatus* including controls, were dissected, removing pleopod, branchial epithelium, antennal gland, gill, heart, and abdominal muscle. Tissues were individually weighted. Tissues were extracted individually using a High Pure Viral Nucleic Acid Kit (Cat. 11858874001, Roche, NSW) as per manufacturer's instructions and subjected to analysis by quantitative real-time PCR (qPCR).

### **4.2.3 Histopathology**

*C. quadricarinatus* were processed for routine histopathology as previously described in 3.5.

#### **4.2.4 Viral purification and transmission electron microscopy**

A caesium chloride purified band (section 3.2.2) and gills from a moribund experimentally infected *C. quadricarinatus* were sent to the Centre for Microscopy and Microanalysis at the University of Queensland for processing as per section 3.2.2. The gill samples were post-fixed in osmium tetroxide, en-bloc stained with uranyl acetate, dehydrated in an ethanol series and embedded in EPON 812 resin using a Pelco Biowave (Ted Pella, Inc.) according to manufacturer's instructions. Sections were cut using a Leica UC6 ultramicrotome at 500 nm and stained with toluidine blue for light microscopy or at 60 nm and contrasted with uranyl acetate and lead citrate for TEM. Both samples were viewed in a JEOL JEM 1011 transmission electron microscope at 80 kV.

#### **4.2.5 Molecular biology**

##### 4.2.5.1 Nucleic acid extraction

Dissected organs from CqDV-injected and control *C. quadricarinatus* (4.2.2) were subjected to total nucleic acid extraction as previously described in 3.3.1.

##### 4.2.5.2 Preparation of synthetic control for quantitative real-time polymerase chain reaction

A synthetic control for qPCR was prepared as previously described in 3.4.1.

##### 4.2.5.3 Standard curve preparation for quantitative real-time PCR

A standard curve was prepared for the qPCR as previously described in 3.4.2.

##### 4.2.5.4 Defining measurement uncertainty

The measurement uncertainty (MU) of the qPCR was calculated for the Ct of each dilution used in the standard curve by multiplying the standard deviation of each dilution by 2. The MU for this assay was defined as the cumulative variability associated with the qPCR run. Sources of variability were from counting colony forming units, plasmid extraction, stability of plasmid after repeated freeze thawing, stability of primers after repeated freeze thawing, pipetting, binding capacity of plastic ware, performance of different batches of core qPCR reagents, the accuracy and precision of the Corbett Rotor-Gene 6000 (Qiagen, VIC) for Ct readings (White and Farrance, 2004). The MU was also calculated for four other published SYBR qPCR assays used to detect penaeid-infecting viruses.

#### 4.2.5.5 Quantitative real-time polymerase chain reaction

The six dissected tissue extracts (pleopod, branchial epithelium, antennal gland, gill, heart, and abdominal muscle) were subjected to a SYBR Green qPCR to determine the tissue tropism of CqDV as previously described in 3.4.3.

#### 4.2.6 Statistical analysis

Mean copy number  $\text{mg}^{-1}$  of tissue was calculated from the qPCR and graphed. The data was log transformed to meet the requirements of Normality and one-way ANOVA with a Fisher's Least Significant Difference test used to identify tissue specific viral copy differences. Statistical analysis was carried out in SPSS version 22.

### 4.3 Results

#### 4.3.1 Infection trial

The infection trial continued until all *C. quadricarinatus* were moribund. The first moribund *C. quadricarinatus* was observed on 17 days post injection. The last *C. quadricarinatus* became moribund 57 days post injection. No mortality was observed in the *C. quadricarinatus* control group.

The first clinical sign of disease was a tendency for *C. quadricarinatus* to migrate to the surface of the water. This was followed by *C. quadricarinatus* being easily handled, with a weak tail flick and *C. quadricarinatus* close to death could not right themselves if placed inverted on their dorsum. Pereiopods and the ventral tips of abdominal segments turned a pink to red colour. The chelipeds and antennae in the majority of *C. quadricarinatus* were lost and the branchial region of the carapace was a reddish pink. The most obvious lesion was on the inner brachial membrane between the carapace and gills which was severely blistered (Figure 4.1A, B) and filled with a viscous gelatinous substance (Figure 4.1C). This extended from one side of the branchial cavity across the top of the underside of the cephalothorax to the other branchial cavity (Figure 4.1D). The branchial carapace was marked with white spots that were etched into the inside of the carapace (Figure 4.1E, F).

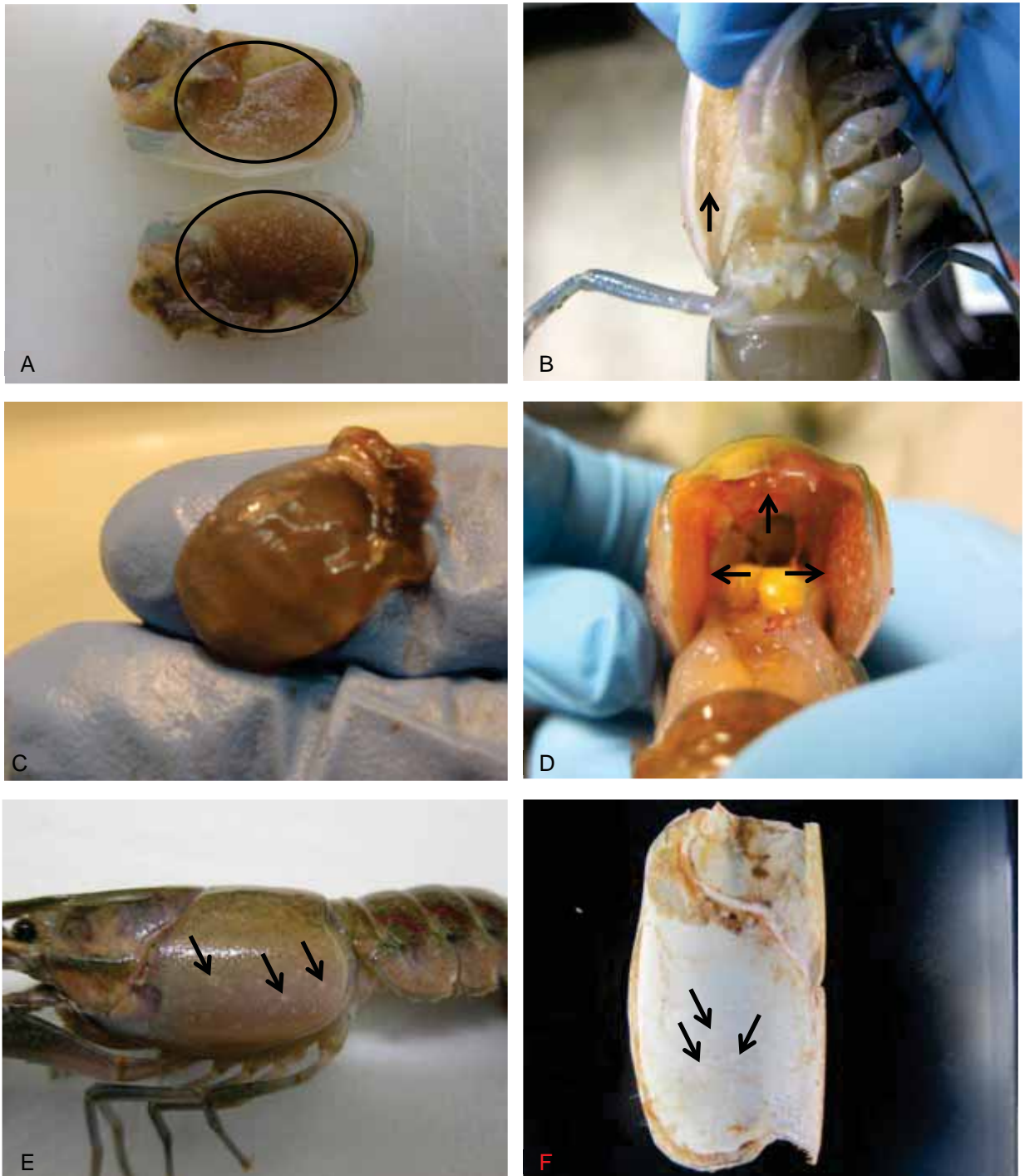


Figure 4.1: Lesions of a moribund *C. quadricarinatus* infected with CqDV. A. blister filling the branchial cavity (black circles). B. arrow indicates blisters filling the branchial chamber between gill and carapace. C. the viscous, gelatinous substance that makes up the blister. D. arrows indicate the blister covers the inside of the cephalothorax, (arrow indicates blisters). E. arrows indicate white spots characteristic of moribund *C. quadricarinatus*. F. arrows point to white spots that are etched on the inside of the brachial carapace.

### 4.3.2 Histopathology

Large basophilic, hypertrophied, intranuclear, Cowdry Type A inclusion bodies (Cowdry, 1934) were observed (Figure 4.2). Ectodermal tissue cells including the gills (Figure 4.2A), cuticular epithelium (Figure 4.2B) and eye-stalk (data not shown) were heavily infected in moribund *C. quadricarinatus*. The ectodermal cells of the gastric sieve were heavily infected (Figure 4.2C) while the *mesoderm* of the midgut epithelium was not infected (Figure 4.2D) but haemocytes containing inclusions were observed in the haemal spaces. Bowater *et al.* (2002) reported infection of the antennal gland but no histopathological changes were observed in this organ (Figure 4.2E). No histopathological change was observed in tail muscle, though the cuticular epidermal tissue was heavily infected (Figure 4.2F). Low numbers of haemocytes with inclusions were also observed in the hepatopancreatic haemocoel but no inclusions were seen in the hepatopancreocytes (Figure 4.2G). The Feulgen stain coloured the inclusion bodies magenta indicating that the inclusions consisted of large quantities of DNA (Figure 4.2H). The Feulgen counterstained with alcoholic picric acid clearly demonstrated the hypertrophied intranuclear, Cowdry Type A inclusion bodies (Figure 4.2G). Of note was the complete lack of apoptosis in affected cells of moribund *C. quadricarinatus*.

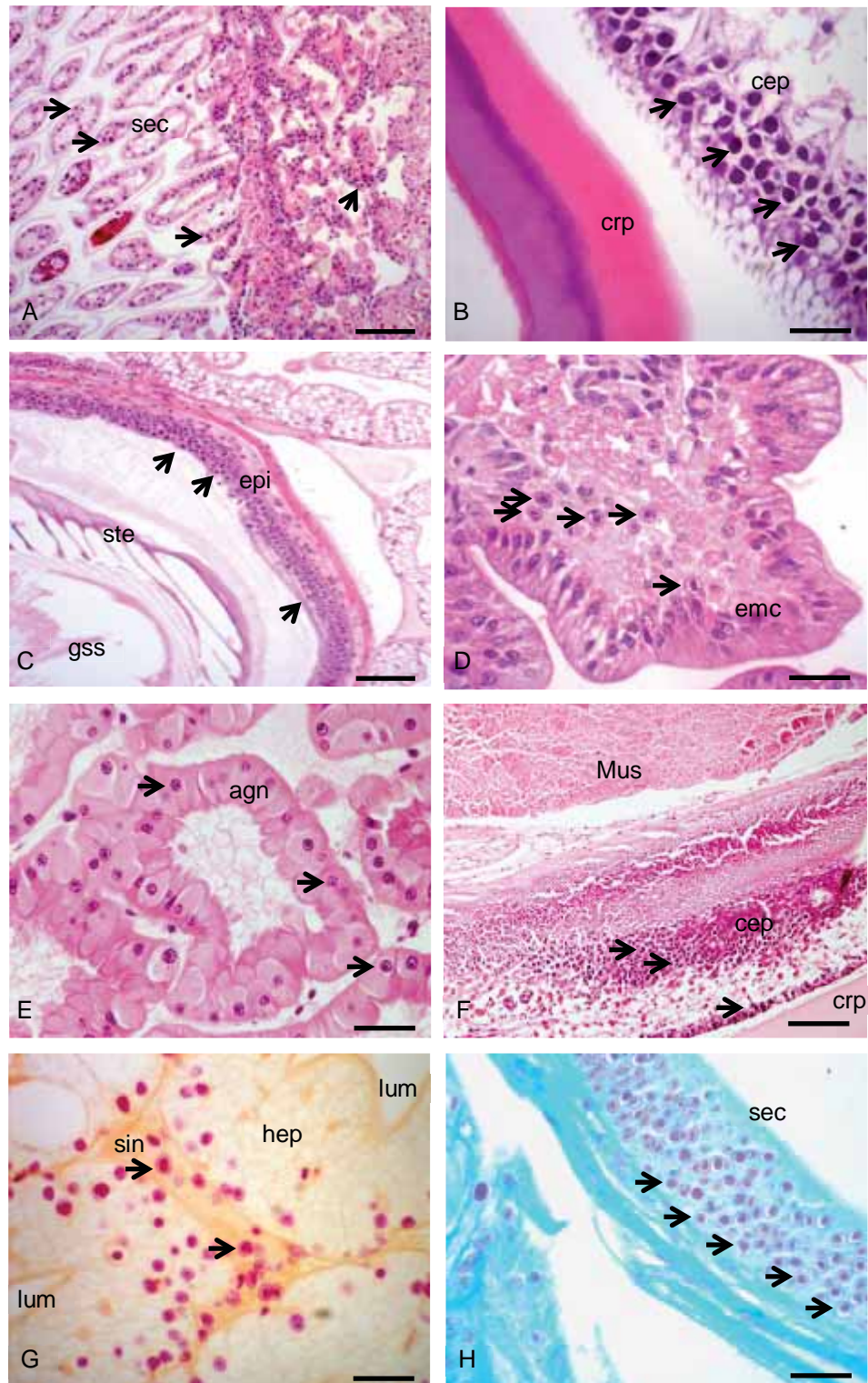


Figure 4.2: A. secondary gill filament (sec) (scale bar: 200 $\mu$ M). B. heavily infected cuticular epidermis (cep) (carapace, crp) with a lack of apoptosis (scale bar: 50 $\mu$ M). C. heavily infected gastric sieve (gss) (setae, ste) epidermis (epi) (scale bar: 200 $\mu$ M). D. midgut epithelium (emc) with infected cells (scale bar: 50 $\mu$ M). E. antennal gland tubules (agn) with healthy cells (scale bar: 50 $\mu$ M). F. abdominal muscle (Mus) with infected cep (scale bar: 200 $\mu$ M). G. hepatopancreas (Hep) with lumen (lum) and the sinus (sin) with infected cells (scale bar: 50 $\mu$ M). H. sec (scale bar: 50 $\mu$ M). Stains: A-F H&E, G: Feulgen stain counterstained with alcoholic picric acid; H: Feulgen stain. Arrows point out basophilic inclusion bodies that are characteristic of CqDV infection.

### 4.3.3 Viral purification and transmission electron microscopy

A single band formed in the caesium chloride gradient (Figure 4.3A). The band was estimated to be  $\sim 1.480 \text{ g mL}^{-1}$ . Observations with the TEM of this band included non-enveloped virions. The viral capsids of complete virions were six sided in profile, indicating an icosahedral three-dimensional structure (Figure 4.3B). These particles were  $24 \pm 1.6 \text{ nm}$  ( $n = 16$ ) in diameter. Empty particles had an electron dense centre (Figure 4.3C).

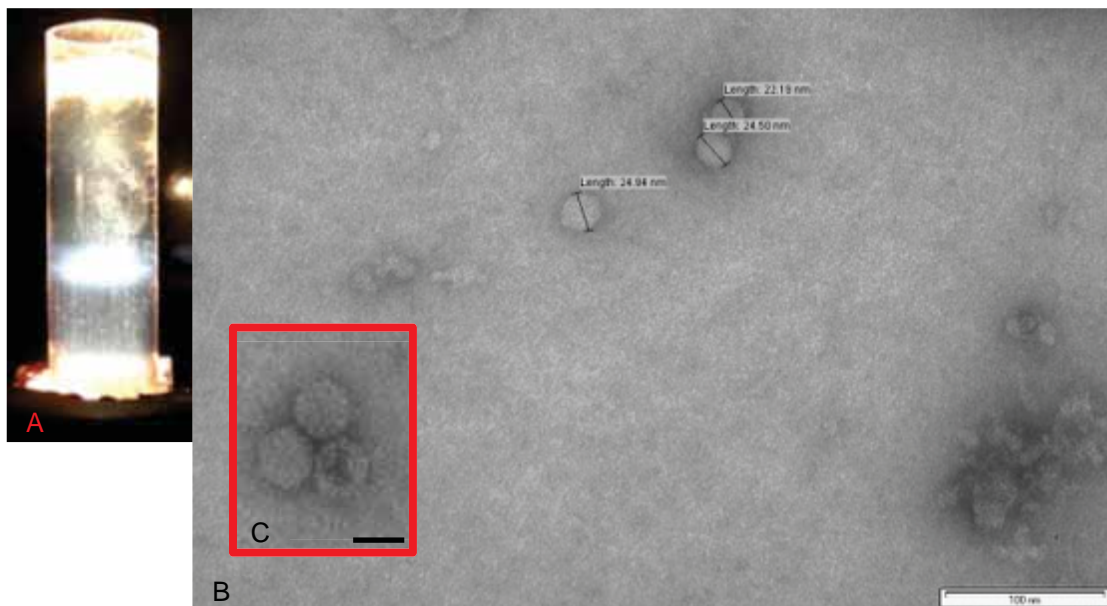


Figure 4.3: A. the first (see 3.2.2) band representing CqDV in caesium chloride. B. viral particles stained with 1% uranyl acetate with size of capsid indicated (scale bar: 100 nm). C. insert (red box) of cluster of capsids, note the empty particle bottom right (scale bar: 25nm).

Using TEM, various cellular changes were observed in CqDV infected tissues. The chromatin was rarefied and reduced to the periphery of the nuclear membrane (Figure 4.4A) while the virogenic stroma became established. The virogenic stroma swelled in the nucleus of the infected cells (Figure 4.4B) producing a halo, condensing and marginalisation of the nucleolus to appear as a signet ring (Figure 4.4C). Mitochondria were numerous, elongated and enlarged (Figure 4.4D). When the virogenic stroma filled the nucleus (Figure 4.4E), virions were readily observed, both empty and encapsulated (not shown) yet no cellular lysis for releasing virions was observed (Figure 4.4F). A single paracrystalline array of virions was observed (Figure 4.5) outside of the nucleus and virions appeared to be adhered to the nuclear membrane (not shown).

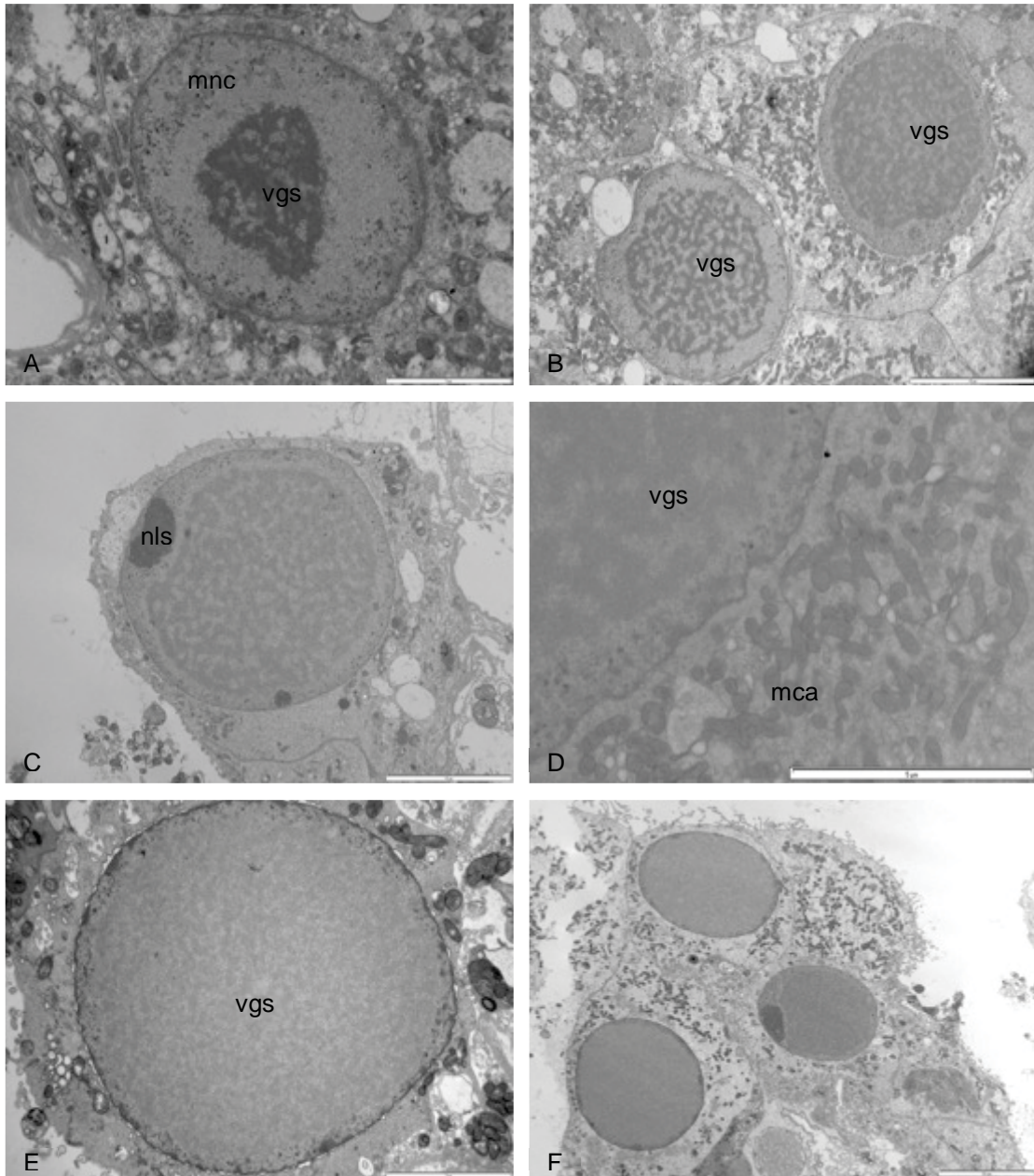


Figure 4.4: A. chromatin is being margined (mnc) and virogenic stroma (vgs) forming (10  $\mu$ m) B. virogenic stroma is established and chromatin is fully margined (10  $\mu$ m) C. signet ring formed with marginated nucleolus (nls) (10  $\mu$ m) D. elongated mitochondria (mca) (1  $\mu$ m) E. virogenic stroma filling the nucleus (5  $\mu$ m) F. intact infected cells with fully formed inclusion bodies (10  $\mu$ m). TEM produced from dissected gill tissue originating from a *C. quadricarinatus* experimentally infected with CqDV.

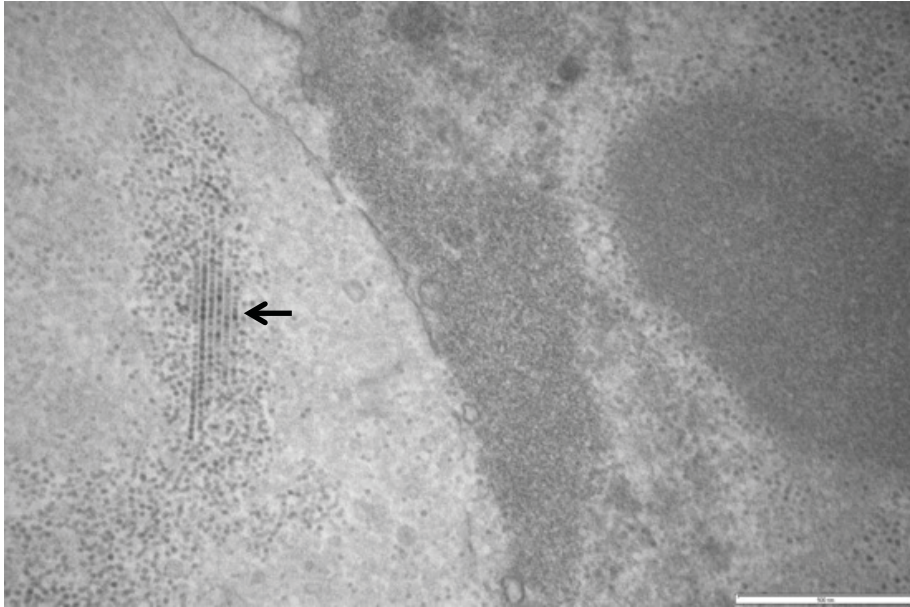


Figure 4.5: Paracrystalline arrays of CqDV (arrow) (scale bar: 1  $\mu\text{m}$ ).

#### 4.3.4 Quantitative real-time polymerase chain reaction

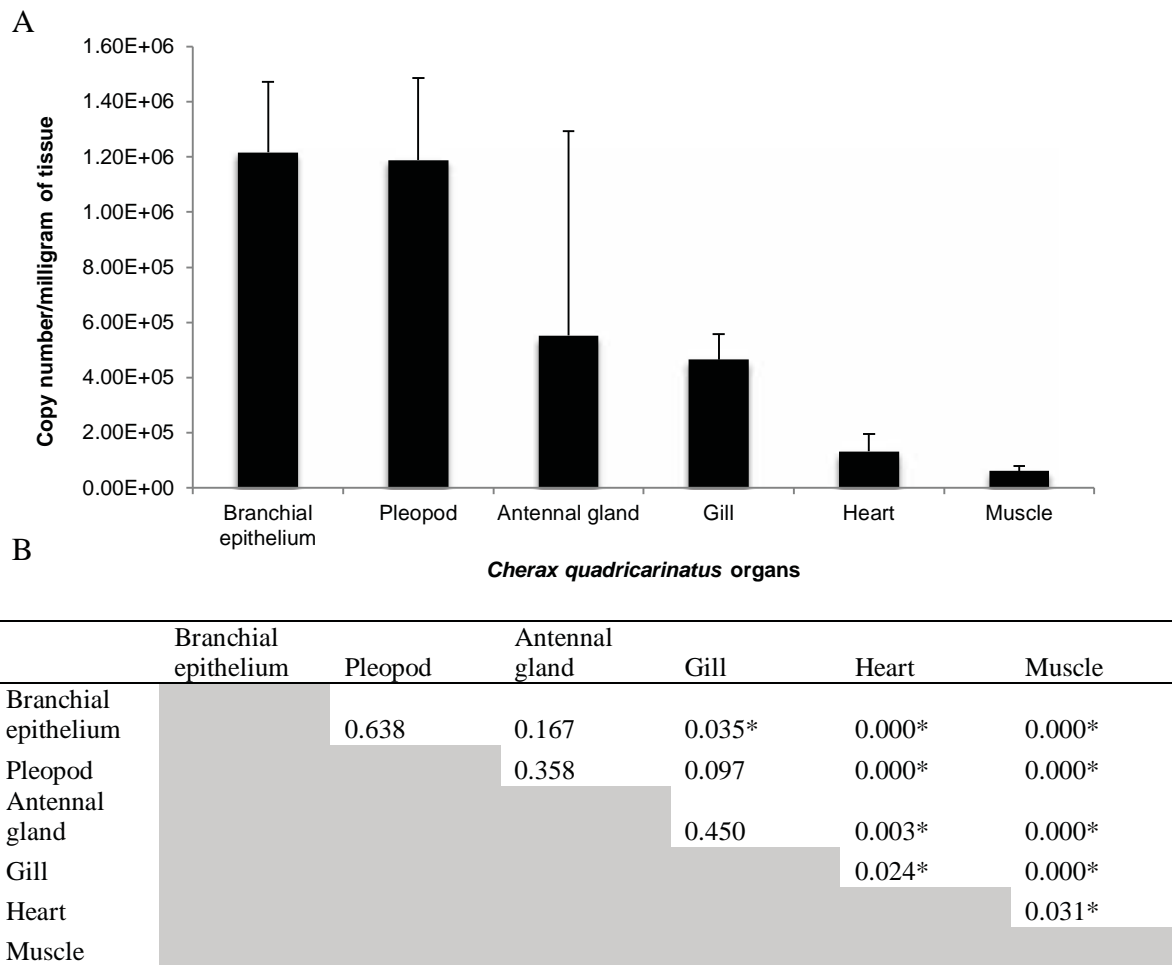
To determine the detection limit of the qPCR, a plasmid standard was constructed. The standard curve quantified the plasmid dilutions between  $10^{-3}$  and  $10^{-8}$ . Excessive fluorescence of standards at dilutions  $10^{-1}$  and  $10^{-2}$  resulted in these dilutions being removed from the standard curve. The MU for each dilution of the standard curve was calculated from seven individual experiments and summarized in Table 4.1. The MU results indicate that there is very little variability in the qPCR set-up and run. To compare the MU of the CqDV assay, the MU was calculated for four other penaeid infecting viruses that use SYBR chemistry, using data from the literature. The MU for these assays was assumed to be the same as those defined here. The CqDV assay MU was similar to assays used to detect viruses in penaeids and therefore fit for purpose.

Table 4.1: Measurement uncertainty of qPCR for detecting CqDV, Taura syndrome virus (TSV); yellow head virus (YHV); *Penaeus stylirostris penstylidensoviurs* (PstDV); white spot syndrome virus (WSSV).

Range of plasmid copies; various assays	CqDV <sup>c</sup>	TSV <sup>ac</sup>	MU		
			YHV <sup>ac</sup>	PstDV <sup>bc</sup>	WSSV <sup>bc</sup>
$2.12 \times 10^6 - 2.42 \times 10^6$	ND	0.53	0.34	ND	ND
$1.88 \times 10^5 - 2.42 \times 10^5$	2.50	1.17	0.22	1.45	0.08
$1.88 \times 10^4 - 2.42 \times 10^4$	0.92	1.06	0.23	1.25	0.45
$1.88 \times 10^3 - 2.42 \times 10^3$	1.13	0.72	0.07	2.03	0.76
$1.88 \times 10^2 - 2.42 \times 10^2$	0.92	0.67	0.46	0.54	0.55
$1.88 \times 10^1 - 2.42 \times 10^1$	1.05	2.49	0.90	0.74	0.84
2.1425 - 12.1	1.16	2.15	0.03	0.93	1.06

<sup>a</sup>(Dhar *et al.*, 2002), <sup>b</sup>(Dhar *et al.*, 2001), <sup>c</sup>SYBR Green chemistry, ND no data

Analysis of tissue tropism using qPCR demonstrated a significant difference ( $F = 13.31$  (5, 54),  $p = 0.000$ ) in copy number between the six tissue types assayed. However, initial testing of extracted DNA from the six organs using the qPCR failed due to the excessive fluorescence from the high initial copy number at the start of cycling. To overcome this, extracted DNA was serially diluted to  $10^{-4}$  and qPCR analysis repeated. Diluted samples had a Ct range between 10 – 22 and a melt temperature of  $83.71 \text{ }^\circ\text{C} \pm 0.06$  and a width (degrees) of  $0.5 \text{ }^\circ\text{C}$ . Over these runs, the coefficient of determination ( $r^2$ ) had a range between 0.98964 and 0.99976. The branchial epithelium had the highest mean copy number  $\text{mg}^{-1}$  of tissue ( $1.22 \times 10^6$ ) followed by pleopod ( $1.19 \times 10^6$ ), antennal gland ( $5.53 \times 10^5$ ), gill ( $4.66 \times 10^5$ ), heart ( $1.32 \times 10^5$ ) and muscle ( $6.12 \times 10^4$ ) (Figure 4.6). Copy number  $\text{mg}^{-1}$  of tissue was significantly different between the six tissue types with the highest level in the branchial epithelium being significantly different to gill, heart and muscle (Figure 4.6), muscle was significantly different to all other tissues. There was no significant difference between sampling days ( $F = 0.464$  (1, 53),  $p = 0.832$ ). The qPCR did not detect any CqDV in *C. quadricarinatus* from the control group (examples of a positive and negative qPCR run can be found in Appendix 4).



\* statistically significant

Figure 4.6: A. average copy number  $\text{mg}^{-1}$  of tissue from six organs ( $n = 10$ ) with error bars showing the standard error of the mean. B. is the trellis diagram showing significant difference values of the one-way ANOVA between the various organs.

## 4.4 Discussion

### 4.4.1 Gross signs of disease

The original discovery of *Cherax quadricarinatus* densovirus was described by Bowater *et al.* (2002). We extended the descriptions of gross pathology of CqDV showing the extent of branchial blistering and additional histopathology using multiple, contrasting stains which make visualisation and rapid screening easier. We show for the first time changes in the nucleoplasm using TEM. We also describe the first qPCR assay for CqDV and examine quantitatively the tissue tropism of CqDV that revealed a varied tissue tropism compared to the original report.

In the original report (Bowater *et al.*, 2002), diseased *C. quadricarinatus* were observed with discolouration and distinctive orange spots on the carapace also seen in our *C. quadricarinatus*. Furthermore, the brachial membrane on the inside of the carapace was severely blistered. This is unique among aquatic crustacean infections, as blisters have not been reported for any crustacean viral infections including others caused by densoviruses namely PstDV (Lightner *et al.*, 1983) or PmeDV (Lightner and Redman, 1985). We hypothesise the observed migration of *C. quadricarinatus* to the surface of the water is because the blister fills the branchial cavity and pushes against the gills reducing oxygen exchange, forcing *C. quadricarinatus* to the surface in search of oxygen. The blisters are extensive under the cephalothorax filling both branchial cavities and extending over the top of the cephalothorax. Histopathology of the gelatinous contents of the blister has proved difficult, as the substance breaks apart during routine processing. Bowater *et al.* (2002) suggested that the blister may be proteinaceous material resembling haemolymph. No infected hepatopancreocytes were seen in the hepatopancreas although the hepatopancreocytes were highly vacuolated. Haemocytes with inclusion bodies were noted in the haemocytes in the haemocoel sinuses of the hepatopancreas.

Of considerable interest were the white spots that developed inside the cuticle during infection with CqDV. White spots in the exoskeleton and epidermis of the cephalothorax of infected prawns is a hallmark of the white spot syndrome virus (WSSV), an enveloped, rod-shaped nucleocapsidated virus (Lo *et al.*, 1996). Shi *et al.* (2000) concluded that *C. quadricarinatus* was experimentally, a potential host and carrier of WSSV. During our TEM observations, no other virions were observed. The CqDV genome does not have any known homology to a chitinase that could cause the white spots observed in infected *C. quadricarinatus* (Bochow *et al.*, 2015). No granulomas indicating possible bacterial infection were observed in the histopathology. In the absence of any other aetiological agent, we hypothesise that CqDV is the cause of the white lesions.

#### 4.4.2 Histopathology

Basophilic hypertrophied intranuclear inclusion bodies were observed in tissues described above with the heaviest infection in cuticular epithelium cells. The Feulgen stain coloured the inclusion bodies magenta indicating that the inclusions are DNA positive as expected. Although the hepatopancreas was not infected, we observed haemocytes with inclusion bodies in the haemal spaces (Figure 4.2G). The mucosal epithelium cells of the midgut, a mesodermal tissue, was not infected but had haemocytes with inclusion bodies in the haemocoel. Bowater *et al.* (2002) reported that the antennal gland and haematopoietic tissues were infected and that CqDV could be found in endodermal, ectodermal and mesodermal cells. However, we were unable to find any sign of CqDV infection in the endodermal cells such as the antennal gland and haematopoietic tissue (however, see the qPCR results below). Our histology results indicate that CqDV preferentially targets ectodermal cells over mesodermal cells and endodermal cells. The infected haemocytes in the haemocoel indicates that CqDV infection is systemic.

#### 4.4.3 Transmission electron microscopy

Comparison of TEM from other reported putative parvoviruses that infect freshwater crustaceans share the classical cellular morphological changes. TEM of hepatopancreatic-infecting parvoviruses of *M. rosenbergii* (Anderson *et al.*, 1990; Gangnonngiw *et al.*, 2009b) were similar to that of CqDV, with marginated chromatin and a virogenic stroma filling the nucleus. However the tissue tropism is different to that of CqDV, as it does not infect the cells of the hepatopancreas in *C. quadricarinatus*. The cellular morphological changes associated with CdSPV (Edgerton *et al.*, 1997) are also similar to that of CqDV. The TEM of CdSPV show the virogenic stroma associated with the nucleolus early and that the stroma is patchy. The CqDV virogenic stroma is also patchy; however, in late stage infection when the CqDV virogenic stroma completely fills the nucleus, the stroma is associated with the nucleolus. Both CqDV and CdSPV genomes are encapsidated in the nucleus of infected cells and are associated with the virogenic stroma. The TEM supports the histopathological observations on H&E and Feulgen stained sections.

#### 4.4.4 Quantitative real-time polymerase chain reaction

The qPCR was specific for detecting CqDV in *C. quadricarinatus* infected with CqDV. The MU range of the CqDV specific qPCR was similar to that of other qPCR used to detect crustacean-infecting virus including TSV (Dhar *et al.*, 2002), YHV (Dhar *et al.*, 2002), PstDV (Dhar *et al.*, 2001), and WSSV (Dhar *et al.*, 2001). The sources of MU of the described assays were assumed to be those described in this study. Based on our results the qPCR for detecting CqDV in *C. quadricarinatus* is fit for purpose.

Tissue tropism analysis generally supported the histopathology. However, the qPCR results of the antennal gland which had no histopathological changes, had a varied but reasonably high copy number of CqDV. Similar results have been reported in PstDV infection of *P. monodon* and *P. vannamei*. *In situ* hybridization and qPCR results of the same organ were variable between specimens (Chayaburakul *et al.*, 2005).

Chayaburakul *et al.* (2005) proposed that the order of infection between tissue types lead to variable viral load depending on which tissue was infected first. Although the gill (mean  $4.66 \times 10^5$ ) is heavily infected (Figure 4.2A and H), there were significantly less copies of CqDV than that found in the branchial epithelium and pleopods. The mesodermal tissue of the heart and muscle (mean  $1.32 \times 10^5$  and  $6.12 \times 10^4$  respectively) had significantly less copies of CqDV than the ectodermal tissue. The detection of CqDV in these tissues is possibly from the systemic nature of CqDV infection, as haemocytes with inclusion bodies were found in the haemocoel of the hepatopancreas and midgut. This is in contrast to penaeid prawns which have a large proportion of fixed phagocytes in the heart capable of phagocytising virus (Chayaburakul *et al.*, 2005).

#### 4.5 Conclusion

The gross disease presentation of CqDV is unique (blistering) and should be easily recognized by farmers of *C. quadricarinatus*. Future sampling for CqDV can use the pleopod as a non-destructive tissue for CqDV detection using qPCR which is particularly useful for broodstock screening. Future work will focus on the host tropism of CqDV in *C. destructor*, another commercially important freshwater *Cherax* spp. in Australia.

**CHAPTER 5: First complete genome of an *Ambidensovirus*,  
Cherax quadricarinatus densovirus, from freshwater redclaw  
*Cherax quadricarinatus***

## 5.1 Introduction

The members of the family *Parvoviridae* infect a wide range of vertebrate and invertebrate hosts. The defining features of this viral family are the isometric, non-enveloped viral capsid and a non-segmented linear ssDNA genome characterised by self-priming hairpins that are essential for the unique rolling-hairpin replication (Tattersall, 2008). The family contains two subfamilies, the *Parvovirinae*, that infects vertebrates and the *Densovirinae* that infects the arthropods (Cotmore *et al.*, 2013).

Members of the subfamily *Densovirinae* have been found in Lepidoptera (moths and butterflies) (Kouassi *et al.*, 2007), Diptera (true flies) (Afanasiev *et al.*, 1991), Orthoptera (crickets, locusts) (Liu *et al.*, 2011), Dictyoptera (termites and cockroaches) (Mukha and Schal, 2003) and commercially important decapod crustaceans (Lightner *et al.*, 1983; La Fauce *et al.*, 2007). Disease presents in insects as anorexia, lethargy, flaccidity, uncoordinated movements and paralysis (Bergoin and Tijssen, 2010). In penaeid prawns, clinical signs include lethargic surface swimming, inverted sinking to the bottom (Bell and Lightner, 1984), poor growth, anorexia, reduced preening activity and increased surface fouling (Lightner and Redman, 1985).

The open reading frames (ORF) of members of the subfamily *Densovirinae* are divided into non-structural (NS) genes and virion protein (VP) genes on a genome of between 4 to 6 kb that is either monosense or ambisense (Bergoin and Tijssen, 2008). A taxonomic classification of the family *Parvoviridae* has been proposed to better reflect the phylogeny of this family (Cotmore *et al.*, 2013). The genomes of the subfamily *Densovirinae* share common functional motifs including nuclear location signals (NLS), NS1 rolling circle replication and endonuclease motifs, and NS1 helicase superfamily 3 motifs. The genera *Ambidensovirus* and *Iteradensovirus* have phospholipase A<sub>2</sub> (PLA<sub>2</sub>) motifs in their capsids. The genus *Ambidensovirus*, within the subfamily *Densovirinae*, is characterized by the ambisense direction of coding regions on the ssDNA genome. At present, this genus contains only insect viruses while the genus *Hepandensovirus* and *Penstyldensovirus* contain aquatic crustacean viruses.

Reported, for the first time, is the genomic sequence of the virus reported by Bowater *et al.* (2002). We conclude this virus is a member of the genus *Ambidensovirus*, and propose the nomenclature as species *Decapod ambidensovirus*, variant *Cherax quadricarinatus densovirus* (CqDV) (GenBank KP410261). This is the first *Ambidensovirus* to be sequenced from a commercially important crustacean and the first virus of the subfamily *Densovirinae* to be sequenced from a freshwater crayfish.

## **5.2 Materials and methods**

### **5.2.1 Purification of virus from *Cherax quadricarinatus***

Virus was purified from *C. quadricarinatus* as previously described in 3.2.1.

### **5.2.2 Molecular biology**

#### **5.2.2.1 Nucleic acid extraction**

Total nucleic acid was extracted as previously described in 3.3.1.

#### **5.2.2.2 Polymerase chain reaction**

Standard PCR was carried out as previously described in 3.3.2. Primers used to sequence the genome are presented in Table 5.1. In the case where single primers were used to walk along the genome or where gaps between sequences were filled, an extension time of 60 seconds was used. Primers were manually selected and were not computer generated.

Table 5.1: Primers used to sequence the CqDV genome

Primer ID	Sequence 5'-3'	Genome position	Tm
Forward Primers			
HPV 470 F	CGC AGT GTA TTT ATM AGY TAT G	Non specific	54
CqDV 379 F	GTA AGC ATG GCT TGC GTA TAC G	379-400	59.4
CqDV 5 F	CGC TGT GGA GAG TGC ACT AGA G	435-454	60.5
CqDV 606 F	GGT ACA AGA GTA TCT CGA TTG GG	606-628	57.4
Primer 2A F	CGT GAG GAG ATT GAT TCA GA	694-713	56.4
CqDV 1272 F	GCA ACG CCT AGA ATT CCA TG	1272-1291	58.4
BgF3	CCG TTG AGC CAA GTA CAT CC	1464-1483	60.5
BgR3 F	CAC CTT CAG CAA CGG AAT GTG	1801-1821	61.3
Primer 14 5-3F	GTT ACA ATC TAT CGA CGT C	2016-2034	53
CqDV 2084 F	CCA GGA GAT GGA CCT GAA TT	2084-2103	58.4
Primer 13 F	GGA GAT GTG ATC CAG AGC TG	2280-2299	57.3
CqDV 2592 F	GCA TTG TAA TTC ACT CAC CTC C	2592-2613	57.4
2444 F	CTC CTG TGT ATC GTA CAC CTG	2838-2858	61.3
2904 F	AGC GGT AGC GCT ATC ATT C	3295-3313	53.8
Primer 12 3-5	CAG CAG AGT CAC CTC TTA	3579-3596	53.9
CqDV 3923 F	GTA ATA ACA GGT GGA GTA GCT G	3923-3944	57.4
Primer 11B F	GTA CCA TAC TGT TTG GCA ATG	4082-4101	57.4
CqDV 4898 F	GGA CCA GAA CTG CCA GAT TTA C	4898-4919	59.4
4552 F	GTA CTA GGT TGC CGT AAA CC	4952-4971	58.4
CqDV 5115 F	CAT CAT GAC GGC TAG GAT CT C	5115-5135	58.4
CqDV 5367 F	GTT CAT ACG CTT TAT CGT GGT C	5367-5388	57.4
CqPV Cr5-3	GGA ATA TTA CGT TCA GCA AGT CC	5846-5868	53.7
Reverse primers			
HPV 1370R	TGG AYC ATA AYC CTC TTG TTA C	Non specific	59
Primer 5 P hP	CCA GTA GTA GTG AAG AAA GC	360-379	56.4
CqPV 5 RcF	CTC TAG TGC ACT CTC CAC AGC	434-454	56.3
CqDV 606 R	CCC AAT CGA GAT ACT CTT GTA CC	606-628	57.4
Primer 2A R	TCT GAA TCA ATC TCC TCA CG	694-713	56.4
CqDV 782 R	CAG TCA TTT CAC TTG TAA GAT ACC	782-805	57.5
BgF3 R	GGA TGT ACT TGG CTC AAC G	1464-1483	57.3
BgR3	CAC ATT CCG TTG CTG AAG GTG	1801-1821	58.4
Primer 14 RC	GAC GTC GAT AGA TTG TAA C	2016-2034	53
Primer 13 R	CAG CTC TGG ATC ACA TCT C	2281-2299	57.3
CqDV 2592 R	GGA GGT GAG TGA ATT ACA ATG C	2592-2613	57.4
2444 R	CAG GTG TAC GAT ACA CAG GAG	2838-2858	61.3
CqDV 2968 R	CTG CCA ATG GAT TTG GCT TC	2968-2987	58.4
2904 RC R	GAA TGA TAG CGC TAC CGC T	3295-3313	57.3
Primer 12 RC	TAA GAG GTG ACT CTG CTG G	3578-3596	57.3
Primer 11B R	ATT GCC AAA CAG TAT GGT AC	4082-4101	54.3
CqDV 4427R	CAT CTA CTG TAA GGA GTG GTG C	4427-4448	59.4
4923R	ACG CAG ATA AGA AAT CTG CTG	4952-4971	57.4
CqDV 5367 R	GAC CAC GAT AAA GCG TAT GAA C	5367-5388	57.4
CqDV 5584 R	GGT AGT ACT GCT CTT GCT GT	5584-5598	58.4
CqDV 5987 R	GCC TGT GGA GCT CCA TAA T	5987-6005	57.3

### 5.2.2.3 Electrophoresis

Amplicons from PCR were visualised as previously described in 3.3.3.

### 5.2.2.4 Cloning

Cloning was carried out as previously described in 3.3.4.

## 5.2.3 Bioinformatical analysis

Sequencing data was analysed as previously described in 3.6.

The evolutionary history was inferred by the Maximum Likelihood method based on the JTT matrix-based model (Jones *et al.*, 1992). The tree with the highest log likelihood (-10803.3290) and (-4255.2068) are shown for the amino acid homology of NS1 subfamily *Densovirinae* and genus *Ambidensovirus* respectively. Initial tree(s) for the heuristic search were obtained automatically by applying Neighbour-Join and BioNJ algorithms to a matrix of pairwise distances estimated using a JTT model, and then selecting the topology with superior log likelihood value. The analysis involved 37 full-length or 13 partial (P.CaDV, P.TgDV, P.EmDV are missing their N terminus) NS1 subfamily *Densovirinae* and genus *Ambidensovirus* amino acid sequences respectively. All positions containing gaps and missing data were eliminated. There were a total of 269 and 180 positions in the final dataset for subfamily *Densovirinae* and genus *Ambidensovirus* respectively. Evolutionary analyses were conducted in MEGA6 (Tamura *et al.*, 2013). Sequences used by Cotmore *et al.* (2013) to construct trees were obtained from the NCBI database (Table 5.2). The Australian *Penaeus monodon* penstyldensovirus (EU675312) isolate was also included in the phylogenetic analysis as this, with CqDV and *Penaeus merguensis* hependensovirus (DQ458781) are the only Australian densoviruses sequenced. Echinoderm parvo-like sequences were also included because of high sequence similarity to CqDV (Gudenkauf *et al.*, 2013; Hewson *et al.*, 2014). Genome ends were analysed using the CentroidFold program at [www.ncrna.org](http://www.ncrna.org).

Table 5.2: Sequences used to construct phylogenetic tree

Genus	Abbreviation	Accession #	Virus or virus variants	
<i>Ambidensovirus</i>	CqDV (Aust)	KP410261	<i>Cherax quadricarinatus</i> densovirus	
	PfDV	AF192260	<i>Periplaneta fuliginosa</i> densovirus	
	BgDV1	AY189948	<i>Blattella germanica</i> densovirus 1	
	CpDV	FJ810126	<i>Culex pipens</i> densovirus	
	PcDV	AY032882	<i>Planococcus citri</i> densovirus	
	DsDV	AF036333	<i>Diatraea saccharalis</i> densovirus	
	GmDV	L32896	<i>Galleria mellonella</i> densovirus	
	HaDV1	JQ894784	<i>Helicoverpa armigera</i> densovirus	
	JcDV	S47266	<i>Junonia coenia</i> densovirus	
	MIDV	AY461507	<i>Mythimna loreyi</i> densovirus	
	PiDV	JX645046	<i>Pseudoplusia includens</i> densovirus	
	AdDV	HQ827781	<i>Acheta domesticus</i> densovirus	
	<i>Brevidensovirus</i>	AaeDV1	M37899	<i>Aedes aegypti</i> densovirus 1
		AalDV1	AY095351	<i>Aedes albopictus</i> densovirus 1
CppDV		EF579756	<i>Culex pipiens pallens</i> densovirus	
AgDV		EU233812	<i>Anopheles gambiae</i> densovirus	
AaeDV2		FJ360744	<i>Aedes aegypti</i> densovirus 2	
AalDV2		X74945	<i>Aedes albopictus</i> densovirus 2	
AalDV3		AY310877	<i>Aedes albopictus</i> densovirus 3	
HeDV		AY605055	<i>Haemagogus equinus</i> densovirus	
<i>Hepandensovirus</i>	PmoHDV1	DQ002873	<i>Penaeus monodon</i> hepandensovirus 1	
	PchDV	AY008257	<i>Penaeus chinensis</i> hepandensovirus	
	PmoHDV2	EU247528	<i>Penaeus monodon</i> hepandensovirus 2	
	PmoHDV3	EU588991	<i>Penaeus monodon</i> hepandensovirus 3	
	PmeDV (Aust)	DQ458781	<i>Penaeus merguensis</i> hepandensovirus	
	PmoHDV4	FJ410797	<i>Penaeus monodon</i> hepandensovirus 4	
	FchDV	JN082231	<i>Fenneropenaeus chinensis</i> hepandensovirus	
<i>Iteradensovirus</i>	BmDV	AY033435	<i>Bombyx mori</i> densovirus	
	CeDV	AF375296	<i>Casphalia extranea</i> densovirus	
	SfDV	JX020762	<i>Sibine fusca</i> densovirus	
	DpDV	AY665654	<i>Dendrolimus punctatus</i> densovirus	
	PpDV	JX110122	<i>Papilio polyxenes</i> densovirus	
	HaDV2	HQ613271	<i>Helicoverpa armigera</i> densovirus	
	<i>Penstyldensovirus</i>	PstDV1	AF27321	<i>Penaeus stylirostris</i> penstyldensovirus 1
PmoPDV1		GQ411199	<i>Penaeus monodon</i> penstyldensovirus 1	
PmoPDV2		AY124937	<i>Penaeus monodon</i> penstyldensovirus 2	
PstDV2		GQ475529	<i>Penaeus stylirostris</i> penstyldensovirus 2	
PmoDV (Aust)		EU675312	<i>Penaeus monodon</i> penstyldensovirus	
Uncharacterised	SSaDV	KM052275	sea star densovirus	
	P.CaDV*		<i>Colobocentrotus atratus</i> parvovirus-like	
	P.TgDV*		<i>Tripneustes gratilla</i> parvovirus-like	
	P.EmDV*		<i>Echinometra mathaei</i> parvovirus-like	

\*Partial sequences kindly provided by Ian Hewson

## 5.3 Results

### 5.3.1 Polymerase chain reaction

PCR products obtained from TAAHL were cloned and sequenced (original primers unknown, see Appendix 3, page 2 for gel). Contig 4 (626 nucleotides (nt)) showed

sequence similarity with AdDV between nt 1294-1326 (NS1) on isolate SgCa12 (KF015280.1) (between 453-485 nt on contig 4) using BLASTn. Using BLASTx, contig 4 shared sequence similarity with several densoviruses including BgDV (AFC75858.1) with homology between amino acids 23-144 (between 129-553 nt on Contig 4). From these results, universal genus *Hepandensovirus* primers 470F and 1370R were designed (see Appendix 3, page 3 for gel). This amplified a 1,595 nt product that had BLASTx homology between 208-1,284 to Denso VP4 superfamily conserved domains on the NCBI database. The contig also shared homology with BgDV (AFC75860) between nt 118-1,128.

From the TAAHL sequence and primers 470F and 1370R genome walking was carried out. New virus specific primers were designed using the sequencing results (Table 5.2). These PCRs yielded more sequencing product that matched with members of the subfamily *Densovirinae*. The depth of sequence coverage was a minimum of 3 sequences reads per nucleotide over the entire published sequence (Appendix 3).

### 5.3.2 Phylogeny

Phylogenetic analysis of full-length NS1 amino acids suggested that CqDV is a member of the genus *Ambidensovirus*. CqDV clustered with blattodean infecting densoviruses (BgDV1P and PfdV) (Figure 5.1). In line with the most recent proposed taxonomic structure of the family *Parvoviridae* (Cotmore *et al.*, 2013), we propose this virus to be named as species *Decapod ambidensovirus*, virus and virus variant Cherax quadricarinatus densovirus. Like CqDV, Australian PmoPDV is most dissimilar from the other members of its' genus *Penstyldensovirus* while Australian PmeDV is more similar to other viruses within its' genus *Hepandensovirus*. Table 5.3 shows the percentage of identical amino acid within the *Ambidensovirus*, CqDV and SSaDV share the next highest homology after the *Lepidopteran ambidensovirus 1* species. Phylogenetic analysis of the genus *Ambidensovirus* also showed that CqDV and SSaDV isolates are highly related and that two partial NS1 echinoderm sequences (P.EmDV and P.TgDV) are also likely candidate *Ambidensovirus* (Figure 5.2).

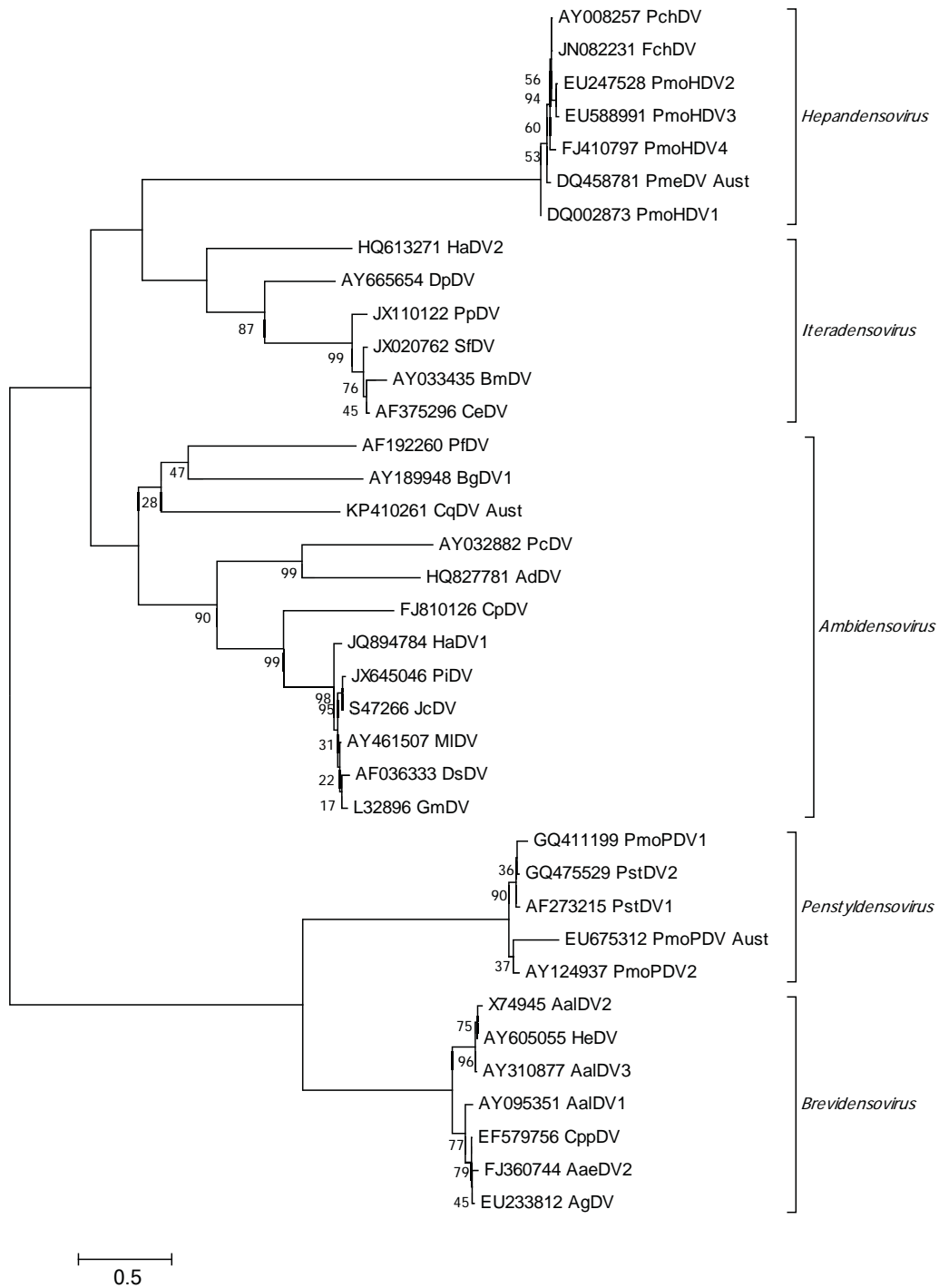


Figure 5.1: Phylogenetic analysis of full-length NS1 amino acids of the subfamily *Densovirinae* by the Maximum Likelihood method. The percentage of trees in which the associated taxa clustered together is shown on branches. Viral genera are bracketed on the right. The tree is drawn to scale, with branch lengths measured in the number of substitutions per site. Abbreviations with the Aust postscript represent Australian isolates.

Table 5.3: Percentage of amino acids that are identical between the *Ambidensovirus* NS1 including CqDV and echinoderm sequences<sup>ab</sup>

	P.CaDV	BgDV1	CpDV	HaDV1	DsDV	PiDV	JcDV	GmDV	MIDV	PfDV	P.EmDV	P.TgDV	SSaDV	CqDV	PcDV	AdDV
P.CaDV		4.9	5.6	6	5.6	5.3	5.3	5.6	5.6	6.1	13.2	10	6.1	5.9	7	4
BgDV1	4.9		26.5	27.3	27.1	26.9	26.9	27.3	27.3	29.8	38.6	19.7	27.7	28.3	24	20.8
CpDV	5.6	26.5		48	49.5	48.6	48.9	48.6	49.3	25.8	39.5	18.7	25.3	26	25.3	25.8
HaDV1	6	27.3	48		87.9	87.7	88.4	87.2	90.3	28	39.5	21.1	28	28.4	25.2	26.4
DsDV	5.6	27.1	49.5	87.9		92.3	92.8	92.1	92.5	27.5	40.9	21.1	28.6	28.6	25.2	26
PiDV	5.3	26.9	48.6	87.7	92.3		97.6	92.8	93.4	27.8	39.8	20.9	28.6	29.1	25.4	25.9
JcDV	5.3	26.9	48.9	88.4	92.8	97.6		92.7	93.9	27.7	40.9	21.1	28.4	28.6	25.5	26.6
GmDV	5.6	27.3	48.6	87.2	92.1	92.8	92.7		94.1	28.6	40.2	20.8	28.2	28.1	25.9	25.2
MIDV	5.6	27.3	49.3	90.3	92.5	93.4	93.9	94.1		28	40.2	20.9	27.9	29.1	26.4	25.5
PfDV	6.1	29.8	25.8	28	27.5	27.8	27.7	28.6	28		45.4	22.5	28.6	27.9	24.6	23.2
P.EmDV	13.2	38.6	39.5	39.5	40.9	39.8	40.9	40.2	40.2	45.4		46.1	44.8	42.8	33.9	28.4
P.TgDV	10	19.7	18.7	21.1	21.1	20.9	21.1	20.8	20.9	22.5	46.1		26	26.5	19.2	14
SSaDV	6.1	27.7	25.3	28	28.6	28.6	28.4	28.2	27.9	28.6	44.8	26		67.6	21.2	19.4
CqDV	5.9	28.3	26	28.4	28.6	29.1	28.6	28.1	29.1	27.9	42.8	26.5	67.6		22.9	20.1
PcDV	7	24	25.3	25.2	25.2	25.4	25.5	25.9	26.4	24.6	33.9	19.2	21.2	22.9		35.4
AdDV	4	20.8	25.8	26.4	26	25.9	26.6	25.2	25.5	23.2	28.4	14	19.4	20.1	35.4	

<sup>a</sup> Accession numbers for genomes are presented in Figure 5.1

<sup>b</sup> Heat map reproduced from Geneious 6.1.8

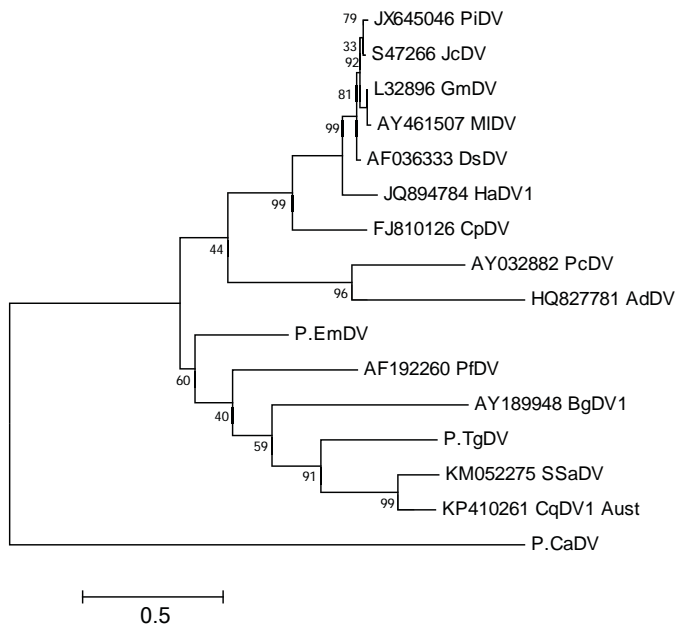


Figure 5.2: Phylogenetic analysis of NS1 amino acids of the genus *Ambidensovirus* by Maximum Likelihood method. The percentage of trees in which the associated taxa clustered together is shown on branches. The tree is drawn to scale, with branch lengths measured in the number of substitutions per site.

### 5.3.3 Genome annotation

Sequencing of the CqDV genome resulted in a single consensus sequence of 6,334 nt. The genome G/C content was 39.9 %. Using the ORF Finder tool at the NCBI set at 100 amino acids, 13 potential ORFs were found on the top strand (coding NS proteins) while 10 ORFs were found on bottom strand (coding VP proteins). Of these, 4 ORFs were considered for further analysis as these ORFs were of similar positions as those of the *Lepidopteran ambidensovirus 1*. The left ORFs coded for NS genes on the top strand while the right ORFs coded for a single VP gene on the bottom strand. Terminal inverted repeats were found at the end of the genome (Figure 5.3).

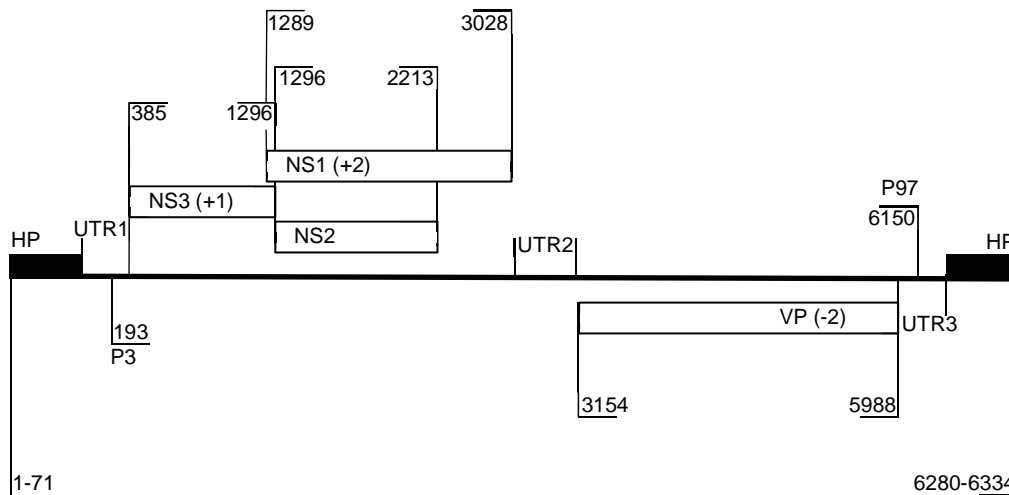


Figure 5.3: Organisation of the CqDV genome, above the line indicates top strand and below the line indicates bottom strand. Filled in boxes indicate hairpins, empty boxes indicate ORFs, bracketed numbers indicate reading frame. ORFs, UTRs and potential promoters are marked with nucleotide positions.

#### 5.3.3.1 ORF 1 – NS3 equivalent

Open reading frame 1 was equivalent to NS3 of the densoviruses. It was 912 nt long starting with an <sup>385</sup>ATG start codon and ending at a stop codon <sup>1296</sup>TAA and coded for a putative 35.55 kDa protein. There was an 8 nt overlap between this ORF and the NS1-like ORF. At the end of ORF1, there was a partial Kozak sequence <sup>1287</sup>CCATG with 5 out of 7 nt similarity (Kozak sequence **RccATGG** (Kozak, 1986) bold indicates CqDV sequence) in the overlap region of NS3-NS1. A polyadenylation signal was found at the end of the NS3 ORF at <sup>1292</sup>AATAA and the overlap region between NS3, NS1 and NS2. BLASTn and BLASTx did not identify any significant homology to other members of the subfamily *Densovirinae*. A manual search of the translated ORF identified three potential zinc finger motifs at <sup>15</sup>CxxC, <sup>18</sup>CxxC and <sup>229</sup>CxxC (Yamagishi *et al.*, 1999).

#### 5.3.3.2 ORF 2 – NS1 equivalent

Open reading frame 2 was equivalent to NS1 of the densoviruses. It was 1,740 nt long starting with an <sup>1289</sup>ATG start codon and ending at stop codon <sup>3029</sup>TAA coding for a putative 67.36 kDa protein. There was a partial Kozak sequence <sup>1287</sup>CCATG 90 nt upstream of a putative NS2 initiation box and a NS1 initiation signal <sup>2313</sup>GTAAATG

was also located followed by a <sup>2413</sup>TATA box 94 nt downstream. A BLASTp search of the translated ORF also identified a region between amino acids 422 and 535 as the conserved helicase domain corresponding to Parvo\_NS1 Pfam domain (pfam01057). Protein alignments of the translated NS1 ORF against other members of the genus *Ambidensovirus* identified the highly conserved H – Hydr (hydrophobic residue) – H – Hydr – Hydr – Hydr – x (any amino acid) (motif 1) and x – x – Y – Hydr – x (motif 2) (Ilyina and Koonin, 1992) which is involved in site-specific nicking and rolling circle replication (Nüesch *et al.*, 1995) (Figure 5.4). Protein homology was also found with the helicase superfamily 3 motifs (Gorbalenya *et al.*, 1990; Koonin, 1993).

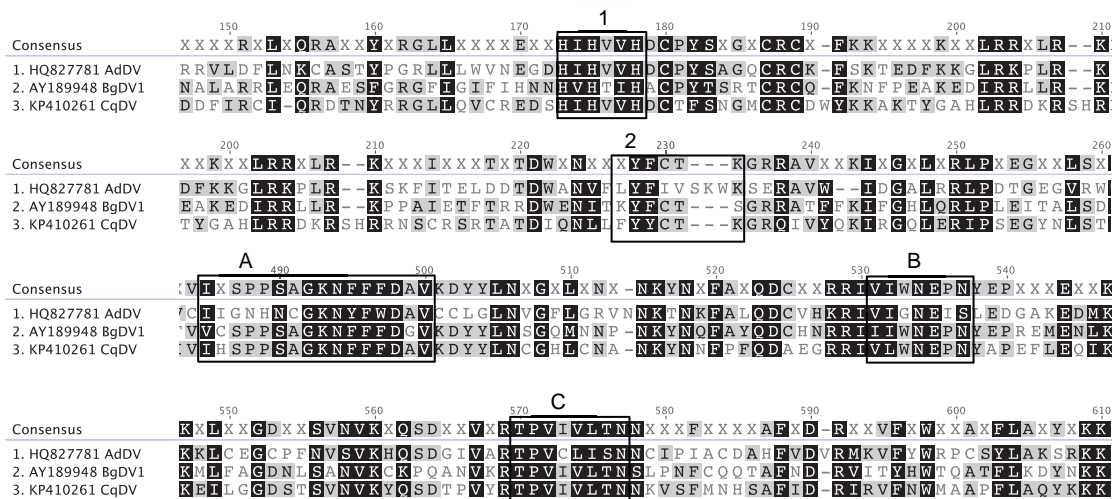


Figure 5.4: Amino acid alignments of CqDV with AdDV and BgDV1. Metal binding domain (motif 1), endonuclease (motif 2), and helicase superfamily 3 motifs (A, B, C).

### 5.3.3.3 ORF 3 – NS2 equivalent

Open reading frame 3 was equivalent to NS2 of the densoviruses. It was unusually large at 918 nt starting with an <sup>1296</sup>ATG start codon and ending at a stop codon <sup>2213</sup>TAA putatively coding for a 35.18 kDa protein. There was a TATA box 118 bp upstream of the NS2 start codon. A BLASTx search of this ORF identified homology to NS1 and NS2 of densoviruses, with the highest homology (62 %) to NS2 of BgDV.

#### 5.3.3.4 ORF 4 – VP equivalent

Open reading frame 4 was equivalent to capsid protein of the subgroup A genus *Ambidensovirus* (Bergoin and Tijssen, 2008). On the bottom strand, the ORF started with a <sup>5988</sup>TAC and finished with a <sup>3154</sup>ATT stop codon. This ORF most likely codes for 4 structural proteins through a leaky scanning mechanism, similar to other members of the species *Lepidopteran ambidensovirus 1*. A BLASTx search of the VP ORF found high homology with Densoviridae VP4 superfamily between nucleotide 3,532-4,607, SSaDV (AIQ82698.1) (E value of 0.0) and BgDV (AFC75860.1) (E value 2e-16). Protein alignment of the VP amino acids with genus *Ambidensovirus* identified a PLA<sub>2</sub> motif (data not shown). The CqDV PLA<sub>2</sub> motif had the conserved <sup>179</sup>YxGxG Ca<sup>2+</sup> binding loop and the <sup>202</sup>HDxxY catalytic site.

#### 5.3.3.5 Inverted terminal repeats and untranslated regions

There were 3 untranslated regions (UTR) within the CqDV genome. UTR1, the 5' hairpin, UTR2 between the NS1 and VP coding regions and UTR3, the 3' hairpin (Figure 5.5). Sequencing of the ends of the genome (see Appendix 3, page 24) revealed a UTR1 and UTR3 of 384 and 346 nt respectively which are inverted terminal repeats as UTR3 can be reverse complemented and aligned against UTR1. The first 71 nucleotide of UTR1 forms a hairpin that folds at <sup>36</sup>TTC although the <sup>22</sup>CATG<sup>25</sup> and <sup>29</sup>CATG<sup>32</sup> are miss-matched and therefore form an imperfect palindrome (Figure 5.5A). This pattern is consistent on UTR3, with the last 55 nucleotides forming a hairpin that folds at <sup>6302</sup>CTT and miss-matches at <sup>6293</sup>CATG<sup>6296</sup> and <sup>6300</sup>CATG<sup>6303</sup> and therefore an imperfect palindrome (Figure 5.5B). The hairpin sequences were able to contig together; however, the 3' hairpin is missing 8 nucleotides at the start, most likely from incomplete cloning. Two potential promoter sequences were identified, the first P3, <sup>193</sup>TATAAAA<sup>200</sup> and the second P97 <sup>6144</sup>TTTTATA<sup>6150</sup>.

UTR2 had a G/C content of 28.8 %. The UTR2 (125 nt) is rich in nucleotides A and T that could make up 3 polyadenylation signals or 8 TATA boxes. This is unusual for members of the genus *Ambidensovirus* as most have an overlapping NS1-VP coding regions or very small nucleotide gap between these two coding regions.

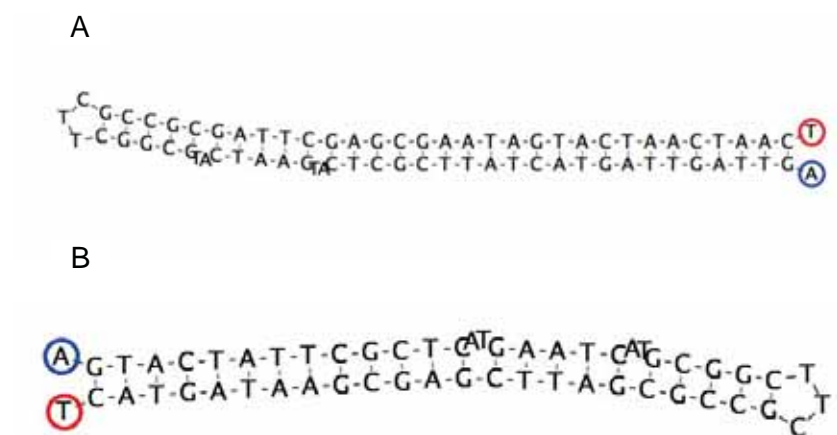


Figure 5.5: Hairpin structures of CqDV. (A) Hairpin of left hand side, note the two TA nucleotides that are not complementary, blue circled A is the terminus. (B) Hairpin on the right and side, note the two AT nucleotides that are not complementary, red circled T is the terminus. The miss-matched nucleotides occur at the same position on both termini.

## 5.4 Discussion

Following an epizootic in juvenile *C. quadricarinatus*, the *Cherax quadricarinatus* parvo-like virus was visualized via TEM. The virus was purified from diseased crayfish and cell-free extract used to recreate the disease in healthy *C. quadricarinatus* (Bowater *et al.*, 2002). The parvo-like virus was re-purified from experimentally infected moribund crayfish and used to re-infect *C. quadricarinatus* at James Cook University 13 years later, to satisfy 3 of 4 Koch's postulates for viruses (Rivers, 1937). TEM of the presumptive parvovirus bands in caesium chloride revealed a classic icosahedral particle of  $24 \pm 1.6$  nm ( $n = 16$ ) (4.3.3). The morphology and size of the CqDV capsid was similar to those of other aquatic *Densovirinae* such as PmoPDV1 (Bonami *et al.*, 1990) and PmonHDV1 (Bonami *et al.*, 1995) and insect *Densovirinae* such as PfdV (Suto *et al.*, 1979; Hu *et al.*, 1994) and BgDV1 (Mukha *et al.*, 2006).

Sequencing of the CqDV genome revealed four of the thirteen ORFs were orientated similar to other members of the genus *Ambidensovirus*. Three ORFs, designated NS3, NS1 and NS2 coded on the top strand and were found on the left side of the genome. The structural protein coded on the bottom strand and was located on the right side of

the genome. This architecture resembles that of the species *Lepidopteran ambidensovirus 1*. There were major differences in UTRs between NS and VP ORFs of CqDV compared to the aforementioned. The 125 nt of UTR2 was considerably longer than other UTRs in members of the genus *Ambidensovirus* genomes (Tijssen *et al.*, 2006), for example: PfdV – 29 nt, BgDV – 2 nt, PcDV – 14 nt, DsDV – 29 nt, HaDV1 – 31 nt, AdDV – 18 nt, and JcDV – 31 nt, while GmDV, MIDV, and PiDV had no UTR with NS and VP ORFs overlapping. Transcriptome analysis has demonstrated that the NS and VP transcripts overlap by various lengths (Tijssen *et al.*, 2003; Fédère *et al.*, 2004; Kapelinskaya *et al.*, 2011; Liu *et al.*, 2011).

The viruses of the family *Parvoviridae* can form three distinct hairpin structures, ‘T’, ‘I’ or ‘Y’. We have cloned and sequenced both the 5’ and 3’ hairpin of CqDV which folded into an ‘I’ organisation, though the 3’ hairpin appears to be missing 8 nucleotides when compared to the 5’ end. The hairpin sequences of CqDV did not form palindromes, though Huynh *et al.* (2012) noted that densoviruses are unstable upon cloning and that many densoviruses in GenBank lack significant parts of their inverted terminal repeats. It is likely that the CqDV ends are incomplete. If the CqDV ends do form the ‘I’ organisation, CqDV would be the first genome to have the *Lepidopteran ambidensovirus 1* genome architecture without the ‘Y’ shaped hairpins. The hairpins are essential for the rolling circle type replication and are characteristic of this group of viruses (Tattersall and Ward, 1976; Cotmore and Tattersall, 1996).

#### **5.4.1 Amino acid homology**

Amino acid domains encoded by the *Parvoviridae* proteins are highly conserved and were found in the CqDV translated ORFs. Analysis of the prokaryotic rolling circle replication initiators found three motifs that are conserved (Ilyina and Koonin, 1992; Nüesch *et al.*, 1995). The intervening amino acid lengths between the Y and the K can vary. The HxHxxx domain is a metal-ion ligand (Koonin and Ilyina, 1993) and functions with the active-site tyrosine (Y) to nick the viral DNA for rolling hairpin replication (Nüesch *et al.*, 1995). The CqDV translated NS1 ORF contained the metal-ion ligand <sup>169</sup>HIHVVH motif followed by the active-site tyrosine <sup>219</sup>YYCTK. Furthermore, the C terminus of the CqDV NS1 translated ORF encoded the helicase

superfamily 3 motifs (Gorbalenya *et al.*, 1990; Koonin, 1993). The NS3 translated ORF contained a zinc finger motif, a structure which mostly binds to nucleic acids. This motif was conserved in GmDV, DsDV, BmDV and JcDV and found in two locations (Yamagishi *et al.*, 1999) although in CqDV NS3, there were three zinc finger motifs. No homology to other proteins was identified for CqDV NS2 on the NCBI database and sequence and amino acid homology was low when compared to other genus *Ambidensovirus* NS2s.

The VP protein of CqDV was encoded on a single large ORF, similar to that of the species *Lepidopteran ambidensovirus 1*. The large ORFs of *Lepidopteran ambidensovirus 1* are un-spliced and use a leaky scanning mechanism to generate 4 structural proteins (Tijssen *et al.*, 2003; Fédère *et al.*, 2004; Huynh *et al.*, 2012). *Ambidensovirus* genomes that contain split structural ORFs, such as AdDV (HQ827781) and BgDV1 (AY189948) are spliced (Kapelinskaya *et al.*, 2011; Liu *et al.*, 2011). The VP ORF of CqDV most likely encodes multiple structural proteins that are generated by a leaky scanning mechanism. Within the CqDV VP translated ORF, a PLA<sub>2</sub> motif was identified. This motif is common to genus *Ambidensovirus* and *Iteradensovirus* but lacking in other members of the subfamily *Densovirinae* that infect aquatic crustaceans. The motif consists of a Ca<sup>2+</sup> binding loop YxGxG and catalytic site HDxxY. The enzyme hydrolyzes the *sn*-2 ester bond of phospholipids (Balsinde *et al.*, 1999). Zádori *et al.* (2001) demonstrated the functionality of this motif in parvoviruses by disrupting the capsid with alkali denaturation and heat shock, which resulted in a 50 to 100 fold increase in PLA<sub>2</sub> activity indicating that the PLA<sub>2</sub> motif is located inside the capsid. Mutant studies on the N terminal end of VP1, have demonstrated that the motif is required for endosomal escape into the cytosol. The CqDV VP PLA<sub>2</sub> was homologous to other viruses in the genus *Ambidensovirus*. Taken together, the results indicate that the ORFs on the top strand encode the NS proteins and the ORFs on the bottom strand encode the VP protein of CqDV.

#### 5.4.2 Phylogeny

We propose CqDV be classified as a new species, *Decapod ambidensovirus*, variant *Cherax quadricarinatus densovirus* within the genus *Ambidensovirus*. Analysis of

phylogeny using the accession numbers provided by Cotmore *et al.* (2013) produced a tree that generally agreed with their proposed phylogeny of the subfamily *Densovirinae* and CqDV meets the proposed outlines (Cotmore *et al.*, 2013) for inclusion into the family *Parvoviridae*; 1. the viral particle has been isolated from an unambiguous host (*Cherax quadricarinatus*); 2. the genome has been sequenced; 3. the genome is non-segmented and contains non-structural and viral particle coding regions that meets the required size constraints and organization; 4. conserved motif patterns are consistent with that of a parvovirus; and 5. observed epizootic and experimentally induced mortalities are compatible with dissemination by infection (Bowater *et al.*, 2002). Based on the phylogeny, the closest relative of CqDV is that of the uncultured SSaDV and is not related to other known viruses of the subfamily *Densovirinae* that infect aquatic crustaceans.

The phylogenetic analysis showed that CqDV clustered with the blattodean-infecting densovirus (PfdV and BgDV). Though not complete, the terminal ends of CqDV also shared the 'I' organisation of the aforementioned. However, the architecture of the CqDV ORFs was similar to that of the *Lepidopteran ambidensovirus 1* and *Dipteran ambidensovirus 1* with a single large VP ORF. Of considerable interest is the high similarity (62 % of identical amino acids in NS1) between the CqDV and SSaDV genomes and their host range. SSaDV was suggested as the cause of sea-star wasting disease, which was linked to epizootics in marine sea stars observed off the east coast of America (Hewson *et al.*, 2014). Three partial urchin-associated parvovirus-like sequences from *Colobocentrotus atratus* (P.CaDV), *Tripneustes gratilla* (P.TgDV) and *Echinometra mathaei* (P.EmDV), kindly provided by Prof. Ian Hewson from a metagenomic study (Gudenkauf *et al.*, 2013), were also included in our phylogenetic tree (Figure 5.2). The partial genomes of P.EmDV, and P.CaDV are not closely related to CqDV while the P.TgDV is somewhat related. Further analysis of the echinoderm sequences identified conserved domains constant with the *Densovirinae* (Table 5.4).

Although CqDV and SSaDV are phylogenetically similar, they are geographically and environmentally distinct from each other. The host range of the *Densovirinae* varies greatly and includes a wide range of arthropod orders. Some *Densovirinae* have a monospecific host range while others have a polyspecific host range, but host range

does not extend outside of the host order. Examples include MIDV which can infect lepidopteran *Spodoptera littoralis*, *Pectinophora gossypiella*, *Sesamia cretica*, *Chilo agamemnon*, and *Ostrinia nubilalis* (Fédière et al., 2004). Other examples include JcDV which can infect a variety of *Lepidoptera* hosts and PfDV which can infect different members of the genus *Periplaneta* (Bergoin and Tijssen, 2008). Polyspecific host range is also observed in the crustacean virus PmoHDV which can infect multiple species of penaeid prawns (Safeena et al., 2012). The CqDV isolate shares attributes from both the *Blattodean ambidensovirus 1* and *2* and *Lepidopteran ambidensovirus 1*, together with SSaDV, are the first isolates that are somewhat related and have been found to infect phylogenetically disparate hosts. They are thus far, unique amongst the *Densovirinae*. The pathogenicity of CqDV or SSaDV in alternative hosts is unknown at this time.

Table 5.4: Motifs present in uncharacterized echinoderm densovirus

Virus	NS1 rolling circle replication motifs		NS1 helicase superfamily 3			PLA <sub>2</sub>	Polyglycine
	<b>1</b>	<b>2</b>	<b>A</b>	<b>B</b>	<b>C</b>		
SSaDV	+	+	+	+	+	+	+
P.CaDV	-	-	-	-	-	ND	ND
P.EmDV	-	-	+	+	+	ND	ND
P.TgDV	-	-	+	+	+	ND	ND

ND no data

## 5.5 Conclusion

The results firmly place CqDV in the genus *Ambidensovirus*. This isolate, along with SSaDV, are the first highly related isolates to infect disparate hosts, making them unique amongst the *Densovirinae*. This was the first parvovirus to have been sequenced from a commercially important freshwater crayfish and the only known *Ambidensovirus* to infect aquatic crustaceans. Trials to assess if this virus infects other commercially important crustaceans that are cultured in Australia are necessary (Chapter 7). We are also studying the transcriptome of CqDV to characterise the transcription strategy, and utilising SDS-PAGE to assess the size and number of structural proteins encoded by CqDV.

**CHAPTER 6: Partial transcriptome of *Cherax  
quadricarinatus* densovirus**

## 6.1 Introduction

*Cherax quadricarinatus* densovirus (CqDV) is a highly pathogenic densovirus of *Cherax quadricarinatus* (Bowater *et al.*, 2002) and is a member of the *Densovirinae*. The genome of the viruses of *Densovirinae* are linear ssDNA between 4 and 6 kb. Their genomes possess two gene cassettes, the non-structural (NS) and the viral protein (VP) encoding genes. NS1 and NS2 are overlapping ORFs that code for proteins that are crucial in the lifecycle (Cotmore and Tattersall, 2014), and are found on the 5' or left hand side of the genome. The VPs are coded by up to three ORF that produce viral proteins from splicing and/or leaking scanning mechanism. The VP ORFs are found on the 3' half or the right side of the genome. The *Ambidensovirus* is only genus that encodes NS3 and has coding capacity on both strands. By convention, the top strand codes for the NS genes, on the left side and the bottom strand codes for the VP genes on the right side of the genome (Bergoin and Tijssen, 2008).

Members of the family *Parvoviridae* utilise a complex mechanism of alternative splicing to increase the coding capacity of their compact genomes from overlapping reading frames (Pintel *et al.*, 1995). The splicing patterns in the *Densovirinae* are varied, even within a genus. The blattodean-infecting densovirus that have multiple VP ORFs, splice both the NS and VP mRNAs while the species *Lepidopteran ambidensovirus 1* that have a single VP ORF, only splice the NS mRNAs. However, not all *Densovirinae* genomes are spliced. Members of the genus *Iteradensovirus* and *Brevidensovirus* do not have spliced genomes.

The genome of CqDV has been sequenced (GenBank: KP410261) with phylogeny placing the isolate in the genus *Ambidensovirus* of the *Densovirinae* (Bochow *et al.*, 2015). The phylogeny places CqDV with the blattodean-infecting densoviruses but the CqDV genome architecture is similar to the species *Lepidopteran ambidensovirus 1*. Infection trials demonstrate that CqDV is a chronic infection, leading to 100 % mortality over approximately 70 days (Bowater *et al.*, 2002). CqDV is the first naturally occurring *Densovirinae* from freshwater crustaceans and the only *Ambidensovirus* from a crustacean to be sequenced.

Two *Densovirinae* have been sequenced from cultured penaeid prawns. *Hepandensovirus* and *Penstyldensovirus* isolates are highly pathogenic to commercially cultured penaeid species (Lightner *et al.*, 1983; Lightner and Redman, 1985; Bonami *et al.*, 1995; Mari *et al.*, 1995; Shike *et al.*, 2000). Only *Penaeus stylirostris* penstyldensovirus 1 (PstDV1, AF273215) has had its transcriptome mapped. As CqDV is the third crustacean-infecting *Densovirinae* isolated and sequenced, and has a unique architecture compared to its phylogeny, we mapped the splice sites of CqDV for comparison to other *Ambidensovirus* members. We also set out to identify the replication cycle of CqDV in the first 120 hours of infection in *C. quadricarinatus*.

## **6.2 Materials and methods**

### **6.2.1 *Cherax quadricarinatus***

*C. quadricarinatus* were sourced from a commercial farm in northern Queensland in March 2015. *C. quadricarinatus* were housed in 3 recirculating systems, with eight 50 L tanks per system attached to a sump filled with bio-balls. Each tank was supplied with an air driven corner filter and PCV piping for hides. Water was maintained at 26 °C; the photoperiod set at 12 h light and 12 h dark. *C. quadricarinatus* were monitored twice daily and fed chicken pellets once daily to satiation. No water was exchanged during the trial period and *C. quadricarinatus* were allowed to acclimate to conditions for 2 weeks.

### **6.2.2 Clarified homogenate**

CqDV was clarified as previously described in 3.2.1.

### **6.2.3 Infection trial**

Twenty *C. quadricarinatus* with a mean body weight of 37.6 grams were randomly distributed between three recirculating systems. Eighteen *C. quadricarinatus* were injected with  $10^7$  copies of CqDV-containing clarified extract using 1 mL luer slip

syringes (Cat. 1018242, SSS Australia Healthcare Supplies, Brisbane) and 30G x 13 mm Microlance needles (Cat. 1263187, SSS Australian Healthcare Supplies, Brisbane). System 1 contained 8 *C. quadricarinatus* in individual tanks, pairs were killed at 3, 6, 9 and 12 hours post-injection. System 2 contained 10 *C. quadricarinatus* in 8 tanks, pairs were killed at 24, 48, 72, 96, and 120 hours post-injection. System 3 contained 2 negative control *C. quadricarinatus* that were killed at 144 hours (Table 6.1).

Table 6.1: Experimental design of *C. quadricarinatus* randomly distributed in three systems.

Accession number	Day	Tank number	Time (hours) killed after injection with CqDV
A15-052.1	1	1 <sup>a</sup>	3
A15-052.2		2 <sup>a</sup>	3
A15-052.3		3 <sup>a</sup>	6
A15-052.4		4 <sup>a</sup>	6
A15-052.5		5 <sup>a</sup>	9
A15-052.6		6 <sup>a</sup>	9
A15-052.7		7 <sup>a</sup>	12
A15-052.8		8 <sup>a</sup>	12
A15-052.9	2	9 <sup>b</sup>	24
A15-052.10		9 <sup>b</sup>	24
A15-052.11	3	10 <sup>b</sup>	48
A15-052.12		10 <sup>b</sup>	48
A15-052.13	4	11 <sup>b</sup>	72
A15-052.14		12 <sup>b</sup>	72
A15-052.15	5	13 <sup>b</sup>	96
A15-052.16		14 <sup>b</sup>	96
A15-052.17	6	15 <sup>b</sup>	120
A15-052.18		16 <sup>b</sup>	120
A15-052.19	7	17 <sup>c</sup>	144
A15-052.20		18 <sup>c</sup>	144

<sup>a</sup>System 1; <sup>b</sup> System 2; <sup>c</sup> System 3, no-injection control.

## 6.2.4 Molecular biology

### 6.2.4.1 Nucleic acid extraction

Total nucleic acid was extracted from approximately 100 mg of gill tissue as previously described in 3.3.1.

#### 6.2.4.2 Total RNA extraction

TRI Reagent Solution (Cat. AM9738, Life Technologies Australia) was used to extract total RNA from approximately 100 mg of gill tissue. Total RNA was resuspended in 70  $\mu$ L of DEPC-treated water (Bioline) as per manufacture's instructions. Extraction was undertaken immediately after *C. quadricarinatus* were killed. Total RNA was checked for salt contamination using a NanoDrop 1000 Spectrophotometer (ThermoFisher Scientific).

Total RNA from above was cleaned using a High Pure Viral Nucleic Acid Kit (Cat. 11858874001 Roche, NSW) with a modified protocol. Total RNA was added to 300  $\mu$ L of binding buffer supplemented with Poly(A) and left on wet ice for 5 minutes before being added to the column. The sample was then washed with inhibitor removal buffer once followed by three washes with wash buffer before being eluted in 70  $\mu$ L of elution buffer. Total RNA was checked for salt contamination using a NanoDrop 1000 Spectrophotometer (ThermoFisher Scientific) before being aliquoted and stored at  $-80^{\circ}\text{C}$ .

#### 6.2.4.3 RNA quality check

Total RNA was run on a 2200 TapeStation using a High Sensitivity RNA ScreenTape (Cat. 5067-5579, Agilent Technologies, USA) chip with a modified protocol. As well as denaturing the sample prior to analysis, a cold sample was run along side the denatured sample for comparison.

#### 6.2.4.4 RNA ligase-mediated rapid amplification of cDNA ends polymerase chain reaction

The 5' RNA ligase mediated rapid amplification of cDNA ends (RLM-RACE) (Cat. AM1700, ThermoFisher Scientific) protocol was used as per manufacture's instructions. The standard reaction requires 10  $\mu$ g starting total RNA. As the yield of RNA was low, the standard reaction started with 16  $\mu$ L (5.8  $\mu$ g) of total RNA (A15-052.9), the maximum possible in the CIP reaction (Part A, Step 1). The small reaction

started with 4  $\mu$ L (1.7  $\mu$ g) of total RNA (A15-052.11). cDNA was stored at  $-20^{\circ}\text{C}$  before PCR.

The 5' RLM-RACE small reaction (4  $\mu$ L (999 ng) of total RNA (A15-052.5)) was modified at Part B; Reverse Transcription. The ligated RNA was incubated at  $94^{\circ}\text{C}$  with random decamer primers for 4 minutes while the remaining reverse transcriptase reaction components were incubated separately at  $25^{\circ}\text{C}$  for 5 minutes. The RNA/random primer mix was added to the reaction mix and incubated for 10 minutes. The remainder of the protocol was followed as per manufacture's instruction. cDNA was stored at  $-20^{\circ}\text{C}$  before PCR.

#### 6.2.4.5 Tetro cDNA synthesis

The Tetro cDNA Kit (Cat. BIO-65042, Bioline, NSW) protocol was modified. Two microliters of total RNA from A15-052.11 was used in the protocol. Two reactions were set up using 4  $\mu$ L and 2  $\mu$ L of total RNA from A15-052.11 and either random hexamers or the 3' adaptor primer from the RLM-RACE kit respectively. The two total RNA/primer mixes were heated to  $94^{\circ}\text{C}$  for 4 minutes. The remaining reverse transcriptase reaction components were incubated separately at  $25^{\circ}\text{C}$  for 5 minutes. The RNA/primer mixes were added to their respective reaction mixes and incubated for 10 minutes at  $25^{\circ}\text{C}$ . The remainder of the protocol was followed as per manufacture's instruction. cDNA was stored at  $-20^{\circ}\text{C}$  before PCR.

#### 6.2.4.6 Polymerase chain reaction

cDNA template from 6.2.4.4 and 6.2.4.5 was used in standard PCR using the primers from Table 6.2 (primers represented on the CqDV genome in Figure 6.1 and 6.2) as previously described in 3.3.2.

#### 6.2.4.7 Cloning

PCR products were cloned into pGEM vectors as previously described in 3.3.4.

#### 6.2.4.8 Preparation of synthetic control for quantitative real-time polymerase chain reaction

A synthetic control for qPCR was prepared as previously described in 3.4.1.

#### 6.2.4.9 Standard curve preparation

A standard curve was prepared for the qPCR as previously described in 3.4.2.

#### 6.2.4.10 Quantitative real-time polymerase chain reaction

Total nucleic acid extracted from gills was subjected to a SensiFast SYBR Green qPCR to determine the copy number of CqDV as previously described in 3.4.3.

Table 6.2: Primers used in the investigation of the CqDV transcriptome

Primer name	Sequence 5' – 3'	CqDV position
<b>Primers used for NS genes</b>		
SP5 CqDV NSF 193 <sup>a</sup>	<b><u>TAT AAA AAC</u></b> TGG TTA GAG GTT ATT TGA AGG	193-222
SP5 CqDV NSF 320 <sup>b</sup>	ATA AAA CCA GCG CGC AGA GC	320-340
SP5 CqDV NSF_342	GTG GAG CTC AGA TCT TCT GC	342-361
SP5 CqDV NSF 385	<b>ATG</b> GCT TGC GTA TAC GGT ATT G	385-406
CqDV 606 F	GGT ACA AGA GTA TCT CGA TTG G	606-627
Primer 2A reverse	TCT GAA TCA ATC TCC TCA CG	694-713
CqDV 1312 R	GTG TTC TGG TGA CAT CTC TTC CA	1312-1334
CqDV 1464 R	GGA TGT ACT TGG CTC AAC GG	1464-1483
CqDV 2281 R	CAG CTC TGG ATC ACA TCT C	2281-2299
CqDV 2592 F	GCA TTG TAA TTC ACT CAC CTC C	5892-2613
CqDV 2838 F	CTC CTG TGT ATC GTA CAC CTG	2838-2858
SP1 CqDV NSR 3004	<b>TTACCCTTCCACCAATTTACTTC</b>	3004-3028
<b>Primers used for VP genes</b>		
SP5 CqDV VPF 6150 <sup>a</sup>	<b><u>TAT AAA AAC</u></b> TGG TTA GAG GTT ATT TGA AGG	6150-6121
SP5 CqDV VPF 6069	TAT ATT TTG GAT TGG TTA ATG TTG AAA ATA	6069-6040
SP5 CqDV VPF 6024 <sup>b</sup>	AAT AAA ACC AGC GCG CAG A	6024-6006
SP5 CqDV VPF 5988	<b>ATG</b> GCT GAG GAA GCC TTC GA	5988-5969
CqDV 5367 R	GTT CAT ACG CTT TAT CGT GGT C	5388-5367
4552 Reverse	GTA CTA GGT TGC CGT AAA CC	4971-4952
CqDV 3923 R	GTA ATA ACA GGT GGA GTA GCT G	3944-3923
CqDV 3295 F	GAA TGA TAG CGC TAC CGC T	3313-3295
SP1 CqDV VPR 3180	CAC CAA AAC AGA CTT CTT ACG AAG	3180-3157
<b>RLM-RACE primers*</b>		
5' RACE Adaptor	GCUGAUGGCGAUGAAUGAACACUGCGUUUGCUGGCU UUGAUGAAA	NA
5' RACE Outer Primer	CTGATGGCGATGAATGAACACTG	NA
5' RACE Inner Primer	CGCGGATCCGAACACTGCGTTTGCTGGCTTTGATG	NA
3' RACE Adapter	GCGAGCACAGAATTAATACGACTCACTATAGGT <sub>12</sub> VN	NA
3' RACE Outer Primer	GCGAGCACAGAATTAATACGACT	NA
3' RACE Inner Primer	CGCGGATCCGAATTAATACGACTCACTATAGG	NA

<sup>a</sup> Primers are similar; <sup>b</sup> Primers supplied in RLM-RACE kit (Cat. AM1700); bold indicates start and stop codons; bold underline indicates promoter sequences.

### 6.2.5 Statistical analysis

Copy number mg<sup>-1</sup> of gill tissue was calculated from the qPCR and analysed in SPSS (IBM, version 23). Each time point-post injection was treated as a replicate. The copies mg<sup>-1</sup> were log<sub>10</sub> transformed to homogenise the variance. A One-Way ANOVA carried out on the transformed data.



Figure 6.1: Left side of CqDV (between nt 1 and 3,153) showing NS genes (orange). The hairpin is marked in yellow, P3 promoter in purple, PCR primers in green and polyadenylation signal in blue.



## 6.3 Results

### 6.3.1 Infection trial

No mortality was observed in the CqDV treatment group or the control group during the infection trial. Gross signs of disease and behavioural changes associated with CqDV infection were not observed.

### 6.3.2 Quantitative real-time polymerase chain reaction

Quantitative real-time PCR was used to assess the replication cycle of CqDV in the first 120 hours of infection. Whilst somewhat noisy, there was no statistical difference ( $P > 0.05$ ) between the time points tested (Figure 6.3).

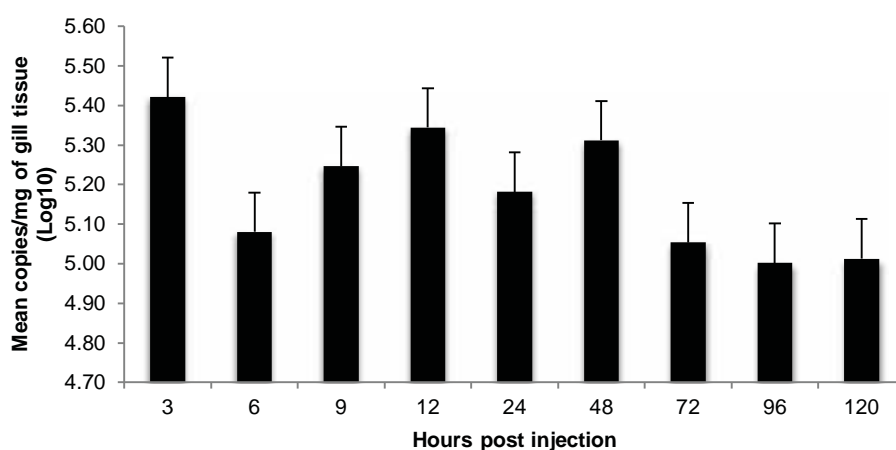


Figure 6.3: Viral copies  $\text{mg}^{-1}$  of CqDV in gill tissue of *C. quadricarinatus* between 3 and 120 hours post-injection of clarified homogenate. There was no significant difference between time points ( $P > 0.05$ ).

### 6.3.3 RNA quality check

The total RNA did not have a strong 28S peak but did have a strong 18S peak. The denaturation step failed to show an appreciable difference between treatments. Figure 6.4 is an example of electropherograms generated from the TapeStation using A15-052.5 extracted RNA. Despite the absence of the 28S peak, the RNA quality below 2000 nt (18S) is intact, where the CqDV transcripts would be found.

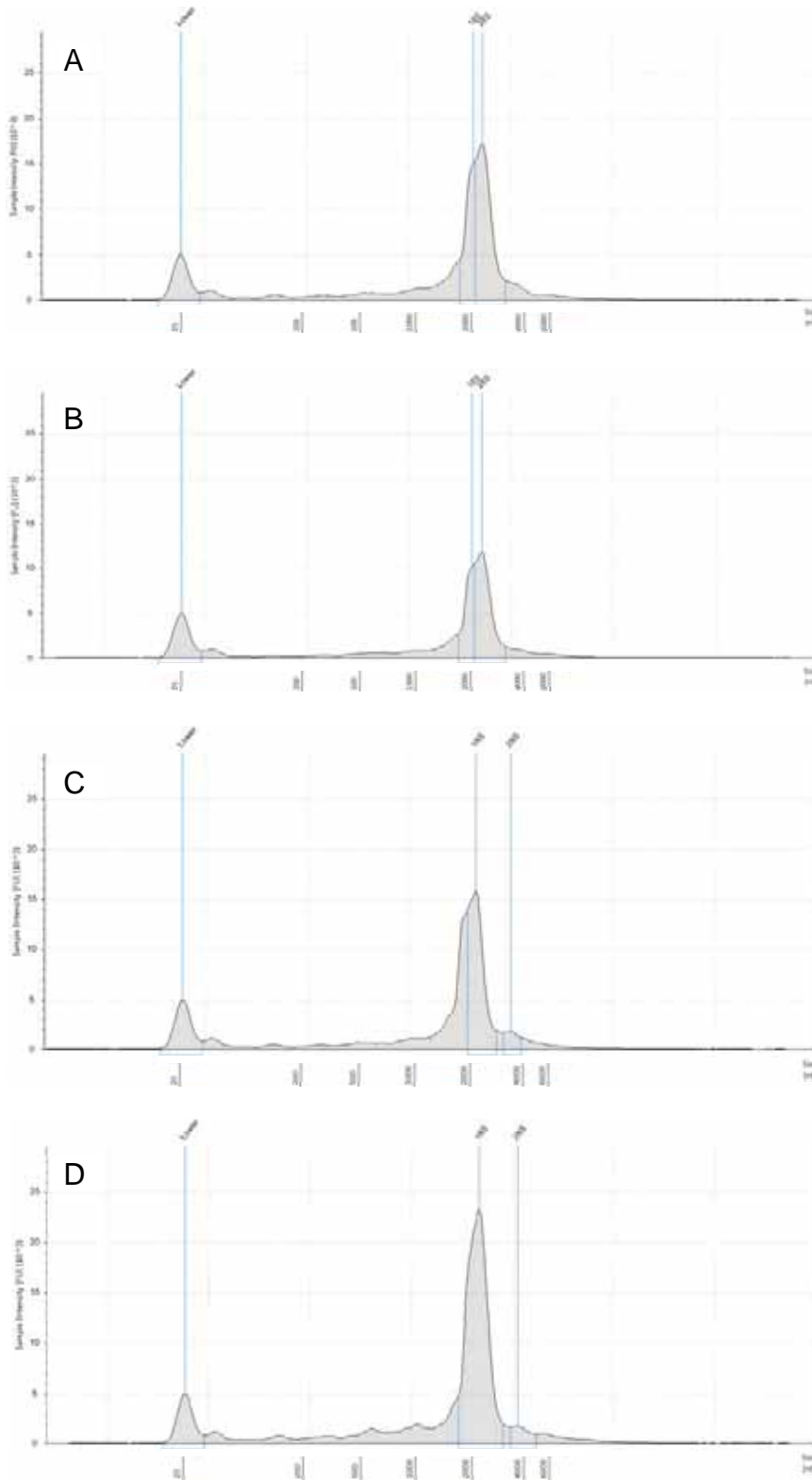


Figure 6.4: Electropherograms of heat denatured total RNA (A, B) and non-denatured RNA (C, D). There was no difference between treatments of the RNA. A and C; B and D are paired samples of A15-052.5 and A15-052.11 respectively. Peaks 5S, 18S and 28S are at approximately nt 25, 2,000 and 4,000 respectively. X-axis represents nucleotides and the Y-axis represents sample intensity.

### 6.3.4 Partial transcriptome analysis

Amplification of the 5' ends of the CqDV transcript using the RLM-RACE protocol and modified protocol failed. Although PCR product was obtained (data not shown) the resulting clones did not contain any CqDV cDNA. Amplification of the 3' ends also failed. Clones from these reactions did contain the 3' adaptor sequence and a poly A tail, but the nucleotide sequence was not CqDV cDNA.

Amplification of splice sites was successful using the Tetro cDNA Kit and random hexamer primers. Four splice sites (Splice A, B, C, D) were amplified on the left hand side of the genome (Figure 6.5A) in the NS genes while no splicing was found in the VP gene (data not shown). Splice A was the most similar to the consensus sequence for splice acceptor and donor sites outlined by Shapiro and Senapathy (1987). However, the splicing could produce new hypothetical proteins. The splice sites of CqDV did not match any found in other *Densovirinae* (Table 6.3).

Table 6.3: Comparison of *Densovirinae* donor and acceptor sites of the NS genes

Species	Splice	Donor site	nt position	Acceptor site	nt position
(Shapiro and Senapathy, 1987)		AG/GTAAGT <sup>a</sup>	NA	CAG/N <sup>a</sup>	NA
CqDV (KP410261)	A	GC/GCAGAG	333	TGT/C	1324
	B	TG/GTAAGC	379	GCA/G	1254
	C	CA/CGAGAA	808	CCA/G	1156
	D	GT/GACAAA	897	AAA/T	1203
PfDV (AB028936)		AC/AAAGCT	312	TAT/A	1120
BgDV (AY189948)		AG/GTACGT	275	GAG/A	1699
CpDV (FJ810126)		CG/GTAAGT	1721	CAG/A	1774
GmDV (L32896)		AG/GTATGT	655	CAG/A	1362
JcDV (S47266)		GG/TATGTC	564	AGA/T	1254
MIDV (AY461507)		AG/GTATGT	653	CAG/A	1356
AdDV (HQ827781)		AG/TAGAAG	241	CCG/T	840
PstDV1 (AF273215)		AT/GTAAGT	288	CAG/A	423

<sup>a</sup> Shapiro and Senapathy (1987) consensus sequence; / indicates splice site

Splice A was sequenced using primer set CqDV NSF 193 and CqDV 1464 R (Figure 6.5A, B) and contained the P3 promoter. Intron A was the largest intron at 991 nucleotides (Figure 6.5B) between nucleotides 333 and 1,324. The intron removed the NS3 ORF and the first 35 and 28 nucleotides of NS1 and NS2 respectively. Removal of the start codons from NS1 and NS2 could destroy the ability of NS 1 and NS2 to be transcribed. To investigate this further, the intron sequence was removed from the CqDV genome and the genome submitted to an ORF find search. Two new ORFs

were identified, ORF 2 $\alpha$  and ORF 3 $\alpha$  (Figure 6.5C).

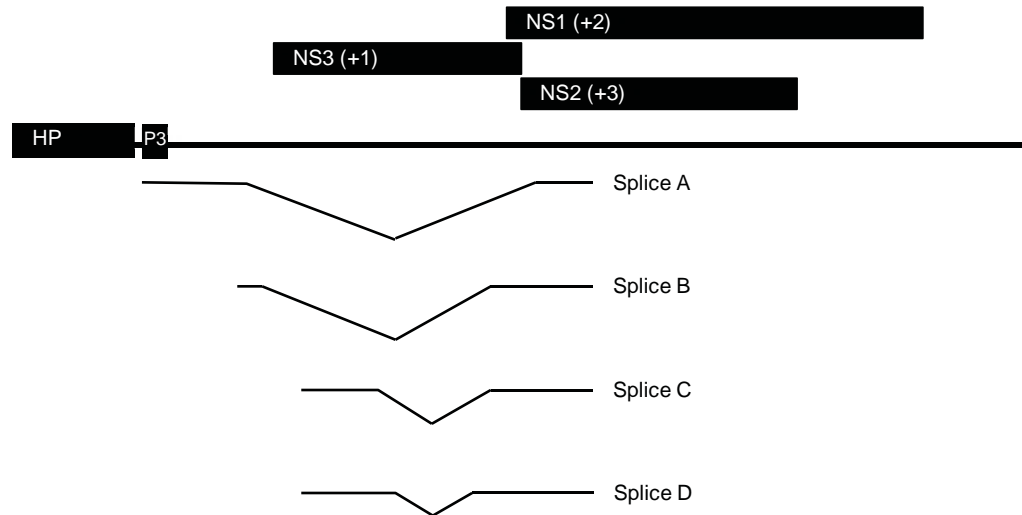
ORF 2 $\alpha$  was 481 amino acids long with a molecular weight of 56.6 kDa. Although the reading frame was +1 (original NS1 ORF 2 was +2) the new ORF 2 $\alpha$  was missing 98 amino acids from the N-terminus, but the remainder was identical to the original NS1 amino acid sequence. On the un-spliced CqDV genome, the new start codon is <sup>1583</sup>ATG; the original stop codon <sup>3026</sup>TAA is the same. There is a weak Kozak sequence (Kozak sequence RccATGG, R represents a purine (A/G) (Kozak, 1986)) at the start of ORF 2 $\alpha$  <sup>1580</sup>GatATGG. The highly conserved endonuclease and helicase amino acid motifs characteristic of parvovirus NS1 were identified in ORF 2 $\alpha$ . The endonuclease motifs were located between amino acids 66-71 and 120-125 and the helicase motifs between amino acids 340-356, 385-391 and 424-431 and were identical to that of the original CqDV NS1 ORF.

ORF 3 $\alpha$  was 270 amino acids long with a molecular weight of 30.9 kDa and had a +2 reading frame. ORF 3 $\alpha$  was equivalent to NS2 ORF 3 with a new start codon <sup>1401</sup>ATG; the original stop codon <sup>2211</sup>TAA is the same. A weak Kozak sequence was also identified at <sup>1398</sup>GgaATGa.

Splice B was sequenced using primer set NSF 342 and CqDV 1464 (Figure 6.5A, B). Intron B was 875 nucleotides long between 379 and 1,253 (Figure 6.5A, B). Intron B removed the majority of the NS3 ORF leaving 43 nucleotides between the end of the intron and the <sup>1294</sup>TAA stop codon of NS3.

Splice C and D were sequenced using primer set CqDV 606 F and CqDV 1464 R. Intron C is 348 nucleotides long between 808 and 1,155 while intron D is 306 nucleotides long between 897 and 1,202. The removal of both intron sequences produces two new NS3 ORFs, NS3 ORF 1 $\alpha$  and NS3 ORF 1 $\beta$ . NS3 ORF 1 $\alpha$  is produced from splice C and is 187 amino acids in length with a molecular weight of 21.8 kDa. NS3 ORF 2 $\beta$  is produced from intron D and is 201 amino acids in length with a molecular weight of 23.3 kDa. Both ORF 1 $\alpha$  and NS3 ORF 2 $\beta$  had a +1 reading frame and had identical amino acids compared to the original NS3 expect the amino acids removed due to splicing in the mRNA. The original start codon <sup>385</sup>ATG and stop codon <sup>1294</sup>TAA remained the same.

A



B

Clone A: <sup>193</sup>TATAAAAA...N<sub>122</sub> <sup>323</sup>AAACCAGCGC/<sup>1324</sup>CACCAGAACA N<sub>140</sub>... <sup>1474</sup>AAGTACATCC  
 Clone B: <sup>342</sup>GTGGAGCTCA...N<sub>17</sub> <sup>369</sup>ACTACTACTG/<sup>1254</sup>GGAACCACCA N<sub>210</sub>... <sup>1474</sup>AAGTACATCC  
 Clone C: <sup>606</sup>GGTACAAGAG...N<sub>182</sub> <sup>798</sup>AATGACTGCA/<sup>1155</sup>GACTGCAAAC N<sub>308</sub>... <sup>1474</sup>AAGTACATCC  
 Clone D: <sup>606</sup>GGTACAAGAG...N<sub>686</sub> <sup>887</sup>TTGGTACAGT/<sup>1203</sup>TACTTATGTG N<sub>261</sub>... <sup>1474</sup>AAGTACATCC

C

NS1 ORF 2 $\alpha$ : <sup>193</sup>TATAAAAA...N<sub>122</sub> <sup>323</sup>AAACCAGCGC/<sup>1324</sup>CACCAGAACA N<sub>293</sub>...  
<sup>1573</sup>CGGGCCAGAT**AT**GGAACAAC N<sub>1426</sub>... <sup>3019</sup>GGAAGGG**TAA**  
 NS2 ORF 3 $\alpha$ : <sup>193</sup>TATAAAAA...N<sub>122</sub> <sup>323</sup>AAACCAGCGC/<sup>1324</sup>CACCAGAACA N<sub>57</sub>...  
<sup>1391</sup>GAAAGACGGA**AT**GACAGCGG N<sub>793</sub>... <sup>2204</sup>ATACAG**TAA**  
 NS3 ORF 1 $\alpha$ : <sup>193</sup>TATAAAAA...N<sub>597</sub>... <sup>798</sup>AATGACTGCA/<sup>1155</sup>GACTGCAAAC N<sub>121</sub>... <sup>1287</sup>CCATGA**TAA**  
 NS3 ORF 1 $\beta$ : <sup>193</sup>TATAAAAA...N<sub>686</sub> <sup>887</sup>TTGGTACAGT/<sup>1203</sup>TACTTATGTG N<sub>74</sub>... <sup>1287</sup>CCATGA**TAA**

Figure 6.5: A. Left hand side of the CqDV genome showing hairpin (HP), promoter (P3) and NS genes. Below the solid black line are the four splice sites A, B, C and D represented by inverted triangles orientated against the NS genes above the black line. B. The sequence of the four clones showing where the splice sites were found. C. New hypothetical ORFs generated from splicing of the mRNA from CqDV. Superscript numbers indicate nucleotide position on the CqDV un-spliced genome. / represent the splice sites. N with subscript represents number of nucleotides between sequences presented. Underlined ATG is the start codon of NS1. Bold ATG indicates new start codons from spliced cDNA. Bold TAA indicates stop codons.

## 6.4 Discussion

Previous results have highlighted that infection of *C. quadricarinatus* with CqDV is chronic. Mortality is slow to start but reaches 100 % 60-73 days post-injection while signs of disease take 17-22 days to present (Bowater *et al.*, 2002) (Chapter 7). These results were repeated here, with no morbidity, mortality or signs of CqDV infection being found within the first 120 hours of infection.

Phylogenetically, CqDV is most related to the SSaDV (KM052275) and blattodean-infecting densovirus (PfDV AF192260 and BgDV AY189948) (Bochow *et al.*, 2015). PfDV and BgDV splice their mRNA during replication (Yamagishi *et al.*, 1999; Yang *et al.*, 2008; Kapelinskaya *et al.*, 2011). To investigate if CqDV used a similar mechanism of splicing during transcription, RLM-RACE was used to identify the 5' and 3' ends of the CqDV mRNA during the early stages of infection. The standard kit protocol and modified versions failed to produce PCR product for cloning despite the RNA being of high quality. The 28S band that is used to assess quality of RNA should appear as a clear band or peak when being analysed; however, the total RNA from Trizol extractions did not form a single 28S peak. Crustaceans and insects contain a hidden break within their 28S RNA, which upon denaturation typically used before analysis, breaks the 28S into two fragments that are approximately the same size as the 18S (Winnebeck *et al.*, 2010; McCarthy *et al.*, 2015). These authors suggest that, despite the poor RNA integrity number (RIN) from degraded 28S peaks, the RNA is still of high quality and is not degraded. Based on the results here, it is likely that, like many other invertebrates, *C. quadricarinatus* 28S has a hidden break that causes the 28S to break and run closer to the 18S. To increase the chance of RACE PCR success in the future, an mRNA Isolation Kit (e.g. Cat. No. 11741985001, Roche) should be used along with pleopod, to recover mRNA from total RNA extractions, removing unwanted rRNA. As the RACE failed, it is unclear where transcription starts and stops, nevertheless, splice sites within the mRNA were identified for the NS ORFs using RT-PCR.

*Cherax quadricarinatus* densovirus is 6,334 nt long and has 4 ORFs. Three NS genes are on the top strand from the 5' end and one, the VP gene, is on the bottom strand

starting from the 5' end. The genome is bracketed by inverted terminal repeats. Like other DNV genomes, CqDV uses alternative splicing to express ORFs for expression of NS proteins. The transcriptome analysis revealed four splices within the NS genes. Splice A completely removes the NS3 ORF and the start codons of NS1 and NS2. However, two new proteins could hypothetically be generated from start codons downstream of Splice A. NS1 ORF 2 $\alpha$  and NS2 ORF 3 $\alpha$  are truncated versions of the original NS1 and NS2 ORFs. NS1 ORF 2 $\alpha$  still retains the functional endonuclease and helicase motifs used by NS1 for various roles during a parvovirus lifecycle (Nüesch *et al.*, 1995; Op De Beeck and Caillet-Fauquet, 1997). One other of the *Densovirinae* has splicing that removes the ATG codon of NS1. Like CqDV, the splice NSSp12 in BgDV (AY189948) mRNA removes all of the NS3 ORF and half of the NS1 NS2 ORF. The resulting mRNA codes for a 501 nucleotide ORF identical to the 3' half of the original BgDV NS1 ORF (Wang *et al.*, 2013). In both instances, it is not known if the new ORFs generate functional NS1 and NS2 like proteins, but as the reading frames are intact, it appears likely.

Splice B of CqDV is similar to those of the blattodean-infecting densoviruses and *Lepidopteran ambidensovirus 1*. PfDV (AB028936) (Yang *et al.*, 2008), BgDV (AY189948) (Kapelinskaya *et al.*, 2011), MIDV (AY461507) (Fédière *et al.*, 2004), GmDV (L32896) (Tijssen *et al.*, 2003), JcDV (S47266) (Wang *et al.*, 2013) and AdDV (Liu *et al.*, 2011) all share a common splice in their NS3 ORF. This single large splice removes the coding capacity of the NS3 ORF. Like these genomes, splice B in the CqDV mRNA also removes the coding capacity of the NS3 ORF. This splice moves the promoter elements and transcription sites closer to the start of NS1 and NS2. As NS1 is in an unfavorable context (poor Kozak sequence), the ribosome can bypass it and move to the second ATG, the start of NS2, leading to leaking scanning mechanism of the mRNA (Tijssen *et al.*, 2003; Yang *et al.*, 2008). However, NS1 of CqDV has a stronger Kozak sequence (<sup>1286</sup>TCCATGA) than that of NS2 (<sup>1293</sup>ATAATGT).

The function of NS3 in the life cycle of the *Ambidensovirus* is thought to contribute to the viral DNA replication (Abd-Alla *et al.*, 2004). CqDV has two unique splices in NS3 that are not found in other *Ambidensovirus* members. Splice C and D remove 348 and 306 nt respectively. These splices can result in two new hypothetical

isoforms of NS3. These splices are unique within the *Ambidensovirus* genes and the functions of the potentially new NS3 isoforms are unknown at this time.

A single TATA box (P3) has been identified at nt 193 and is the hypothetical promoter that drives CqDV NS expression. Other members of the *Ambidensovirus*, such as BgDV (Kapelninskaya *et al.*, 2011), PfDV (Yang *et al.*, 2008), MIDV (Fédière *et al.*, 2004) and GmDV (Tijssen *et al.*, 2003) use a single promoter upstream of their NS start codons to drive NS expression. Northern blotting of RNA from these viruses also show that the spliced transcripts are generated from the large un-spliced NS transcript. Although RACE failed to identify the start of the CqDV NS transcripts, it is likely that the P3 promoter drives expression of the NS transcripts as no other promoter-like sequence has been identified. It is also likely that a single CqDV NS transcript is spliced to generate the smaller transcripts, although northern blotting and RACE PCR is needed to confirm this. However, the CqDV clone containing Splice A was detected using primer SP CqDV NSF 193 which binds to the P3 promoter. It is unclear if this is the true start of the NS transcript of CqDV, as NS transcription starts upstream of the NS3 start codon but down stream of the promoter elements in other *Ambidensovirus* species.

The qPCR results are consistent with those of Chapter 7. In the first week post-injection with a CqDV-containing homogenate, CqDV copy number remained flat in the first week (see Figure 7.3, Chapter 7). These results are consistent with the finding presented here. In the first 120 hours after injection, there was no statistically significant change in copy number and CqDV does not appear to have a high replication rate in the first week of infection. This significance of this is unknown; however, it is clear that in the following weeks the copy number more than doubles (see Figure 7.3, Chapter 7).

## **6.5 Conclusion**

Future work should focus on sequencing the 5' and 3' ends of the CqDV transcripts. This will answer the question of where transcription starts and finishes and identify if the CqDV transcript starts at the P3 promoter. The new ORFs generated should be

expressed as proteins and tested for their function in CqDV to assess their role in the lifecycle of CqDV. Using the samples generated here; transcriptome analysis should be performed on all time points of this experiment to determine the temporal order of splicing during replication. If qPCR is to be performed on the cDNA extracts in future, then a new qPCR will need to be developed as the DNA region that is targeted by the current qPCR primers is spliced out between transcription and translation. Thus the current qPCR would not give an accurate representation of copy number.

**CHAPTER 7: Translocation of *Cherax* species crayfish  
across zoogeographical zones within Australia; potential to  
spread highly pathogenic *Cherax quadricarinatus*  
densovirus**

## 7.1 Introduction

The Australian freshwater crustacean industry produces various species for the aquarium, live feed and restaurant trades. The main crayfish cultured include *Cherax quadricarinatus* in northern Australia valued in 2013 \$USD 715,000, *C. destructor* in southeastern and western Australia valued at \$USD 698,000 and *C. tenuimanus* in southwestern Australia valued at \$USD 1,822,000 (FAO). Production systems are purpose-built earthen ponds or agricultural farm dams and are considered semi-intensive (Merrick and Lambert, 1991). Intensive hatchery based production of craylings has been developed in the *C. quadricarinatus* industry of northern Queensland.

A number of uncharacterised potential pathogens have been identified in the Australian freshwater crayfish industry. These include *Achlya*-like fungus, *Psorospermium*, *Thelohania* sp. (Carstairs, 1978; Herbert, 1987), *Cherax* baculovirus (Anderson and Prior, 1992), *Cherax* Giardiavirus-like virus (Edgerton *et al.*, 1994) *Cherax quadricarinatus* bacilliform virus (Edgerton, 1996), *Cherax destructor* systemic parvo-like virus (Edgerton *et al.*, 1997), a *Coxiella rickettsia* (Tan and Owens, 2000), presumptive hepatopancreatic reovirus and putative gill parvovirus (Edgerton *et al.*, 2000). Surveys have also identified pathological lesions of interest (Edgerton and Owens, 1999; Jones and Lawrence, 2001). There are no reports suggesting that these pathogens cause mass mortality events in cultured freshwater crayfish. However mass mortality events in *C. quadricarinatus* due to vibriosis have been reported (Eaves and Ketterer, 1994). Except for *Cherax* reovirus (Hayakijkosol and Owens, 2011), these pathogens have not been isolated, characterised or used to recreate disease in their respective hosts. Their prevalence and effect on the culture of freshwater crayfish in Australia remains unknown.

In December 1999 to January 2000, an epizootic occurred that was attributed to a suspected parvovirus at a *C. quadricarinatus* farm in northern Queensland. On going morbidity and mortality occurred over three-months that affected juvenile and adult *C. quadricarinatus*. The parvovirus was isolated and used in infection trails to successfully recreate the disease. Using histopathology and transmission electron

microscopy, the virus was named *Cherax quadricarinatus* parvovirus-like (Bowater *et al.*, 2002). The virus was re-isolated from tissue originating from the first, and only, outbreak and its genome sequenced (Bochow *et al.*, 2015). The virus has been re-classified as *Cherax quadricarinatus* densovirus (CqDV) (GenBank KP410261) of the subfamily *Densovirinae*, genus *Ambidensovirus* and shares 75 % nucleotide homology across the entire genome with sea star-associated densovirus (SSaDV) (KM52275).

Some members of the *Densovirinae* have been shown to have a wide host range. Penaeid prawns have suffered epizootics from *Penaeus stylirostris* penstyldensovirus (PstDV) (Lightner *et al.*, 1983) and *Penaeus monodon* hependensovirus (PmoHDV) (Lightner and Redman, 1985). PstDV causes severe mortality in *P. stylirostris* but runt deformity syndrome in *P. vannamei* and *P. monodon*. Infection can be identified in both species by histopathology (Bell and Lightner, 1984). Members of the *Ambidensovirus*, of which CqDV is a member, can also have broad host ranges. *Mythimna loreyi* densovirus (MIDV) has been isolated from five different genera (Fédière *et al.*, 2004), while *Periplaneta fuliginosa* densovirus (PfDV) can infect different members of the *Periplaneta*. *Junonia coenia* densovirus (JcDV) can infect multiple members of the *Lepidoptera* (Bergoin and Tijssen, 2008). SSaDV has been found in two families and orders (*Asteriidae* (order *Forcipulatida*) and *Asterinidae* (order *Valvatida*)) of asteroids a unique feature among the *Densovirinae*, and at least twenty different species (Hewson *et al.*, 2014).

Given that a restricted host range seems uncommon and CqDV and the multihost SSaDV are related, we set out to investigate if CqDV could infect another commercially cultured freshwater crayfish. *C. destructor* was chosen because the southern and northern most ranges for culture of *C. quadricarinatus* and *C. destructor* respectively overlap. The aim of this experiment was to assess if CqDV could (i) cause gross signs of disease, particularly blistering of the branchial membrane, a unique feature of CqDV infection in *C. quadricarinatus*, (ii) cause histopathological changes similar to those found in CqDV infected *C. quadricarinatus*, (iii) determine if the copy number of CqDV in *C. destructor* is similar to that of *C. quadricarinatus* using quantitative real-time PCR (qPCR).

## 7.2 Materials and methods

### 7.2.1 Experimental *Cherax* species

*C. quadricarinatus* and *C. destructor* were sourced from commercial farms in northern Queensland and NSW respectively in June 2014. Dead-on-arrival *C. destructor* were immediately frozen. Crayfish were housed at James Cook University's Aquatic Pathology Laboratory in individually recirculating 1,000 L plastic tanks (Table 7.1) as previously described in 3.1.

Table 7.1: Distribution of crayfish in CqDV infection trial

Tank number	<i>n</i>	Species	Treatment group
A14-029	11	<i>C. destructor</i>	Negative control, no injection
A14-030	11	<i>C. destructor</i>	CqDV injection
A14-031	14	<i>C. destructor</i>	CqDV injection
A15-032	14	<i>C. destructor</i>	CqDV injection
A15-033	15	<i>C. quadricarinatus</i>	Positive control, CqDV injection

### 7.2.2 Experimental trial

The aim of the trial was to investigate if CqDV could cause disease in *C. destructor*. *C. quadricarinatus* were used to confirm that the homogenate containing CqDV was infectious. The negative control, no injection *C. destructor* were used to confirm that CqDV was not present in the *C. destructor* upon starting the trial and that no contamination occurred during the trial. Therefore these control components were not replicated to meet the principle of active animal ethics, reducing the number of animals used in experimentation.

Each crayfish was numbered by removing a pleopod in a sequential order. To standardise dose for weight differences, *C. destructor* (mean weight 15.8 g, *n* = 43) and *C. quadricarinatus* (22.4 g, *n* = 15) were injected with 60  $\mu$ L and 90  $\mu$ L respectively of CqDV clarified supernatant (as per section 3.2.1) (approximately 4  $\mu$ L g<sup>-1</sup> or 10<sup>-8</sup> copies g<sup>-1</sup>), using 1 mL luer slip syringes (Cat. 1018242, SSS Australia Healthcare Supplies, Brisbane) and 30G x 13 mm Microlance needles (Cat. 1263187, SSS Australian Healthcare Supplies, Brisbane). A14-029 (negative control, no injection *C. destructor*) were bled at week 1, and the crayfish in the other tanks

were infected on successive days (week 1) and bled every 7 days starting at week 2 for 8 weeks. Approximately 100 – 200 µL of hemolymph was drawn directly into Binding Buffer (Cat. 11858874001 Roche, NSW) from the heart sinus using syringes and needles described above. *C. destructor* in triplicate treatments, were injected with CqDV while a single *C. quadricarinatus* treatment was used as CqDV positive control (Table 7.1). Moribund crayfish were removed from tanks, euthanised and frozen at -20 °C. All mortalities were recorded.

### **7.2.3 Histopathology**

During the trial, moribund crayfish were killed by severing the cephalothorax from the abdomen and processed for histology as previously described in 3.5.

### **7.2.4 Molecular biology**

#### 7.2.4.1 Nucleic acid extraction

Viral nucleic acid was extracted from haemolymph as previously described in 3.3.1.

#### 7.2.4.2 Preparation of synthetic control for quantitative real-time polymerase chain reaction

A synthetic control for qPCR was prepared as previously described in 3.4.1.

#### 7.2.4.3 Standard curve preparation

A standard curve was prepared for the qPCR as previously described in 3.4.2.

#### 7.2.4.4 SYBR Green quantitative real-time polymerase chain reaction

Total nucleic acid extracted from gills was subjected to a SensiFast SYBR Green qPCR to determine the copy number of CqDV as previously described in 3.4.3.

### 7.2.5 Statistical analysis

Copy number  $\text{mg}^{-1}$  of haemolymph was calculated from the qPCR and analysed in SPSS (IBM, version 23). The three *C. destructor* (Table 7.1) replicate treatments infected with CqDV were pooled into a single treatment after preliminary statistics showed no significant differences between replicates and a univariate ANOVA was carried out on copy numbers  $\log_{10}$  transformed to homogenise the variances.

Mortality was treated the same, with *C. destructor* infected with CqDV pooled into a single treatment. Survival graphs and analysis was carried out in Prism (GraphPad software, Inc, version 6.0h).

## 7.3 Results

### 7.3.1 Infection trial

On arrival to the laboratory, the *C. destructor* appeared highly stressed. Their pereopods were reddish-pink and four were dead on arrival. Mortalities were also observed leading up to the start of the trial. Of the original 61 *C. destructor* stocked into the 4 tanks, 50 were remaining at the start of the trial. All *C. quadricarinatus* appeared healthy on arrival and no mortalities were observed leading up to the start of the trial.

Daily observations of the *C. destructor* treatment groups showed no signs of obvious morbidity throughout the trial. *C. destructor* were highly active, especially during feeding, and started to breed during the trial. During weekly bleeding, the *C. destructor* were handled, and showed strong tail flicking and actively avoided capture. *C. quadricarinatus* showed similar behaviour for the first 22 days. However after this, *C. quadricarinatus* became lethargic, migrated to the surface of the water, were easily handled with weak tail flicks and were unable to right themselves when placed on their dorsal side. The carapace was a reddish pink colour and white spots developed on the branchial carapace. The defining feature was the severely blistered inner brachial membrane between the carapace and the gills.

For statistical analysis, the null hypothesis was that *C. destructor* would not be affected by CqDV. The survival analysis showed that there was no significant difference between the negative control *C. destructor* and the *C. destructor* + CqDV treatments (Mantel-Cox = 3.287, d.f. = 1,  $p = 0.0698$ ). Survival curves indicated that positive control *C. quadricarinatus* suffered the highest mortality at the end of the trial (Figure 7.1).

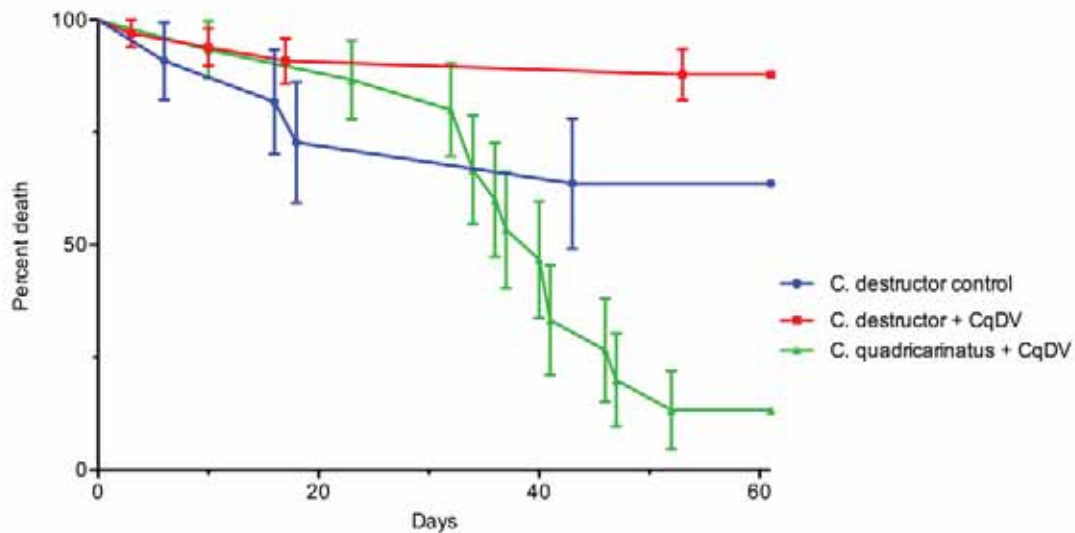


Figure 7.1: Mortality of *Cherax* species over 61 days of the trial. Although the negative control *C. destructor* apparently suffered higher mortalities than the *C. destructor* + CqDV treatment, it was not statistically significant ( $P > 0.05$ ).

### 7.3.2 Histology

Negative control *C. destructor* did not present any lesions. Despite the detection of CqDV in the *C. destructor* + CqDV treatment groups (see below), histopathological changes associated with CqDV infection were not observed in any tissue in this group (Figure 7.2). In contrast, *C. quadricarinatus* were heavily infected and produced large basophilic inclusion bodies in tissues including the gills and cuticular epithelium (Figure 7.2). The labyrinth/coelomosac complex of the antennal gland was sparsely infected while the tubules of the antennal gland were not infected.

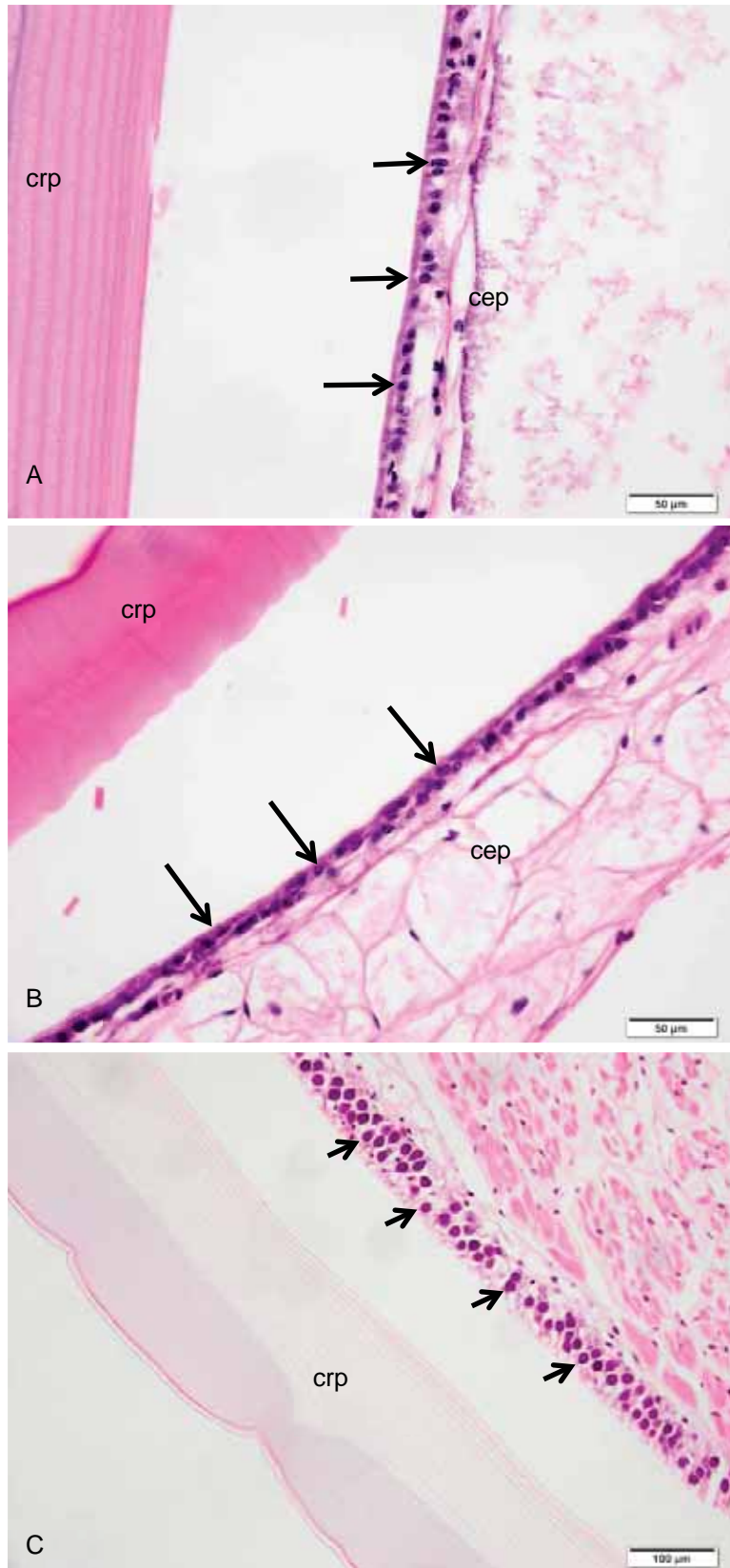


Figure 7.2: Epithelial cells of the three control and treatment groups. A. *C. destructor* control group did not show any lesions (long arrows). B. *C. destructor* + CqDV did not show basophilic inclusion bodies characteristic of CqDV (long arrows). C. *C. quadricarinatus* + CqDV, short arrows indicate large basophilic inclusion bodies. cep: cuticular epidermis, crp: carapace. All figures are stained with H&E.

### 7.3.3 Quantitative real-time polymerase chain reaction

The number of copies of CqDV  $\text{mg}^{-1}$  of haemolymph was significantly different between all treatment groups ( $p = < 0.0001$ ). CqDV could not be detected in negative control *C. destructor* over the course of the trial. *C. destructor* infected with CqDV had on average, lower copies of CqDV compared to that of *C. quadricarinatus*. The apparent trend was as follows: Copy numbers in *C. destructor* + CqDV increased rapidly to 1,320 copies in the first week of the trial before dropping between weeks 2 to 5 to 716 copies at which time copy number increased again to 1,261 copies (Figure 7.3). However, there was no statistically significant difference in copy numbers between weeks in the *C. destructor* + CqDV treatment. It is likely that the high individual variance of copy number masks statistical significance.

Copy numbers increased in *C. quadricarinatus* between weeks 2 to 4 topping at 1,744,130 copies and then precipitously declined as *C. quadricarinatus* died. After day 28 (week 4), mortalities started to occur and continued for the remainder of the trial. The mortalities corresponded to *C. quadricarinatus* that had the highest copy number which caused the treatment copy number to decrease as infected *C. quadricarinatus* were removed from the trial by mortality (data not shown). At week 6, only two *C. quadricarinatus* remained, A14-033.1 and A14-033.2. *C. quadricarinatus* A14-033.1 was negative for CqDV at weeks 7 and 8 while A14-033.2 had a copy numbers below detectible levels throughout the entire trial (presumptively not infected).

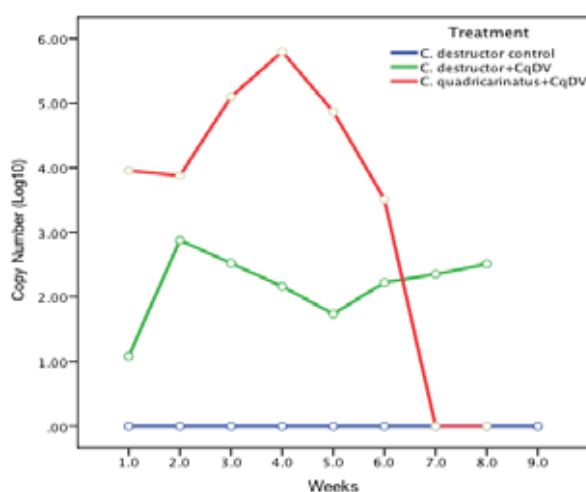


Figure 7.3: Mean copy number of CqDV  $\text{mg}^{-1}$  of hemolymph of each treatment group.

## 7.4 Discussion

CqDV is the first viral pathogen infecting *Cherax* spp. to be isolated and its genome characterised (Bochow *et al.*, 2015). Histopathology, transmission electron microscopy (TEM) and qPCR have been developed which have identified the tissue tropism of CqDV (Chapter 4). The partial transcriptome has also been sequenced which in the future will lead to a better understanding of the CqDV replication strategy (Chapter 7). CqDV was further characterised by studying its' impact on another commercially cultured freshwater crayfish, *C. destructor*.

There have been four published reports, indicating that parvovirus infect freshwater *Cherax* species. The first report was a single moribund *C. destructor* submitted for histology and TEM, revealing Cowdry Type A intranuclear inclusions and icosahedral virion particles of approximately 20 nm (Edgerton *et al.*, 1997). A putative gill parvovirus was also found in *C. quadricarinatus* during a failed gill-associated virus transmission trial (Edgerton *et al.*, 2000). Also, the presumptive parvovirus, spawner-isolated mortality virus was detected by gene probe in *C. quadricarinatus* (Owens and McElnea, 2000). The only parvovirus proven to cause an epizootic is CqDV, first isolated by Bowater *et al.* (2002), and the only *C. quadricarinatus* infecting densovirus to be sequenced (Bochow *et al.*, 2015). There is limited information on viral infection studies in *C. quadricarinatus* and no information for *C. destructor* as crayfish specific viral pathogens have not been characterised from these crayfish. This represents the first study assessing the host susceptibility of a different freshwater crayfish to CqDV.

The positive control *C. quadricarinatus* infected with CqDV showed typical signs of CqDV infection. These included white spots on the inside of the carapace, reddish colouration of the abdomen and pereopods, migration to the surface, and uniquely to CqDV, branchial membrane blistering and finally morbidity. Clearly the dose was infective with CqDV. Of the 15 *C. quadricarinatus* infected, only two survived to the end of the trial. *C. quadricarinatus* A14-033.1 was infected from weeks 1 to 6 before CqDV was undetectable with the qPCR. *C. quadricarinatus* A14-033.2 was presumptively negative throughout the trial. Perhaps this *C. quadricarinatus* may not

have not have received a CqDV injection at the start of the trial. In contrast, all *C. destructor* appeared healthy and showed no clinical signs of CqDV infection throughout the trial and even started breeding during the trial. It is unclear why there were mortalities in the negative control *C. destructor* which remained below detectable levels (nominal negatives) for CqDV throughout the trial. On histopathological examination, they had no noticeable lesions from any known agent (see below).

The results of the infection trial indicate that CqDV can be detected in *C. destructor* eight weeks post-injection. During the first week, CqDV increased almost two logs in *C. destructor* before falling away at week 5 where perhaps another half-log increase in CqDV copy number was detected. In penaeid prawns, stress can cause persistent viral infections to become lethal (Flegel and Pasharawipas, 1998). Throughout the trial, the routine of observations, animal husbandry and haemolymph collection remained constant, as were the environmental conditions. A stress event was not perceived at week 5 that could have caused the possible increase in viral copy number in *C. destructor*.

Histopathology of negative control and infected *C. destructor* did not show any lesions. Histopathological examination of the negative control *C. destructor* and *C. destructor* + CqDV revealed both treatments to be healthy despite the qPCR detecting CqDV copies in the *C. destructor* + CqDV treatment group. There were no observed cytoplasmic or nuclear inclusions indicative of viral infection found in either treatment. Granulomas, melanisation, necrosis, bacteraemia and fungi were not observed in any tissues of the *C. destructor* groups. In the absence of any histopathological changes to give a lead, further molecular investigation was deemed impractical. There are also no published reports of natural infections of penaeid prawn viruses infecting *Cherax* species. However, *C. quadricarinatus* have been shown experimentally to carry *Penaeus merguensis* densovirus for up to 30 days which greatly stressed the *C. quadricarinatus* allowing other pathogens to kill almost 50% of the *C. quadricarinatus* (La Fauce and Owens, 2007).

In comparison, the positive control, *C. quadricarinatus* + CqDV presented with typical large basophilic Cowdry Type A inclusion bodies (Bowater *et al.*, 2002).

However, Bowater *et al.* (2002) showed that the antennal gland tubules were infected (their Figure 6) but we were unable to find viral inclusions in this part of the gland.

*Densovirinae* have been reported in penaeid prawns that can show varied responses to infection. For example, PstDV is highly pathogenic to *P. stylirostris* causing 80% to 99% mortality (Lightner *et al.*, 1983). However, infection of *P. vannamei* does not show significant mortality (Lightner *et al.*, 1983) but does cause runt deformity syndrome (Kalagayan *et al.*, 1991). In *P. monodon*, PstDV is generally considered as subclinical (Flegel, 2006). Using PCR, *P. monodon* were found to be PCR positive for PstDV but were histologically negative (Flegel *et al.*, 2004), however it was later found that the primers used in that study cross-reacted with endogenous viral elements of PstDV (Tang and Lightner, 2006) in *P. monodon* which may explain these contrary results. Similarly, Chayaburakul *et al.* (2005) found identical results, with grossly normal *P. monodon* being PCR-positive for PstDV but histologically negative. To confirm their results, Chayaburakul *et al.* (2005) used TEM to show paracrystalline arrays of virions of approximately 22 nm in diameter. It is possible that the qPCR detected the original viral inoculum injected into *C. destructor* and that *C. destructor* were unable to clear CqDV during the trial period. Further investigation is needed to clarify this; CqDV should be re-isolated from *C. destructor* and injected into *C. quadricarinatus*. Tissue from CqDV-positive *C. destructor* should also be fed to *C. quadricarinatus*. Finally, mRNA from CqDV-positive *C. destructor* should be used in PCR to determine if CqDV is replicating. However, because of the splicing pattern of CqDV (see Chapter 6) a new quantitative real-time PCR will need to be developed to assess replication of CqDV.

Although CqDV infects *C. quadricarinatus*, CqDV is an *Ambidensovirus* and is not related to other known crustacean infecting densovirus (Bochow *et al.*, 2015). Most members of the *Ambidensovirus* are known to have a wide host range and infect multiple genera (Fédière *et al.*, 2004; Bergoin and Tijssen, 2008; Hewson *et al.*, 2014). The closest known relative of CqDV is SSaDV which shares 75% nucleotide homology and has been reputed to cause sea star wasting disease in up to twenty different species of asteroids (Hewson *et al.*, 2014). CqDV did not cause clinical signs of infections in *C. destructor*, but the virus was present, the number of copies was statistically stable and therefore it was not cleared over weeks suggesting prolonged

carrier status, indicative of a wider host range similar to other members of the *Densovirinae*

## 7.5 Conclusion

*Cherax destructor* may be classified as asymptomatic carriers of CqDV as the copy number did not statistically decrease and was trending to increase when the trial ended. Because of the lack of identifiable lesions, *in situ* hybridization followed by TEM should be performed to identify target cells of CqDV infection in *C. destructor*. Future research should focus on identifying if CqDV can be re-isolated from *C. destructor* and if CqDV can then re-infect *C. quadricarinatus* via feeding of infected tissue and/or injected clarified homogenate. These experiments should include other commercially cultured freshwater crayfish such as *C. tenuimanus*.

Assuming that *C. destructor* can, at the very least, be a carrier of CqDV, this has implications for translocation of freshwater crayfish within Australia. If *C. quadricarinatus* viruses can be carried by *C. destructor* and vice-versa, their translocation across zoogeographical zones may pose a risk to established farms. There is currently no diagnostic testing of freshwater crayfish being moved within Australia.

## **CHAPTER 8: General discussion**

## 8.1 Background

Early reports of viral disease in Australian *Cherax* spp. were observational and opportunistic in nature. Viral pathogens were characterised based on their histopathological presentation and transmission electron microscopy. These reports led to the pathogens being identified in high taxonomic rankings. No work has been reported to characterise, in detail, the viral pathogens of Australian *Cherax* species (Anderson and Prior, 1992; Edgerton *et al.*, 1994; Edgerton, 1996; Edgerton *et al.*, 2000; Jones and Lawrence, 2001; Hayakijkosol and Owens, 2011). The prevalence and pathogenicity of these viral pathogens remains unknown.

The most extensively studied viral pathogen of *C. quadricarinatus* is *Cherax quadricarinatus* densovirus (CqDV) (reported by Bowater *et al.* (2002) as *Cherax quadricarinatus* parvo-like virus (CqPV)). CqDV was isolated from an epizootic event affecting juvenile and adult *Cherax quadricarinatus* on a single farm in northern Queensland. The isolate was used to recreate disease in the laboratory, and was characterised with histopathology and transmission electron microscopy.

We obtained the isolate from staff from the Queensland Government's former Tropical and Aquatic Animal Health Laboratory. The aims of this thesis were; 1. recreate the disease, confirm the results of Bowater *et al.* and characterise the tissue tropism using quantitative real-time PCR (qPCR); 2. sequence the genome of the suspected parvovirus and propose a formal taxonomic standing; 3. characterise the transcriptome and 4. assess the CqDV's ability to infect and cause disease in another commercially cultured *Cherax* species. The overall aim was to characterize, in detail, a *Cherax* spp. infecting virus and fill in the knowledge gaps (presented in Table 8.1).

## 8.2 Results

Clarified homogenate was used to successfully recreate the disease. Grossly healthy *C. quadricarinatus* became lethargic, moved to the surface of the water column and changed colour. The most striking lesion was blistering that covered both inner branchial membranes and membrane around the top of the cephalothorax. Diseased

*C. quadricarinatus* presented with typical *Densovirinae* histopathology; Cowdry Type A inclusion bodies with hypertrophic nuclei that were Fluorogen-positive. In the case of CqDV and like *Penaeus merguensis* hepadensovirus (PmoHDV) (Lightner and Redman, 1985), but unlike *Penaeus stylirostris* penstyldensovirus (PstDV) (Lightner *et al.*, 1983), inclusions stained basophilic with hematoxylin and eosin. The qPCR demonstrated that CqDV preferentially targeted tissue of ectodermal origin, which was supported by the histopathology. The gross signs of disease, unique blistering, histopathology and qPCR should aid the rapid diagnosis of CqDV infection in *C. quadricarinatus* in the future.

Sequencing of viral DNA from cesium chloride purified virus and infected tissue resulted in the genome sequence of CqDV (KP410261). The viral genome is 6,334 nt in length with four open reading frames (ORFs) bracketed by terminal inverted repeats on a ssDNA. The ORFs contained conserved amino acid motifs typical of the family *Parvoviridae*; these included endonuclease, helicase, phospholipase A<sub>2</sub>, and nuclear location signals. The orientation of the ORFs was also consistent with other *Densovirinae*, particularly the *Ambidensovirus*.

The phylogeny was consistent with genome architecture (size, number and orientation of ORFs). Using the non-structural protein 1 (NS1) amino acids, phylogeny was recreated using the accession numbers from Cotmore *et al.* (2013). The phylogeny firmly placed CqDV in *genus Ambidensovirus*, species *Decapod ambidensovirus*, variant *Cherax quadricarinatus densovirus*. However, CqDV grouped closer to blattodean infecting densovirus despite the CqDV genome architecture being more similar to the *Lepidopteran ambidensovirus 1*. Of considerable interest was 75 % homology between sea star-associated densovirus (SSaDV) (discussed in more detail below). Taken together, the data demonstrates unequivocally that the original isolate reported by (Bowater *et al.*, 2002) is indeed a *Densovirinae*.

The transcriptome of CqDV, despite being incomplete, demonstrates a unique splicing pattern. The NS transcript is spliced four times, potentially producing new NS1, NS2 and NS3 isoforms. The hypothetical isoforms of NS1 and NS2 still contain their conserved motifs but are N-terminally truncated. Like the phylogeny, the

splicing was similar to both blattodean-infecting densoviruses and the *Lepidopteran ambidensovirus 1*.

There are three *Cherax* spp. commercially cultured in Australia. These include *C. quadricarinatus*, *C. destructor* and *C. tenuimanus*. We set out to test if CqDV could cause disease in *C. destructor*. Although there was no significant difference in CqDV copy number between weeks, and no gross signs of disease, CqDV was detected throughout the 8-week trial in *C. destructor* injected with CqDV-containing clarified homogenate.

This work has filled in significant gaps within the virology of *Cherax* species. As demonstrated in Table 8.1, the penaeid prawn infecting densoviruses have been comparatively well characterised. In comparison, the suspected parvo-like viruses of *Cherax* spp. are poorly characterised. We were able to successfully characterise CqDV and fill in many gaps in knowledge. This will provide a strong basis for future work in this field and will assist future researchers in this field to better direct their studies.

Table 8.1: Comparison of the characterisation between penaeid infecting *Densovirinae* and *Cherax* spp. infecting parvovirus showing the knowledge gaps in CqDV filled by this study

Pathogen	Histology	TEM	Transmission trial	Genome sequence	Transcriptome sequence	qPCR	Treatment
<b>PstDV1<sup>a</sup></b>	Lightner <i>et al.</i> (1983)	Lightner <i>et al.</i> (1983)	Bell and Lightner (1984)	Shike <i>et al.</i> (2000)	Dhar <i>et al.</i> (2010)	Tang and Lightner (2001), Dhar <i>et al.</i> (2002)	ND
<b>PmeDV<sup>a</sup></b>	Lightner and Redman (1985)	Bonami <i>et al.</i> (1995)	Catap <i>et al.</i> (2003)	Sukhumsirichart <i>et al.</i> (2006)	ND	Owens <i>et al.</i> (2014)	Owens <i>et al.</i> (2014)
<b>SMV<sup>ab</sup></b>	(Owens <i>et al.</i> , 1998) <sup>b</sup> Owens and McElnea (2000)	Owens <i>et al.</i> (1998) <sup>b</sup>	Owens <i>et al.</i> (1998) <sup>b</sup>	ND	ND	ND	ND
<b>CqDV<sup>b</sup></b>	Bowater <i>et al.</i> (2002), Chapter 4	Bowater <i>et al.</i> (2002), Chapter 4	Bowater <i>et al.</i> (2002), Chapter 4-7	(Bochow <i>et al.</i> , 2015)	Chapter 6	Chapter 4	ND
<b>CdSPV</b>	Edgerton <i>et al.</i> (1997)	Edgerton <i>et al.</i> (1997)	ND	ND	ND	ND	ND
<b>Putative gill parvovirus<sup>b</sup></b>	Edgerton <i>et al.</i> (2000)	Edgerton <i>et al.</i> (2000)	ND	ND	ND	ND	ND

<sup>a</sup> *P. monodon*, <sup>b</sup> *C. quadricarinatus*, ND no data

### 8.3 Future work

Future work is needed to finish characterising CqDV. Perhaps the most pressing issue is the development of a new qPCR. The current qPCR targets a 281 nt region on NS3 that, if used with cDNA, will not provide an accurate copy number because of CqDV's splicing pattern. A newly designed qPCR will aid in experiments investigating CqDV's ability to replicate and cause disease in other commercially cultured *Cherax* species.

Attempts should be made to complete the CqDV transcriptome. The results presented here demonstrate that CqDV is slow to replicate in the first week of infection. Future experiments should isolate mRNA from *C. quadricarinatus* 2 weeks post-injection with CqDV. This may yield higher amount of viral mRNA, increasing the success of rapid amplification of cDNA ends PCR.

Experiments need to be carried out to identify if CqDV is infectious and capable of replication in other *Cherax* species. CqDV-containing homogenate should be injected into *C. destructor* and *C. tenuimanus*, reisolated, and fed and injected back into *C. quadricarinatus* to test if CqDV is still infectious. RNA from CqDV injected *C. destructor* and *C. tenuimanus* should be isolated and tested using qPCR to identify if CqDV is actively replicating in these hosts and its preferred tissue tropism in these new hosts. These experiments should demonstrate CqDV's ability to cause disease in these hosts, and will have implications for translocation of these species across zoological boundaries.

### 8.4 Implications

There are two *Densovirinae* characterised in commercially cultured crustaceans. These are PmoHDV (Lightner and Redman, 1985) which belongs to the *Hepandensovirus* and PstDV (Lightner *et al.*, 1983) which belongs to the *Penstyldensovirus*. There have been four parvo-like viruses described in *Cherax* species. These include *Cherax destructor* systemic parvo-like virus (Edgerton *et al.*, 1997), putative gill parvovirus of *C. quadricarinatus* (Edgerton *et al.*, 2000), spawner isolated mortality virus in *C. quadricarinatus* (Owens and McElnea, 2000) and the now characterised CqDV that

belongs to the *Ambidensovirus*. It cannot be assumed that the *Cherax* spp. infecting parvo-like viruses are members of *Hepandensovirus* or *Penstyldensovirus* as CqDV is clearly a member of the *Ambidensovirus*. Indeed, in other crustaceans worldwide, it cannot be safely assumed that all basophilic inclusion bodies will be *Hepandensovirus* as has been assumed for those in, for instance, *Macrobrachium* (section 2.5).

Although CqDV and SSaDV are phylogenetically similar, they are geographically and environmentally distinct from each other. Some *Densovirinae* have a monospecific host range while others have a polyspecific host range, but host range does not extend outside of the host order. However, SSaDV has been found in two families belonging to two different orders (*Asteriidae* (order *Forcipulatida*) and *Asterinidae* (order *Valvatida*)), a unique feature among the *Densovirinae*. CqDV and SSaDV are, besides the *Lepidopteran ambidensovirus 1*, the next most related isolates within the *Densovirinae*. The question of whether or not CqDV and SSaDV can infect and cause disease in sea stars and crayfish respectively should be investigated.

If the crayfish industry is to progress, the need for characterisation of disease is paramount. This will facilitate the development of fast diagnostic tests and better surveillance. These measures can reduce the risk posed by the movement of stock between farms, interstate, and internationally. At present there are no molecular diagnostic tests and very limited biosecurity. Histopathology is the main method of investigation to propose a suspected pathogen. If the industry as a whole is to move forward, then this need to be rectified (Herbert, 1987). The industry needs to become more proactive as it grows and culture intensification technologies become more widely available.

## APPENDIX 1

### Media and buffers

#### Lysogeny broth (LB)

Component	Weight (grams litre <sup>-1</sup> )
Yeast	5
Tryptone	10
Sodium chloride	5

#### LB agar

Component	Weight (grams litre <sup>-1</sup> )
Yeast	5
Tryptone	10
Sodium chloride	5
Bacteriological agar	15

#### Blood agar

Component	Weight (grams litre <sup>-1</sup> )
Enzymatic digest of Casein	7.5
Enzymatic Digest of animal tissue	7.5
Liver digest	2.5
Yeast extract	5
Sodium chloride	5
Bacteriological agar	12g
Sheeps blood	100 mL

#### Preparation of stock solutions for cloning media

Component	Volume to prepare	Mass required <sup>a</sup>	Stock concentration
Isopropyl $\beta$ -D-1-thiogalactopyranoside (IPTG)	5 mL	0.12 g	500 mM
5-bromo-4-chloro-3-indolyl- $\beta$ -D-galactopyranoside (X-Gal)	2 mL (in dimethylformamide)	0.1 g	50 mg mL <sup>-1</sup>

Additions to LB and LB agar for cloning

Component	Stock concentration	Final required	Dilution of stock required
(IPTG)	500 mM	0.5 mM	1000
(X-Gal)	50 mg mL <sup>-1</sup>	80 ug mL <sup>-1</sup>	625
Ampicillin <sup>a</sup>	100000 ug mL <sup>-1</sup>	100 ug mL <sup>-1</sup>	1000
Ampicillin <sup>b</sup>	100000 ug mL <sup>-1</sup>	50 ug mL <sup>-1</sup>	2000

<sup>a</sup> pGEM T Easy; <sup>b</sup> TOPO TA Cloning

Davidsons fixative

Component	mL
Acetic acid	115
Absolute ethanol	313
Formaldehyde	220
Water	352

TNH buffer

Component	Final concentration to 1 litre
<i>Tris</i> -HCl	0.02 M
<i>NaCl</i>	0.4 M
4-hexylresorcinol <sup>a</sup>	0.5 %

<sup>a</sup> pre-prepared and filter before adding

TN buffer

Component	Final concentration to 1 litre
<i>Tris</i> -HCl	0.02 M
<i>NaCl</i>	0.4 M

## APPENDIX 2

### Publications

Work published as part of this thesis:

Bochow, S., Condon, K., Elliman, J. and Owens, L. (2015) First complete genome of an *Ambidensovirus*; *Cherax quadricarinatus* densovirus, from freshwater crayfish *Cherax quadricarinatus*. *Marine Genomics* **24**, Part 3: 305-312

Poster presentation at XVI<sup>th</sup> International Parvovirus Workshop, Ajaccio, Corsica.

Title of Poster: Characterisation of *Cherax quadricarinatus* densovirus

This poster won best poster presentation at the workshop.

Proposed publications from this thesis

Tissue tropism of *Cherax quadricarinatus* densovirus using histopathology, TEM and quantitative real-time PCR. *Aquaculture*.

Partial transcriptome of *Cherax quadricarinatus* densovirus. *Marine Genomics*. (This is expected to be a note.)

Translocation of *Cherax* species crayfish across zoogeographical zones within Australian has the potential to spread highly pathogenic *Cherax quadricarinatus* densovirus. *Aquaculture*.

## REFERENCE LIST

- Abd-Alla, A., Jousset, F.X., Li, Y., Fédière, G., Cousserans, F. and Bergoin, M. (2004) NS-3 protein of the *Junonia coenia* densovirus is essential for viral DNA replication in an Ld 652 cell line and *Spodoptera littoralis* larvae. *Journal of Virology* **78**: 790-797
- Afanasiev, B.N., Galyov, E.E., Buchatsky, L.P. and Kozlov, Y.V. (1991) Nucleotide sequence and genomic organization of *Aedes densonucleosis* virus. *Virology* **185**: 323-336
- Anderson, I.G., Law, A.T., Shariff, M. and Nash, G. (1990) A parvo-like virus in the giant freshwater prawn, *Macrobrachium rosenbergii*. *Journal of Invertebrate Pathology* **55**: 447-449
- Anderson, I.G. and Prior, H.C. (1992) Baculovirus infections in the mud crab, *Scylla serrata*, and a freshwater crayfish, *Cherax quadricarinatus*, from Australia. *Journal of Invertebrate Pathology* **60**: 265-273
- Azarkh, E., Robinson, E., Hirunkanokpun, S., Afanasiev, B., Kittayapong, P., Carlson, J. and Corsini, J. (2008) Mosquito densonucleosis virus non-structural protein NS2 is necessary for a productive infection. *Virology* **374**: 128-137
- Balsinde, J., Balboa, M.A., Insel, P.A. and Dennis, E.A. (1999) Regulation and inhibition of phospholipase A2. *Annual Review of Pharmacology and Toxicology* **39**: 175-189
- Baquerizo-Audiot, E., Abd-Alla, A., Jousset, F.X., Cousserans, F., Tijssen, P. and Bergoin, M. (2009) Structure and expression strategy of the genome of *Culex pipiens* densovirus, a mosquito densovirus with an ambisense organization. *Journal of Virology* **83**: 6863-6873
- Baulcombe, D. (2004) RNA silencing in plants. *Nature* **431**: 356-363
- Bell, T.A. and Lightner, D.V. (1984) IHNV virus: Infectivity and pathogenicity studies in *Penaeus stylirostris* and *Penaeus vannamei*. *Aquaculture* **38**: 185-194
- Bell, T.A. and Lightner, D.V. (1988) A handbook of normal penaeid shrimp histology. World Aquaculture Society, Baton Rouge, Louisiana.
- Bergoin, M. and Tijssen, P. (2008) Parvoviruses of Arthropods. In: B.W.J. Mahy and M.H.V.v. Regenmortel (Eds), *Encyclopedia of Virology* (Third Edition), pp. 76-85. Academic Press, Oxford.
- Bergoin, M. and Tijssen, P. (2010) Densoviruses: A highly diverse group of arthropod parvoviruses. In: J.K. Asgari S (Ed), *Insect Virology*, pp. 57-90. Horizon Scientific Press, Norwich, United Kingdom.
- Berns, K.I. (1990) Parvovirus replication. *Microbiological Reviews* **54**: 316-329
- Bertani, G. (1951) Studies on lysogenesis I.: The mode of phage liberation by lysogenic *Escherichia coli*. *Journal of Bacteriology* **62**: 293-300
- Bochow, S., Condon, K., Elliman, J. and Owens, L. (2015) First complete genome of an Ambidensovirus; *Cherax quadricarinatus* densovirus, from freshwater crayfish *Cherax quadricarinatus*. *Marine Genomics* **24, Part 3**: 305-312
- Bonami, J.R., Mari, J., Poulos, B.T. and Lightner, D.V. (1995) Characterization of hepatopancreatic parvo-like virus, a second unusual parvovirus pathogenic for penaeid shrimps. *Journal of General Virology* **76**: 813-817

- Bonami, J.R., Trumper, B., Mari, J., Brehelin, M. and Lightner, D.V. (1990) Purification and characterization of the infectious hypodermal and haematopoietic necrosis virus of penaeid shrimps. *Journal of General Virology* **71**: 2657-2664
- Bonami, J.R. and Vago, C. (1971) A virus of a new type pathogenic to crustacea. *Experientia* **27**: 1363-1364
- Boonyaratpalin, S., Supamattaya, K., Kasornchandra, J., Direkbusaracom, S., Aekpanithanpong, U. and Chantanachooklin, C. (1993) No-occluded baculo-like virus, the causative agent of yellow head disease in black tiger shrimp (*Penaeus monodon*). *Gyobyo Kenkyu* **28**: 103-109
- Bowater, R.O., Wingfield, M., Fisk, A., Condon, K.M., Reid, A., Prior, H. and Kulpa, E.C. (2002) A parvo-like virus in cultured redclaw crayfish *Cherax quadricarinatus* from Queensland, Australia. *Diseases of Aquatic Organisms* **50**: 79-86
- Carstairs, I.L. (1978) Report of microsporidial infestation of the freshwater crayfish, *Cherax destructor*. *Freshwater Crayfish* **4**: 343-347
- Cassinotti, P., Weitzand, M. and Tratschin, J.D. (1988) Organization of the adeno-associated virus (AAV) capsid gene: Mapping of a minor spliced mRNA coding for virus capsid protein. *Virology* **167**: 176-184
- Catap, E.S., Lavilla-Pitogo, C.R., Maeno, Y. and Travina, R.D. (2003) Occurrence, histopathology and experimental transmission of hepatopancreatic parvovirus infection in *Penaeus monodon* postlarvae. *Diseases of Aquatic Organisms* **57**: 11-17
- Chang, P.S., Chen, H.C. and Wang, Y.C. (1998) Detection of white spot syndrome associated baculovirus in experimentally infected wild shrimp, crab and lobsters by *in situ* hybridization. *Aquaculture* **164**: 233-242
- Chayaburakul, K., Lightner, D.V., Sriurairattana, S., Nelson, K.T. and Withyachumnarnkul, B. (2005) Different responses to infectious hypodermal and hematopoietic necrosis virus (IHHNV) in *Penaeus monodon* and *P. vannamei*. *Diseases of Aquatic Organisms* **67**: 191-200
- Claydon, K., Bradford, C. and Owens, L. (2004) OIE white spot syndrome virus PCR gives false-positive results in *Cherax quadricarinatus*. *Diseases of Aquatic Organisms* **62**: 265-268
- Cotmore, S.F., Agbandje-McKenna, M., Chiorini, J.A., Mukha, D.V., Pintel, D.J., Qiu, J., Soderlund-Venermo, M., Tattersall, P., Tijssen, P., Gatherer, D. and Davison, A.J. (2013) The family *Parvoviridae*. *Archives of Virology*: 1-9
- Cotmore, S.F., D'Abramo Jr, A.M., Carbonell, L.F., Bratton, J. and Tattersall, P. (1997) The NS2 polypeptide of parvovirus MVM is required for capsid assembly in murine cells. *Virology* **231**: 267-280
- Cotmore, S.F., Hafenstein, S. and Tattersall, P. (2010) Depletion of virion-associated divalent cations induces parvovirus minute virus of mice to eject its genome in a 3' - to -5' direction from an otherwise intact viral particle. *Journal of Virology* **84**: 1945-1956
- Cotmore, S.F. and Tattersall, P. (1996) Parvovirus DNA replication, In: DNA replication in eukaryotic cells, edited by M.L. DePamphilis. 1058 pp. Cold Springs Harbor, USA.
- Cotmore, S.F. and Tattersall, P. (2013) Parvovirus diversity and DNA damage responses. *Cold Spring Harbor Perspectives in Biology* **5**: 1-12
- Cotmore, S.F. and Tattersall, P. (2014) Parvoviruses: Small does not mean simple. *Annual Review of Virology* **1**: 517-537

- Couch, J.A. (1974a) An enzootic nuclear polyhedrosis virus of pink shrimp: Ultrastructure, prevalence, and enhancement. *Journal of Invertebrate Pathology* **24**: 311-331
- Couch, J.A. (1974b) Free and occluded virus similar to BaculoŌirus in hepatopancreas of pink shrimp. *Nature* **247**: 229-231
- Cowdry, E.V. (1934) The problem of intranuclear inclusions in virus diseases. *Archives of Pathology* **18**: 527-542
- Croizier, L., Jousset, F.X., Veyrunes, J.C., Ferber, M.L., Bergoin, M. and Croizier, G. (2000) Protein requirements for assembly of virus-like particles of Junonia coenia densovirus in insect cells. *Journal of General Virology* **81**: 1605-1613
- Dhar, A.K., Kaizer, K.N. and Lakshman, D.K. (2010) Transcriptional analysis of Penaeus stylirostris densovirus genes. *Virology* **402**: 112-120
- Dhar, A.K., Roux, M.M. and Klimpel, K.R. (2001) Detection and quantification of infectious hypodermal and hematopoietic necrosis virus and white spot virus in shrimp using real-time quantitative PCR and SYBR Green chemistry. *Journal of Clinical Microbiology* **39**: 2835-2845
- Dhar, A.K., Roux, M.M. and Klimpel, K.R. (2002) Quantitative assay for measuring the taura syndrome virus and yellow head virus load in shrimp by real-time RT-PCR using SYBR Green chemistry. *Journal of Virological Methods* **104**: 69-82
- Doerig, C., Hirt, B., Antonietti, J.P. and Beard, P. (1990) Nonstructural protein of parvoviruses B19 and minute virus of mice controls transcription. *Journal of Virology* **64**: 387-396
- Dworetzky, S.I., Landford, R.E. and Feldherr, C.M. (1988) The effects of variations in the number and sequence of targeting signals on nuclear up take. *Journal of Cell Biology* **107**: 1279-1287
- Eaves, L.E. and Ketterer, P.J. (1994) Mortalities in red claw crayfish *Cherax quadricarinatus* associated with systemic *Vibrio mimicus* infection. *Diseases of Aquatic Organisms* **19**: 233-237
- Edgerton, B. (1996) A new bacilliform virus in Australian *Cherax destructor* (Decapoda: Parastacidae) with notes on *Cherax quadricarinatus* bacilliform virus (= *Cherax baculovirus*). *Diseases of Aquatic Organisms* **27**: 43-52
- Edgerton, B. (2004) Susceptibility of the Australian freshwater crayfish *Cherax destructor albidus* to white spot syndrome virus (WSSV). *Diseases of Aquatic Organisms* **59**: 187-193
- Edgerton, B. and Owens, L. (1997) Age at first infection of *Cherax quadricarinatus* by *Cherax quadricarinatus* bacilliform virus and *Cherax* Giardiavirus-like virus, and production of putative virus-free crayfish. *Aquaculture* **152**: 1-12
- Edgerton, B., Owens, L., Glasson, B. and De Beer, S. (1994) Description of a small dsRNA virus from freshwater crayfish *Cherax quadricarinatus*. *Diseases of Aquatic Organisms* **18**: 63-69
- Edgerton, B., Owens, L., Harris, L., Thomas, A. and Wingfield, M. (1995) A health survey of farmed redclaw crayfish, *Cherax quadricarinatus* (von Martens), in tropical Australia. *Freshwater Crayfish* **10**: 322-338
- Edgerton, B., Webb, R., Anderson, I.G. and Kulpa, E. (2000) Description of a presumptive hepatopancreatic reovirus, and a putative gill parvovirus, in the freshwater crayfish *Cherax quadricarinatus*. *Diseases of Aquatic Organisms* **41**: 83-90
- Edgerton, B., Webb, R. and Wingfield, M. (1997) A systemic parvo-like virus in the freshwater crayfish *Cherax destructor*. *Diseases of Aquatic Organisms* **29**: 73-78

- Edgerton, B.F., Evans, L.H., Stephens, F.J. and Overstreet, R.M. (2002) Synopsis of freshwater crayfish diseases and commensal organisms. *Aquaculture* **206**: 57-135
- Edgerton, B.F. and Owens, L. (1999) Histopathological surveys of the redclaw freshwater crayfish, *Cherax quadricarinatus*, in Australia. *Aquaculture* **180**: 23-40
- Farr, G.A., Zhang, L.g. and Tattersall, P. (2005) Parvoviral virions deploy a capsid-tethered lipolytic enzyme to breach the endosomal membrane during cell entry. *Proceedings of the National Academy of Sciences of the United States of America* **102**: 17148-17153
- FAO (Food and Agriculture Organization of the United Nations) Global Aquaculture production. <http://www.fao.org/fishery/statistics/global-aquaculture-production/query/en>. Accessed February 2016.
- Fédière, G., El-Far, M., Li, Y., Bergoin, M. and Tijssen, P. (2004) Expression strategy of densovirus from *Mythimna loreyi*. *Virology* **320**: 181-189
- Feldherr, C.M., Kallenbach, E. and Schultz, N. (1984) Movement of a karyophilic protein through the nuclear pore of oocytes. *Journal of Cell Biology* **99**: 2216-2222
- Flegel, T.W. (2006) Detection of major penaeid shrimp viruses in Asia, a historical perspective with emphasis on Thailand. *Aquaculture* **258**: 1-33
- Flegel, T.W. (2012) Historic emergence, impact and current status of shrimp pathogens in Asia. *Journal of Invertebrate Pathology* **110**: 166-173
- Flegel, T.W., Nielsen, L., Thamavit, V., Kongtim, S. and Pasharawipas, T. (2004) Presence of multiple viruses in non-diseased, cultivated shrimp at harvest. *Aquaculture* **240**: 55-68
- Flegel, T.W. and Pasharawipas, T. (1998) Active viral accommodation: A new concept for crustacean response to viral pathogens. Advances in shrimp biotechnology. National Centre for Genetic Engineering and Biotechnology, Bangkok.
- Fraser, C.A. and Owens, L. (1996) Spawner-isolated mortality virus from Australian *Penaeus monodon*. *Diseases of Aquatic Organisms* **27**: 141-148
- Gangnonngiw, W., Kiatpathomchai, W., Sriurairatana, S., Laisutisan, K., Chuchird, N., Limsuwan, C. and Flegel, T.W. (2009a) Parvo-like virus in the hepatopancreas of freshwater prawns *Macrobrachium rosenbergii* cultivated in Thailand. *Diseases of Aquatic Organisms* **85**
- Gangnonngiw, W., Kiatpathomchai, W., Sriurairatana, S., Laisutisan, K., Chuchird, N., Limsuwan, C. and Flegel, T.W. (2009b) Parvo-like virus in the hepatopancreas of freshwater prawns *Macrobrachium rosenbergii* cultivated in Thailand. *Diseases of Aquatic Organisms* **85**: 167-173
- Ghanawi, J. and Saoud, I.P. (2012) Molting, reproductive biology, and hatchery management of redclaw crayfish *Cherax quadricarinatus* (von Martens 1868). *Aquaculture* **358-359**: 183-195
- Gorbalenya, A.E., Koonin, E.V. and Wolf, Y.I. (1990) A new superfamily of putative NTP-binding domains encoded by genomes of small DNA and RNA viruses. *FEBS Letters* **262**: 145-148
- Groff, J.M., McDowell, T., Friedman, C.S. and Hedrick, R.P. (1993) Detection of a nonoccluded baculovirus in the freshwater crayfish *Cherax quadricarinatus* in North America. *Journal of Aquatic Animal Health* **5**: 275-279
- Gudenkauf, B.M., Eaglesham, J.B., Aragundi, W.M. and Hewson, I. (2013) Discovery of urchin-associated densoviruses (family *Parvoviridae*) in coastal waters of the Big Island, Hawaii. *Journal of General Virology* **95**: 652-658

- Han, Y., Wang, Q., Qiu, Y., Wu, W., He, H., Zhang, J., Hu, Y. and Zhou, X. (2013) *Periplaneta fuliginosa* densovirus nonstructural protein NS1 contains an endonuclease activity that is regulated by its phosphorylation. *Virology* **437**: 1-11
- Hauck, K., Michael, M., Joseph, L. and Russell, L. (2001) A new finding and range extension of bacilliform virus in the freshwater redclaw crayfish in Utah, USA. *Journal of Aquatic Animal Health* **13**: 158-162
- Hayakijkosol, O., Burgess, G., La Fauce, K. and Owens, L. (2012) The complete sequence of the Australia recognizate of *Macrobrachium rosenbergii* nodavirus which causes white tail disease. *Aquaculture* **366–367**: 98-104
- Hayakijkosol, O. and Owens, L. (2011) Investigation into the pathogenicity of reovirus to juvenile *Cherax quadricarinatus*. *Aquaculture* **316**: 1-5
- Herbert, B. (1987) Notes on diseases and epibionts of *Cherax quadricarinatus* and *C. tenuimanus* (Decapoda: *Parastacidae*). *Aquaculture* **64**: 165-173
- Hewson, I., Button, J.B., Gudenkauf, B.M., Miner, B., Newton, A.L., Gaydos, J.K., Wynne, J., Groves, C.L., Hendler, G., Murray, M., Fradkin, S., Breitbart, M., Fahsbender, E., Lafferty, K.D., Kilpatrick, A.M., Miner, C.M., Raimondi, P., Lahner, L., Friedman, C.S., Daniels, S., Haulena, M., Marliave, J., Burge, C.A., Eisenlord, M.E. and Harvell, C.D. (2014b) Densovirus associated with sea-star wasting disease and mass mortality. *Proceedings of the National Academy of Sciences* **111**: 17278-17283
- Hickman, A.B. and Dyda, F. (2005) Binding and unwinding: SF3 viral helicases. *Current Opinion in Structural Biology* **15**: 77-85
- Hsieh, C.Y., Chuang, P.C., Chen, L.C., Chien, T., Chien, M.S., Huang, K.C., Kao, H.F., Tung, M.C. and Tsai, S.S. (2006) Infectious hypodermal and haematopoietic necrosis virus (IHHNV) infections in giant freshwater prawn, *Macrobrachium rosenbergii*. *Aquaculture* **258**: 73-79
- Hu, Y., Zheng, J., Iizuka, T. and Bando, H. (1994) A densovirus newly isolated from the smoky-brown cockroach *Periplaneta fuliginosa*. *Archives of Virology* **138**: 365-372
- Hueffer, K. and Parrish, C.R. (2003) Parvovirus host range, cell tropism and evolution. *Current Opinion in Microbiology* **6**: 392-398
- Huynh, O.T.H., Pham, H.T., Yu, Q. and Tijssen, P. (2012) Pseudoplusia includens densovirus genome organization and expression strategy. *Journal of Virology* **86**: 13127-13128
- Ilyina, T.V. and Koonin, E.V. (1992) Conserved sequence motifs in the initiator proteins for rolling circle DNA replication encoded by diverse replicons from eubacteria, eucaryotes and archaebacteria. *Nucleic Acids Research* **20**: 3279-3285
- Jones, C.M. (1990) The biology and aquaculture potential of *Cherax quadricarinatus*. Queensland Department of Primary Industries and Fisheries. This document was submitted to the Reserve Bank of Australia Rural Credits Development Fund as a final report for the project "The Assessment of *Cherax quadricarinatus* as a Candidate for Aquaculture". Project No. QDPI/8860.
- Jones, C.M., Medley, P.B. and Avault Jr, J.W. (1994) Redclaw crayfish, *Cherax quadricarinatus*: Production, economics and marketing. *World Aquaculture* **25**: 6-13
- Jones, D.T., Taylor, W.R. and Thornton, J.M. (1992) The rapid generation of mutation data matrices from protein sequences. *Computer applications in the biosciences* **8**: 275-282

- Jones, J.B. and Lawrence, C.S. (2001) Diseases of yabbies (*Cherax albidus*) in Western Australia. *Aquaculture* **194**: 221-232
- Kalagayan, H., Godin, D., Kanna, R., Hagino, G., Sweeney, J., Wyban, J. and Brock, J. (1991) IHVN Virus as an etiological factor in runt-deformity syndrome (RDS) of juvenile *Penaeus vannamei* cultured in Hawaii. *Journal of the World Aquaculture Society* **22**: 235-243
- Kapelinskaya, T.V., Martynova, E.U., Schal, C. and Mukha, D.V. (2011) Expression strategy of densovirus from the German cockroach, *Blattella germanica*. *Journal of Virology* **85**: 11855-11870
- King, J.A., Dubielzig, R., Grimm, D. and Kleinschmidt, J.A. (2001) DNA helicase-mediated packaging of adeno-associated virus type 2 genomes into preformed capsids. *The EMBO Journal* **20**: 3282-3291
- Kivovich, V., Gilbert, L., Vuento, M. and Naides, S.J. (2012) The putative metal coordination motif in the endonuclease domain of human parvovirus B19 NS1 is critical for NS1 induced S phase arrest and DNA damage. *International Journal of Biological Sciences* **8**: 79-92
- Koonin, E.V. (1993) A common set of conserved motifs in a vast variety of putative nucleic acid-dependent ATPases including MCM proteins involved in the initiation of eukaryotic DNA replication. *Nucleic Acids Research* **21**: 2541-2547
- Koonin, E.V. and Ilyina, T.V. (1993) Computer-assisted dissection of rolling circle DNA replication. *Biosystems* **30**: 241-268
- Kouassi, N., Peng, J.x., Li, Y., Cavallaro, C., Veyrunes, J.C. and Bergoin, M. (2007) Pathogenicity of *Diatraea saccharalis* densovirus to host insects and characterization of its viral genome. *Virologica Sinica* **22**: 53-60
- Kozak, M. (1986) Point mutations define a sequence flanking the AUG initiator codon that modulates translation by eukaryotic ribosomes. *Cell* **44**: 283-292
- Kozak, M. (1995) Adherence to the first-AUG rule when a second AUG codon follows closely upon the first. *Proceedings of the National Academy of Sciences* **92**: 2662-2666
- Kozlova, E.N. and Mukha, D.V. (2015) Mammalian cell culture as a model for studying the intracellular traffic of densovirus proteins. *Russian Journal of Genetics* **51**: 218-222
- La Fauce, K. and Owens, L. (2012) RNA interference with special reference to combating viruses of crustacea. *Indian Journal of Virology* **23**: 226-243
- La Fauce, K.A., Elliman, J. and Owens, L. (2007) Molecular characterisation of hepatopancreatic parvovirus (PmergDNV) from Australian *Penaeus merguensis*. *Virology* **362**: 397-403
- La Fauce, K.L. and Owens, L. (2007) Investigation into the pathogenicity of *Penaeus merguensis* densovirus (PmergDNV) to juvenile *Cherax quadricarinatus*. *Aquaculture* **271**: 31-38
- Labow, M.A., Graf, L.H. and Berns, K.I. (1987) Adeno-associated virus gene expression inhibits cellular transformation by heterologous genes. *Molecular and Cellular Biology* **7**: 1320-1325
- Leisi, R., Ruprecht, N., Kempf, C. and Ros, C. (2013) Parvovirus B19 uptake is a highly selective process controlled by VP1u, a novel determinant of viral tropism. *Journal of Virology* **87**: 13161-13167
- Li, X. and Rhode 3rd, S.L. (1991) Nonstructural protein NS2 of parvovirus H-1 is required for efficient viral protein synthesis and virus production in rat cells *in vivo* and *in vitro*. *Virology* **184**: 117-130

- Li, X. and Rhode 3rd, S.L. (1993) The parvovirus H-1 NS2 protein affects viral gene expression through sequences in the 3' untranslated region. *Virology* **194**: 10-19
- Lightner, D.V. and Redman, R.M. (1985) A parvo-like virus disease of penaeid shrimp. *Journal of Invertebrate Pathology* **45**: 47-53
- Lightner, D.V. and Redman, R.M. (1998) Shrimp diseases and current diagnostic methods. *Aquaculture* **164**: 201-220
- Lightner, D.V., Redman, R.M. and Bell, T.A. (1983) Infectious hypodermal and hematopoietic necrosis, a newly recognized virus disease of penaeid shrimp. *Journal of Invertebrate Pathology* **42**: 62-70
- Lightner, D.V., Redman, R.M., Poulos, B.T., Mari, J.L., Bonomi, J.R. and Mohamed Din, M.S. (1994) Distinction of HPV-type viruses in *Penaeus chinensis* and *Macrobrachium rosenbergii* using a DNA probe. *Asian Fisheries Science* **7**: 267-272
- Lin, C.K. and Boonyaratpalin, M. (1988) An analysis of biological characteristics of *Macrobrachium rosenbergii* (de Man) in relation to pond production and marketing in Thailand. *Aquaculture* **74**: 205-215
- Liu, K., Li, Y., Jousset, F.-X., Zadori, Z., Szelei, J., Yu, Q., Pham, H.T., Lépine, F., Bergoin, M. and Tijssen, P. (2011) The Acheta domesticus densovirus, isolated from the european house cricket, has evolved an expression strategy unique among parvoviruses. *Journal of Virology* **85**: 10069-10078
- Lo, C.F., Ho, C.H., Peng, S.E., Chen, C.H., Hsu, H.C., Chiu, Y.L., Chang, C.F., Liu, K.F., Su, M.S., Wang, C.H. and Kou, G.H. (1996) White spot syndrome baculovirus (WSBV) detected in cultured and captured shrimp, crabs and other arthropods. *Diseases of Aquatic Organisms* **27**: 215-225
- Lombardo, E., Ramírez, J.C., Garcia, J. and Almendral, J.M. (2002) Complementary roles of multiple nuclear targeting signals in the capsid proteins of the parvovirus minute virus of mice during assembly and onset of infection. *Journal of Virology* **76**: 7049-7059
- Longshaw, M. (2011) Diseases of crayfish: A review. *Journal of Invertebrate Pathology* **106**: 54-70
- Mari, J.L., Lightner, D.V., Bonnie, T.P. and Bonami, J.R. (1995) Partial cloning of the genome of an unusual shrimp parvovirus (HPV): Use of gene probes in disease diagnosis. *Diseases of Aquatic Organisms* **22**: 129-134
- Martynova, E.U., Kapelinskaya, T.V., Schal, C. and Mukha, D.V. (2014) Intracellular localization of regulatory proteins of the German cockroach Blattella germanica densovirus. *Molecular Biology* **48**: 301-304
- McCarthy, S.D., Dugon, M.M. and Power, A.M. (2015) 'Degraded' RNA profiles in *Arthropoda* and beyond. *PeerJ* **3**:e1436
- Mello, M.V.C., Aragão, M.E.F.d., Torres-Franklin, M.L.P., Neto, J.M.d.O. and Guedes, M.I.F. (2011) Purification of infectious myonecrosis virus (IMNV) in species of marine shrimp *Litopenaeus vannamei* in the State of Ceará. *Journal of Virological Methods* **177**: 10-14
- Merrick, J.R., Lambert, N.C. (1991) The yabby, marron and red claw: production and marketing. J.R. Merrick Publications, Artamon, N.S.W
- Mills, B.J. and McCloud, P.I. (1983) Effects of stocking and feeding rates on experimental pond production of the crayfish *Cherax destructor clark* (Decapoda: Parastacidae). *Aquaculture* **34**: 51-72

- Moffatt, S., Yaegashi, N., Tada, K., Tanaka, N. and Sugamura, K. (1998) Human parvovirus B19 nonstructural (NS1) protein induces apoptosis in erythroid lineage cells. *Journal of Virology* **72**: 3018-3028
- Momoeda, M., Wong, S., Kawase, M., Young, N.S. and Kajigaya, S. (1994) A putative nucleoside triphosphate-binding domain in the nonstructural protein of B19 parvovirus is required for cytotoxicity. *Journal of Virology* **68**: 8443-8446
- Morrissy, N.M. (1979) Experimental pond production of marron, *Cherax tenuimanus* (Smith) (Decapoda: *Parastacidae*). *Aquaculture* **16**: 319-344
- Mukha, D.V., Chumachenko, A.G., Dykstra, M.J., Kurtti, T.J. and Schal, C. (2006) Characterization of a new densovirus infecting the German cockroach, *Blattella germanica*. *Journal of General Virology* **87**: 1567-1575
- Mukha, D.V. and Schal, K. (2003) A densovirus of German cockroach *Blattella germanica*: Detection, nucleotide sequence, and genome organization. *Molecular Biology* **37**: 513-523
- Munasinghe, D.H.N., Burrige, C.P. and Austin, C.M. (2004) Molecular phylogeny and zoogeography of the freshwater crayfish genus *Cherax* Erichson (Decapoda: *Parastacidae*) in Australia. *Biological Journal of the Linnean Society* **81**: 553-563
- Naeger, L.K., Cater, J. and Pintel, D.J. (1990) The small nonstructural protein (NS2) of the parvovirus minute virus of mice is required for efficient DNA replication and infectious virus production in a cell-type-specific manner. *Journal of Virology* **64**: 6166-6175
- Naeger, L.K., Salomé, N. and Pintel, D.J. (1993) NS2 is required for efficient translation of viral mRNA in minute virus of mice-infected murine cells. *Journal of Virology* **67**: 1034-1043
- Nüesch, J.P.F., Cotmore, S.F. and Tattersall, P. (1995) Sequence motifs in the replicator protein of parvovirus MVM essential for nicking and covalent attachment to the viral origin: Identification of the linking tyrosine. *Virology* **209**: 122-135
- Nykky, J., Vuento, M. and Gilbert, L. (2014) Role of mitochondria in parvovirus pathology. *PLoS ONE* **9**: e86124
- Obbard, D.J., Gordon, K.H.J., Buck, A.H. and Jiggins, F.M. (2009) The evolution of RNAi as a defence against viruses and transposable elements. *Philosophical Transactions of the Royal Society B: Biological Sciences* **364**: 99-115
- Ohshima, T., Iwama, M., Ueno, Y., Sugiyama, F., Nakajima, T., Fukamizu, A. and Yagami, K. (1998) Induction of apoptosis in vitro and in vivo by H-1 parvovirus infection. *Journal of General Virology*: 3067-3071
- Op De Beeck, A. and Caillet-Fauquet, P. (1997) The NS1 protein of the autonomous parvovirus minute virus of mice blocks cellular DNA replication: A consequence of lesions to the chromatin? *Journal of Virology* **71**: 5323-5329
- Overstreet, R.M., Lightner, D.V., Hasson, K.W., McIlwain, S. and Lotz, J.M. (1997) Susceptibility to taura syndrome virus of some penaeid shrimp species native to the Gulf of Mexico and the southeastern United States. *Journal of Invertebrate Pathology* **69**: 165-176
- Owens, L. (2013) Bioinformatical analysis of nuclear localisation sequences in penaeid densoviruses. *Marine Genomics* **12**: 9-15
- Owens, L., Condon, K., Rai, P. and Karunasagar, I. (2014) Diet-delivery of therapeutic RNA interference in live *Escherichia coli* against pre-existing *Penaeus merguensis* hepadensovirus in *Penaeus merguensis*. *Aquaculture* **437**: 360-365

- Owens, L., Haqshenas, G., McElnea, C. and Coelen, R. (1998) Putative spawner-isolated mortality virus associated with mid-crop mortality syndrome in farmed *Penaeus monodon* from northern Australia. *Diseases of Aquatic Organisms* **34**: 177-185
- Owens, L. and McElnea, C. (2000) Natural infection of the redclaw crayfish *Cherax quadricarinatus* with presumptive spawner-isolated mortality virus. *Diseases of Aquatic Organisms* **40**: 219-223
- Pham, H.T., Jousset, F.X., Perreault, J., Shike, H., Szelei, J., Bergoin, M. and Tijssen, P. (2013) Expression strategy of Aedes albopictus densovirus. *Journal of Virology* **87**: 9928-9932
- Pillai, R.S., Bhattacharyya, S.N. and Filipowicz, W. (2007) Repression of protein synthesis by miRNAs: How many mechanisms? *Trends in Cell Biology* **17**: 118-126
- Pintel, D.J., Gersappe, A., Haut, D. and Pearson, J. (1995) Determinants that govern alternative splicing of parvovirus pre-mRNAs. *Seminars in Virology* **6**: 283-290
- Poulos, B.T., Tang, K., Pantoja, C., Bonami, J.R. and Lightner, D.V. (2006) Purification and characterization of infectious myonecrosis virus of penaeid shrimp. *Journal of General Virology* **87**: 987-996
- Rivers, T.M. (1937) Viruses and Koch's Postulates. *Journal of Bacteriology* **33**: 1-12
- Robalino, J., Bartlett, T., Shepard, E., Prior, S., Jaramillo, G., Scura, E., Chapman, R.W., Gross, P.S., Browdy, C.L. and Warr, G.W. (2005) Double-stranded RNA induces sequence-specific antiviral silencing in addition to nonspecific immunity in a marine shrimp: Convergence of RNA interference and innate immunity in the invertebrate antiviral response? *Journal of Virology* **79**: 13561-13571
- Robalino, J., Browdy, C.L., Prior, S., Metz, A., Parnell, P., Gross, P. and Warr, G. (2004) Induction of antiviral immunity by double-stranded RNA in a marine invertebrate. *Journal of Virology* **78**: 10442-10448
- Romero, X. and Jiménez, R. (2002) Histopathological survey of diseases and pathogens present in redclaw crayfish, *Cherax quadricarinatus* (Von Martens), cultured in Ecuador. *Journal of Fish Diseases* **25**: 653-667
- Ros, C., Gerber, M. and Kempf, C. (2006) Conformational changes in the VP1-unique region of native human parvovirus B19 lead to exposure of internal sequences that play a role in virus neutralization and infectivity. *Journal of Virology* **80**: 12017-12024
- Rosenfeld, S.J., Yoshimoto, K., Kajigaya, S., Anderson, S., Young, N.S., Field, A., Warrenner, P., Bansal, G. and Collett, M.S. (1992) Unique region of the minor capsid protein of human parvovirus B19 is exposed on the virion surface. *The Journal of Clinical Investigation* **89**: 2023-2029
- Rusaini. (2013) Suppression subtractive hybridization to investigate viruses in the lymphoid organ of *Penaeus merguensis* and the gills of *Cherax quadricarinatus* PhD Thesis, James Cook University.
- Rusaini, Ariel, E., Burgess, G. and Owens, L. (2013) Investigation of an idiopathic lesion in redclaw crayfish *Cherax quadricarinatus* using suppression subtractive hybridization. *Journal of Virology & Microbiology* **2013**: 1-15
- Safeena, M.P., Rai, P. and Karunasagar, I. (2012) Molecular biology and epidemiology of hepatopancreatic parvovirus of penaeid shrimp. *Indian Journal of Virology* **23**: 191-202

- Shapiro, M.B. and Senapathy, P. (1987) RNA splice junctions of different classes of eukaryotes: Sequence statistics and functional implications in gene expression. *Nucleic Acids Research* **15**: 7155-7174
- Shi, Z., Huang, C., Zhang, J., Chen, D. and Bonami, J.R. (2000a) White spot syndrome virus (WSSV) experimental infection of the freshwater crayfish, *Cherax quadricarinatus*. *Journal of Fish Diseases* **23**: 285-288
- Shike, H., Dhar, A.K., Burns, J.C., Shimizu, C., Jousset, F.X., Klimpel, K.R. and Bergoin, M. (2000) Infectious hypodermal and hematopoietic necrosis virus of shrimp is related to mosquito *Brevidensovirus*. *Virology* **277**: 167-177
- Simpson, A.A., Chipman, P.R., Baker, T.S., Tijssen, P. and Rossmann, M.G. (1998) The structure of an insect parvovirus (*Galleria mellonella* densovirus) at 3.7 Å resolution. *Structure* **6**: 1355-1367
- Stentiford, G.D., Bonami, J.R. and Alday-Sanz, V. (2009) A critical review of susceptibility of crustaceans to taura syndrome, yellowhead disease and white spot disease and implications of inclusion of these diseases in European legislation. *Aquaculture* **291**: 1-17
- Sukhumsirichart, W., Attasart, P., Boonsaeng, V. and Panyim, S. (2006) Complete nucleotide sequence and genomic organization of hepatopancreatic parvovirus (HPV) of *Penaeus monodon*. *Virology* **346**: 266-277
- Suto, C., Kawamoto, F. and Kumada, N. (1979) A new virus isolated from the cockroach, *Periplaneta fuliginosa* (Serville). *Microbiology and Immunology* **23**: 207-211
- Tamura, K., Stecher, G., Peterson, D., Filipinski, A. and Kumar, S. (2013) MEGA6: Molecular evolutionary genetics analysis version 6.0. *Molecular Biology and Evolution* **30**: 2725-2729
- Tan, C.K. and Owens, L. (2000) Infectivity, transmission and 16S rRNA sequencing of a rickettsia, *Coxiella cheraxi* sp. nov., from the freshwater crayfish *Cherax quadricarinatus*. *Diseases of Aquatic Organisms* **41**: 115-122
- Tang, K.F.J. and Lightner, D.V. (2001) Detection and quantification of infectious hypodermal and hematopoietic necrosis virus in penaeid shrimp by real-time PCR. *Disease of Aquatic Organisms* **44**: 79-85
- Tang, K.F.J. and Lightner, D.V. (2006) Infectious hypodermal and hematopoietic necrosis virus (IHHNV)-related sequences in the genome of the black tiger prawn *Penaeus monodon* from Africa and Australia. *Virus Research* **118**: 185-191
- Tattersall, P. (2008) Parvoviruses: General features. In: B.W.J.M. Editors-in-Chief: and M.H.V.v. Regenmortel (Eds), *Encyclopedia of Virology* (Third Edition), pp. 90-97. Academic Press, Oxford.
- Tattersall, P. and Ward, D.C. (1976) Rolling hairpin model for replication of parvovirus and linear chromosomal DNA. *Nature* **263**: 106-109
- Tijssen, P., Bando, H., Li, Y., Jousset, F.X., Zádori, Z., Fediere, G., El-Far, M., Szelei, J. and Bergoin, M. (2006) Evolution of densovirus. *Parvoviruses*, edited by R.J. Kerr, Cotmore, S. F., Bloom, M. E., Linden, R. M., Parrish, C. R. Hodder Arnold, London, United Kingdom.
- Tijssen, P., Li, Y., El-Far, M., Szelei, J., Letarte, M. and Zádori, Z. (2003) Organization and expression strategy of the ambisense genome of densovirus of *Galleria mellonella*. *Journal of Virology* **77**: 10357-10365
- Vago, C. (1966) A virus disease in crustacea. *Nature* **209**: 1290

- Vihinen-Ranta, M., Wang, D., Weichert, W.S. and Parrish, C.R. (2002) The VP1 N-terminal sequence of canine parvovirus affects nuclear transport of capsids and efficient cell infection. *Journal of Virology* **76**: 1884-1891
- Wang, J., Wu, J. and Gu, J. (2015) Identification of microRNA-like viral small RNAs from AaeDV. *Bing Du Xue Bao* **31**
- Wang, Y., Abd-Alla, A.M.M., Bossin, H., Li, Y. and Bergoin, M. (2013) Analysis of the transcription strategy of the *Junonia coenia* densovirus (JcDENV) genome. *Virus Research* **174**: 101-107
- White, G.H. and Farrance, I. (2004) Uncertainty of measurement in quantitative medical testing: A laboratory implementation guide. *The Clinical Biochemist Reviews* **25**: S1-S24
- Wilson, G.M., Jindal, H.K., Yeung, D.E., Chen, W. and Astell, C.R. (1991) Expression of minute virus of mice major nonstructural protein in insect cells: Purification and identification of ATPase and helicase activities. *Virology* **185**: 90-98
- Winnebeck, E.C., Millar, C.D. and Warman, G.R. (2010) Why does insect RNA look degraded? *Journal of Insect Science* **10**
- Yamagishi, J., Hu, Y., Zheng, J. and Bando, H. (1999) Genome organization and mRNA structure of *Periplaneta fuliginosa* densovirus imply alternative splicing involvement in viral gene expression. *Archives of Virology* **144**: 2111-2124
- Yang, B., Cai, D., Yu, P., Dong, X., Liu, Z., Hu, Z., Cao, X., Zhang, J. and Hu, Y. (2009) Non-structural proteins of *Periplaneta fuliginosa* densovirus inhibit cellular gene expression and induce necrosis in Sf9 cell cultures. *Virus Genes* **38**: 478-486
- Yang, B., Dong, X., Cai, D., Wang, X., Liu, Z., Hu, Z., Wang, H., Cao, X., Zhang, J. and Hu, Y. (2008) Characterization of the promoter elements and transcription profile of *Periplaneta fuliginosa* densovirus nonstructural genes. *Virus Research* **133**: 149-156
- Yang, B., Zhang, J., Cai, D., Li, D., Chen, W., Jiang, H. and Hu, Y. (2006) Biochemical characterization of *Periplaneta fuliginosa* densovirus non-structural protein NS1. *Biochemical and Biophysical Research Communications* **342**: 1188-1196
- Yu, Q. and Tijssen, P. (2014) Gene expression of five different *Iteradensovirus*s: *Bombyx mori* densovirus, *Casphalia extranea* densovirus, *Papilio polyxenes* densovirus, *Sibine fusca* densovirus, and *Danaus plexippus* densovirus. *Journal of Virology* **88**: 12152-12157
- Zádori, Z., Szelei, J., Lacoste, M.-C., Li, Y., Gariépy, S., Raymond, P., Allaire, M., Nabi, I.R. and Tijssen, P. (2001) A viral Phospholipase A2 is required for parvovirus infectivity. *Developmental Cell* **1**: 291-302
- Zamore, P.D., Tuschl, T., Sharp, P.A. and Bartel, D.P. (2000) RNAi: Double-stranded RNA directs the ATP-dependent cleavage of mRNA at 21 to 23 nucleotide intervals. *Cell* **101**: 25-33